Exploring the Potential of Electron Paramagnetic Resonance for in Personal Healthcare, and Assessment of Free Radical Content in Coffee

by

Husain Maki

A Thesis Presented in Partial Fulfillment
of the Requirements for the Degree
Master of Science

Approved April 2022 by the
Graduate Supervisory Committee:

Nathan Newman, Chair
Terry Alford
Ralph V. Chamberlin

ARIZONA STATE UNIVERSITY

May 2022

ABSTRACT

Electron Paramagnetic Resonance (EPR) has facilitated great scientific advancements in many fields, like material science, engineering, medicine, biology, and health. EPR provided the ability to investigate samples on molecular level to detect chemical composition and identify harmful substances like free radicals. This thesis aims to explore current health and diagnostics EPR research and investigate the free radical content in related paramagnetic centers. Examining paramagnetic diagnostic markers of Cancer, Sicklecell disease, oxidative stress, and food oxidation. After exploring current literature on EPR, an experiment is designed and conducted to test seven different coffee samples (Turkish coffee, Espresso Coffee, European Coffee, Ground Arabic Coffee, American Coffee, Roasted Arabic Coffee, and Green Arabic Coffee), using Bruker ELEXSYS E580 spectrometer at x-band and under both room temperature (298 K) and low temperature (106 -113 K). Several microwave powers (1, mW, 0.25 mW, 0.16 mW, 0.06 mW, 0.04 mW) and different modulation frequency (10 G, 5 G, 3 G) are used. The results revealed average g-value was 2.009, highest linewidth was 16.312. Espresso coffee had the highest concentration of radicals, and green Arabic coffee beans had the lowest. Obtained spectra showed signals of Reactive Oxygen Species (ROS) radicals; believed to be result of natural oxidation process, as well as trace amounts of Fe^{3+} and other transition metals impurities, likely to be naturally found in coffee or resulting from the process of coffee production.

ACKNOWLEDGMENTS

I am truly grateful to my supervisor Professor Nathan Newman. He has been very supportive throughout this thesis. He was available for me every week to discuss my progress. We also overcame the difficulty with me doing my thesis remotely with his support. I would also like to sincerely thank Marco Flores, and Siddhesh Gajare who helped in completion of my experiment. My gratitude also goes to the committee members; Professor Terry Alford, and Professor Ralph V. Chamberlin, who were generous in their time and cordiality.

TABLE OF CONTENTS

Page

CHAPTER Page

CHAPTER Page

LIST OF TABLES

Table Page

LIST OF FIGURES

Figure Page

Figure Page

CHAPTER 1

INTRODUCTION & BACKGROUND

1.1 Material Properties

Materials have distinct classes of properties such as mechanical, electrical, thermal, optical, and magnetic; those properties have considerable influences on our life since they are implemented in various vital applications and technologies [1].

1.2 Magnetism

There are several types of magnetism including paramagnetism, diamagnetism, ferriagnetism, antiferromagnetsim, and ferromagnetism. All materials exhibit some type of magnetism as a result of their spin, electron orbital and nuclear magnetic moments [2] [3].

1.3 The Nature of Magnetism

The magnetic properties of materials can be characterized using vibrating magnetic sample (VSM) and superconducting quantum interference device (SQUIDs) magnetometers.

There are two sources of electronic magnetic moments that arise from electrons. The first is the orbital motion of an electron around the nucleus; considering it is a moving charge, an electron may be thought of as a tiny current loop that generates a very small magnetic field and has a magnetic moment along its rotational axis. The second magnetic moment is generated by the spin of this electron, which is directed along the spin axis. According to relativistic quantum mechanics, spin magnetic moments can only be in one of two directions: up or antiparallel down. The smallest unit for an electron"s magnetic moment is the Bohr magneton and is equal to $9.27\times10^{-24}A.m^2$ [4] [5] [6].

1.4 Paramagnetism

Paramagnetism occurs when a substance contains uncoupled unpaired electrons. These materials are attracted by an externally applied magnetic field as a result of induced dipoles in the direction of the applied magnetic field. This results in a small, positive magnetic susceptibility. This makes the amplitude of the field within a paramagnetic material larger than that in a vacuum. The magnitude of the magnetic susceptibility of a paramagnetic result from both the spin and orbital moments of the electrons. The susceptibilities range for most paramagnetic material around 10^{-5} to 10^{-2} [2]. Because the internal magnetic field is induced, paramagnetic materials are only magnetic when in a magnetic field [7]. Oxygen gas, oxidized metmyoglobin, deoxyhemoglobin, reactive oxygen species, nitric oxide, melanin, caffeine and tumor tissue are some examples of paramagnetic materials [8] [9] [10].

CHAPTER 2

ELECTRON PARAMAGNETIC RESONANCE

2.1 EPR Background

Electron paramagnetic resonance (EPR) is a non-destructive method of spectroscopy that examines materials with unpaired electrons using a combination of a magnetic field and microwave radiation [11]. This technique can quantify the number of paramagnetic centers in a material, as well as identity the atomic constituency. It is particularly adept at characterizing transition metal complexes. The nature of the EPR signals depends on the site"s valence and spin state and can be used to quantitatively measure the concentration of a certain species. EPR is also widely used to identify irradiation damage sites in medicines, foods, and chemicals [11] [12]. When an unpaired electron in a paramagnetic material is exposed to an external magnetic field, the electron"s energy level splits into two quantum states with an energy difference proportional to the applied magnetic field. This is commonly called the Zeeman effect. Both resulting magnetic moments and the magnetic spin quantum number MS have 2S+1 values [13]. The absorption of a microwave photon with the Zeeman energy will excite the electron to a higher energy level [14].

2.2 EPR History

In 1944 Russian physicist Yevgenii Zavoiskii successfully observed and reported the first EPR spectra of manganese sulfate, copper, and chromium. Since then, EPR has been used extensively in a wide range of areas including physics, chemistry, biology, food sciences, and medicine [15].

2.3 EPR Spectrometer

Spectroscopy is the measurement and interpretation of energy difference between atomic or molecular states, the absorption of electromagnetic energy leads an electron to migrate from the lower energy state to the higher one [11] [12].

An EPR spectrometer typically consists of a radiation source, electromagnet, sample holder, detector, a phase sensitive detector, attenuator, and an amplifier. The sample is placed in the holder centered on the electromagnet, as microwaves are applied through an iris, the electromagnet magnifies the samples" signals to enable detection [16] [17]. The energy difference ΔE is equal to $\Delta E = hv$. Energy absorption leads to a transition from lower energy states to higher energy states [18].

EPR spectra can be carried out at different frequency bands, the majority of EPR instruments have microwave frequencies around 10 GHz, referred to as X-band. For practical reasons, the frequency is fixed, and the magnetic field is swept.

EPR spectroscopy is similar to all spectroscopies and is most similar to nuclear magnetic resonance (NMR) [14]. Its technique depends on the absorption of electromagnetic radiation; molecules and atoms have distinct states, each with a corresponding energy value; EPR measures and interprets energy differences between spin/orbital states. With knowledge of these energy differences, the identity, structure, and properties can be determined.

The species to be studied can be either in a paramagnetic ground state, or may have been excited into a paramagnetic state, for instance, by ultraviolet light, or high-energy electron or ion irradiation [17] [19].

2.4 EPR Applications

EPR has a wide array of applications in many fields like, material science and engineering, chemistry, quantum physics, biology, medicine and health, geology, and archeology. Some of

the prominent medical applications include study of oxygen species linked to the pathogenesis of numerous diseases, clinical applications like reliable measurement of partial pressure of oxygen (pO_2), measurement and localization of nitric oxide for cardiac disease diagnosis, as well as detection and characterization of free radicals for pharmacological applications [15] [20].

2.5 Molecular orbital theory

The molecular orbital theory explains the electronic structure of a multiatom molecule. By illustrating electron distribution amongst atoms, it enables distinction of physical and chemical characteristics. Magnetism is one of the characteristics that can be observed through molecular orbitals" electron distribution. Using EPR, only paramagnetic molecules can be detected [21]. Paramagnetism and diamagnetism can be clearly identified through molecular orbitals, for example O_2 is paramagnetic, molecular orbital show single electrons as seen in Figure (2.1) [22].

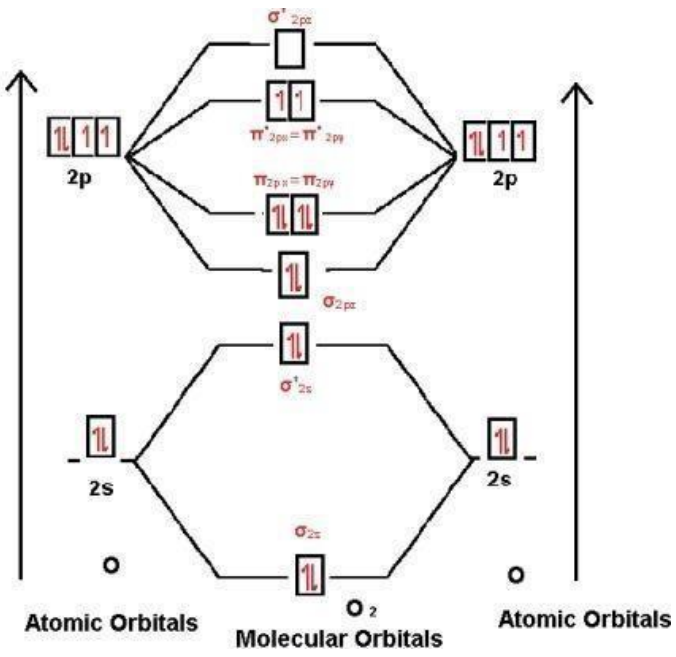

Figure 2.1: Oxygen Molecular orbital [22]

From the molecular orbital, it"s clear that N_2 is diamagnetic, which is illustrated in Figure (2.2) [23].

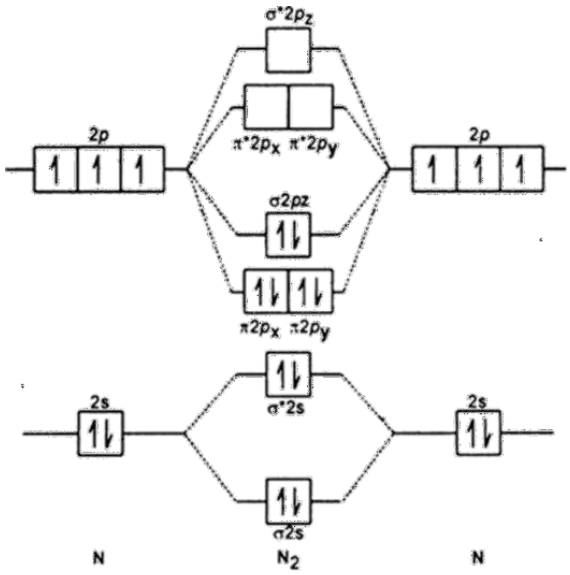

Figure 2.2: Nitrogen Molecular orbital [23]

Methanol (CH_3OH) is paramagnetic, as shown in Figure (2.3) [24].

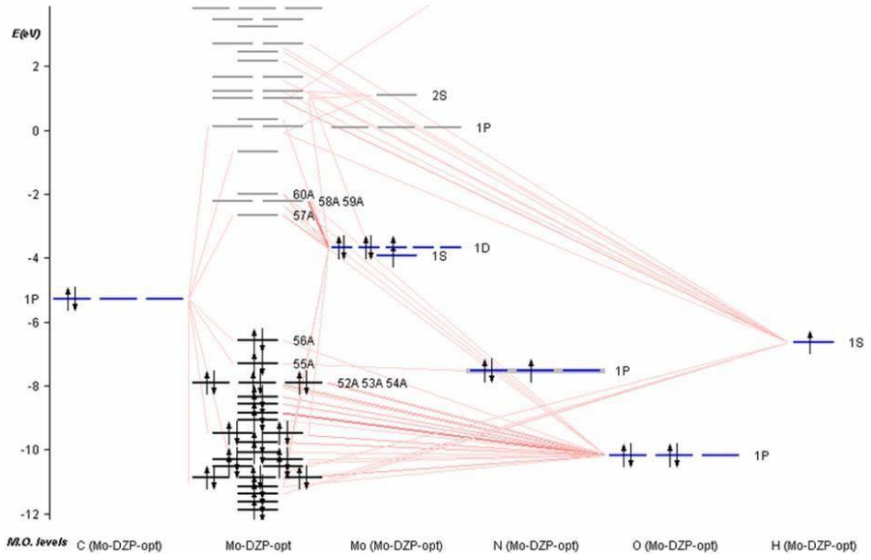

Figure 2.3: Methanol Molecular orbital [24]

Ethylene molecular orbital is illustrated in Figure (2.4) [25].

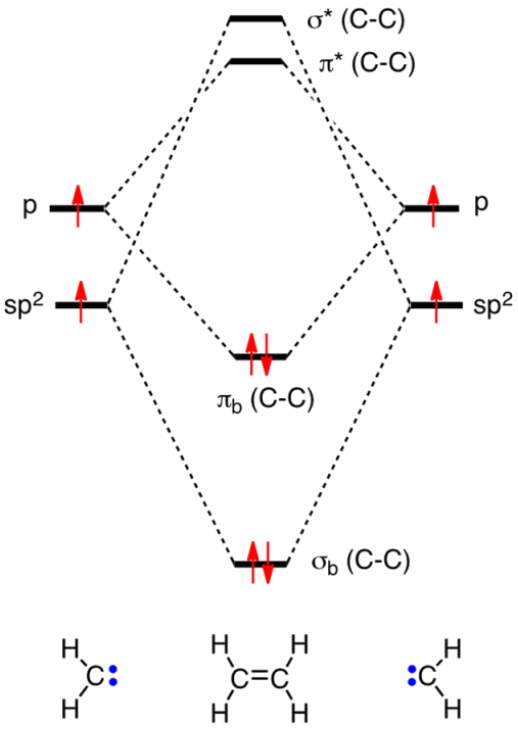

Figure 2.4: Ethylene Molecular orbital [25]

The molecular orbital of Acetone is shown in Figure (2.5) [26].

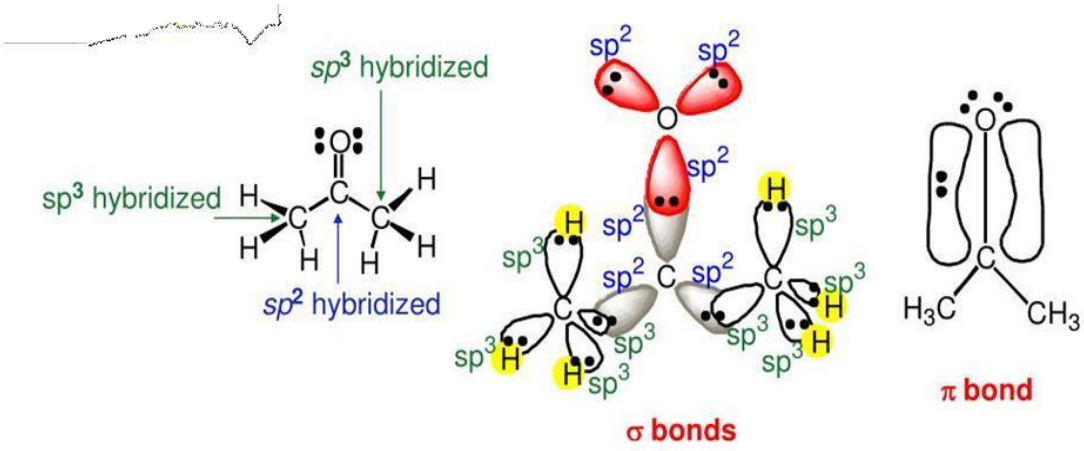

Figure 2.5 Acetone Molecular orbital [26]

NH_3 is diamagnetic; this is illustrated in Figure (2.6) [27].

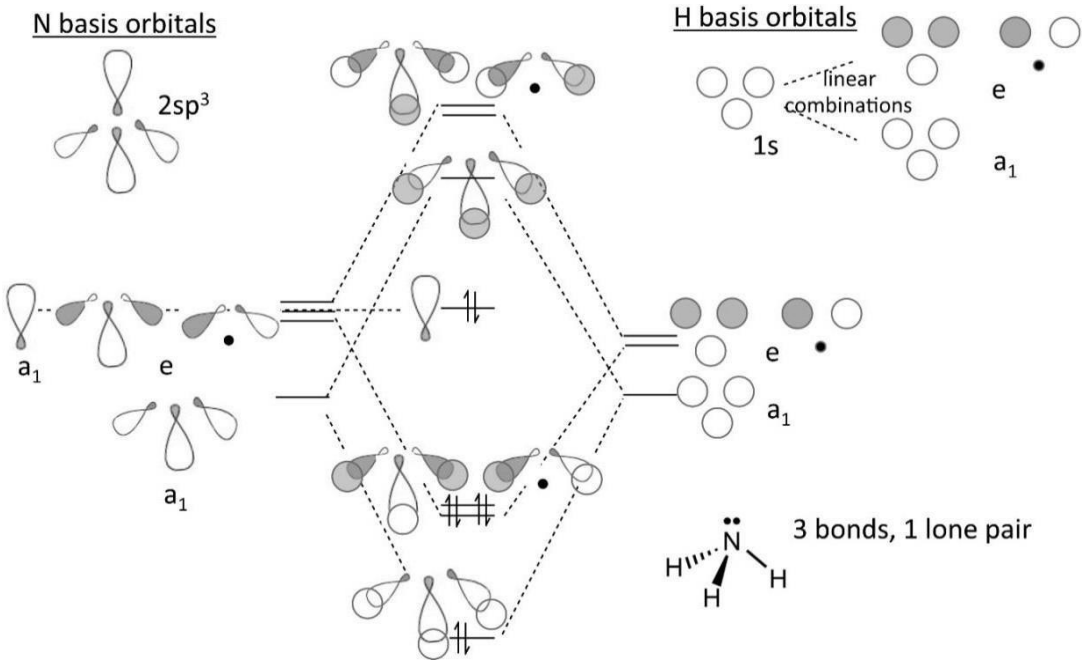

Figure 2.6: Ammonia Molecular orbital [27]

CO is diamagnetic, the molecular orbital of carbon monoxide is illustrated in Figure (2.7) [28].

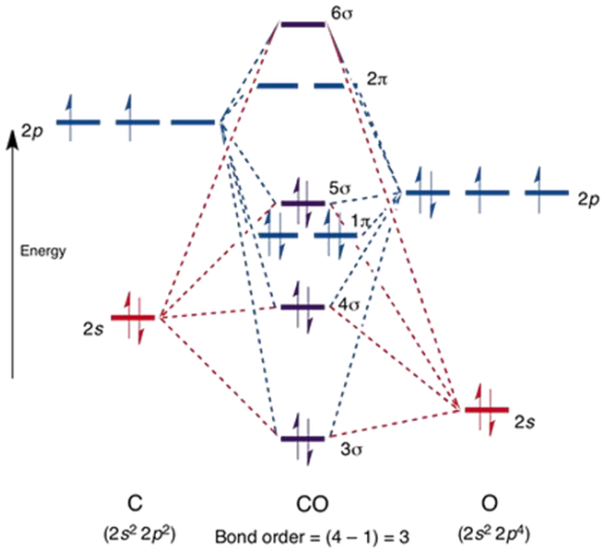

Figure 2.7: Carbon Monoxide Molecular orbital [28]

NO is paramagnetic, this can be seen in Figure (2.8) [29].

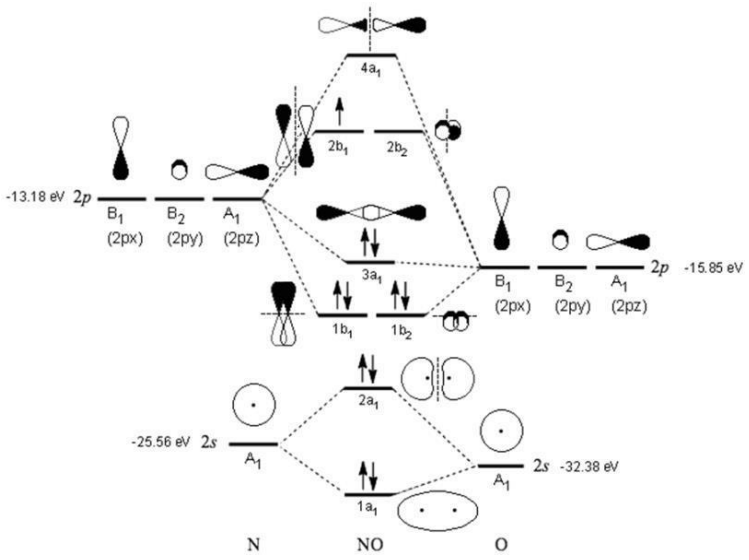

Figure 2.8: Nitric oxide Molecular orbital [29]

Water is diamagnetic; this is shown in Figure (2.9) where there is no free electron in the outer shell [30].

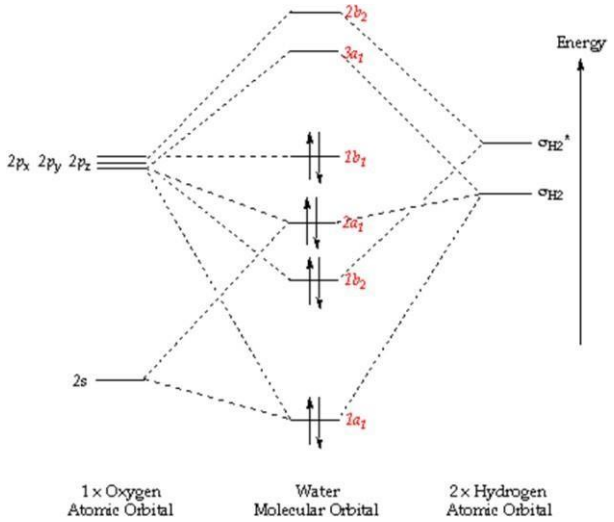

Figure 2.9: Water Molecular orbital [30]

Methane is diamagnetic as shown in Figure (2.10) [31].

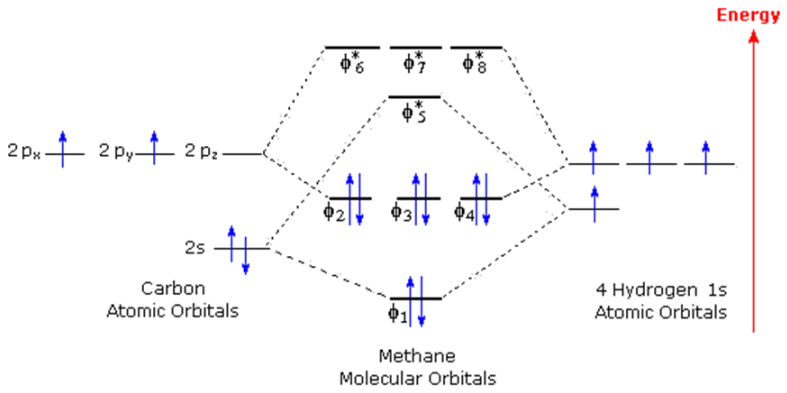

Figure 2.10: Methane Molecular orbital [31]

2.6 Free Radical Nature

Free radicals can be defined as the chemical substance that possesses an unpaired electron in the outer shell of the molecule. The nature of free radicals is paramagnetic and the most effective technique in their detection is EPR.

2.7 The aim of the thesis

The aim of this thesis is to systematically review EPR research in the area of health assessment and disease diagnosis. As well as developing an experiment to examine one of the EPR applications on a deeper level. Coffee is known to have beneficial effect, but its" content of free radicals is concerning as radicals have been linked to chronic diseases. Monitoring free radical concentration, in the globally popular drink, enables measurement of relative benefits and harms of coffee consumption.

CHAPTER 3

LITERATURE REVIEW

3.1 Literature Review Introduction

This thesis will be reviewing the existing evidence to explore the capabilities of EPR in health-related applications and investigate coffee in depth using EPR.

It has been established that EPR facilitates characterization of atoms and molecules containing paramagnetic centers. EPR applications in clinical biochemistry can provide essential information that enables development of advanced early diagnosis methods such as the detection of NO in cardiac and endothelial tissue lining the blood vessels. EPR can be used to quantify the diagnostic markers (e.g., reactive oxygen and nitrogen species) of neurological diseases [32]. These reactive species contribute to a misbalance between free radicals (reactive oxygen species (ROS)) and antioxidants, which is known as oxidative stress. This condition has been linked to the development of cardiovascular, cerebrovascular, and neurodegenerative diseases, as well as chronic kidney and lung diseases. Oxidative stress also contributes to aging and the development of cancer. Additionally, NO plays a significant role as a transmitter in the vascular as well as throughout the nervous system [33] [34].

The discovery of nitrosylated heme/nonheme iron (Containing Fe and Nitric Oxide (NO)) in the mid-1960s led to the discovery of NO as L-arginine in endogenous tissue, and its role in the transmission of signals throughout the body systems [35].

Free radicals, including O^{-2} and NO^{+}, are detectable by EPR as they have unpaired electrons. Detecting NO by EPR can be done in the gaseous state e.g., polluted air. However, detecting NO in tissue has a small spin lifetime and thus requires the use of a spin trap [36].

While EPR can be expensive and more complicated than other methods of detection and measuring of NO, it has some advantages: It can be used on optically opaque or murky samples such as human tissue and blood. EPR provides the ability to define the source of detected NO.

Spin trapping NO using (N-methyl-D-glucamine)2-Fe (II)-NO is able to provide adequate NO measurement due to stability and longer half-life than most NO radicals [36] [37].

In an experiment examining pregnant human subjects, it has been established that placenta oxidative stress is an essential element for the health of the mother and fetus throughout the 3 trimesters. NO is important for the formation of essential amino acid L-arginine, making it vital for the development of the placenta (and proteins, that make up most other human tissue). However, too high a level of oxidative stress leads to pre-eclampsia. Pre-eclampsia is a condition characterized by dangerously high blood pressure due to vascular malfunction and can be life-threatening to both the pregnant woman and fetus. The experiment found that tissue samples of pre-eclamptic placenta had significantly lower concentrations of NO [38].

Ischemia is a condition characterized by severely low oxygenation levels. In rat studies, EPR determined that high concentrations of NO are present in ischemic brain tissue. Melatonin, an antioxidant, which was used to combat the impact of the free radical NO and was found to be successful in decreasing the NO concentration and by that decreasing the damage caused [39].

Interestingly, NO can permeate the blood brain barrier, excess NO and O free radicals contribute to increased oxidative stress and vascular diseases including hypertension, cardiac and cerebrovascular diseases [40].

The basic measurement process is described in a study [24]; NO scavengers were administered to ensure accurate measurement of the NO resulting from the intended experiment. Sample is collected, rinsed with saline solution (NaCl) then frozen using liquid Nitrogen (77 K), EPR spectroscopy is done. The result of NO concentration is determined based on the intensity of the NO–Fe–DETC spectrum and its comparison with the calibration curve. Thus, EPR provides non-invasive way to detect and quantify NO, O, and other radicals, and while spin traps are useful in the detection of NO, they can be used to reduce its concentration. Ultimately reducing oxidative stress. This may aid in the development of medication and other pharmaceuticals to prevent diseases or slow their progression [41].

3.2 Blood studies using EPR

One of the most interesting EPR applications is the investigation of blood. This work has enabled the detection of paramagnetic misbalances that indicate the presence of disease, oxidation, or malignancy. EPR is an easy, minimally invasive method to detect disease. It is also highly accurate and sensitive enough to assist in the diagnosis.

3.2.1 Components of the blood

Examining the basic components of blood enables identification and detection of anomalies related to disease development. Red blood cells (RBCs) compose 41% of the blood content and are responsible for oxygen delivery and circulation. White blood cells (WBCs) comprise about 4% and have several types (lymphocytes, basophil, eosinophil, monocyte, neutrophil). WBCs are responsible for the body"s immune response, to protect health and attack pathogens [42]. Plasma composes 55% of the total blood. Plasma carries nutrients hormones, and proteins, it also carries waste products and is responsible for the transportation of blood cells (blood flow). It contains, plasma proteins; albumin, globulins, fibrinogen, clotting factors and inhibitors, and complement proteins. The proteins maintain pH slightly alkaline by binding the extra hydrogen ions in the blood. Plasma also contains electrolytes, amino acids, nitrogenous compounds, nutrients, and dissolved gases [43]. Additionally, methemalbumin (MetHB)is an abnormal component of blood plasma in certain diseases associated with excessive hemolysis. It is oxidized hemoglobin.

Moreover, Heme Oxygenase-1 is a cytoprotective enzyme, responsible for prevention of vascular inflammation. It reduces oxidative stress by catalyzing oxidative degradation of heme, bilirubin, free iron, and carbon monoxide. It responds to stressors like hypoxia, hyperthermia, oxidative stress, and others [44]. It is suggested that increased HO-1 protects against oxidative stress and stress-related injury. Bilirubin is a biproduct of RBCs breakdown. It is managed by the liver and is excreted in the stool. Increased Bilirubin levels are due to inefficient liver or bile duct function, resulting in bilirubinemia. This condition can be treated by phototherapy, through a healthy

nutritional diet and treatment of underlying conditions [45] [46]. For infants, exposure to a healthy nutritional diet is very effective in treating this condition.

3.2.2 Iron and EPR

Iron is an essential blood component. Fe^{3+} is one type of iron in the blood, it is noteworthy that only a few of the Fe-containing species in the blood are paramagnetic. EPR can monitor the level of iron oxidation and its different types in the blood.

Male-humans contain about 4,000 mg of iron, of which 2,500 mg are within erythrocytes; 1,000 mg is stored in splenic and hepatic macrophages, and the rest is distributed in various proteins such as Myoglobin, cytochromes, or other ferroproteins. Only about 3 mg are bound to plasma transferrin and constitute the mobile iron compartment which supplies the various intracellular iron stores. 1-2 mg of iron is lost every day through skin and enteric desquamation and minor blood losses [47] [48].

3.2.3 Oxidative damage

Reactive oxygen species (ROS) are one of the biological oxidation markers which have been linked to increased oxidative damage. Oxidation leads to deterioration of the body organs' function and intracellular signal transduction. EPR was used to assess blood samples collected from healthy young adults, older healthy adults, young and old individuals with health problems like sarcopenia; degenerative loss of muscle mass, Mild cognitive impairment (MCI); the very early stage of cognitive function and memory loss, and sporadic Amyotrophic Lateral Sclerosis (sALS); a progressive neurodegenerative disease that affects both central and peripheral parts of the nervous system, which occur at random. Higher concentration of ROS was found in blood samples of older individuals as well as those with health problems. EPR is evidenced to provide a safe way to measure ROS concentration and changes, as it can be done in vitro and in vivo. ROS are linked to increased oxidation and can be used as an indicator for disease prognosis. It is

suggested that it may be useful in examining the efficacy of therapeutic drugs as well as drug screening [49].

3.2.4 Albumin

Albumin is the most abundant protein in the human blood; it is produced by the liver and accounts for more than half of the plasma proteins. In cancer patients, tumor cells produce proteins that bind to albumin; these proteins can indicate the characteristics of tumors and impact on the body"s systems. Binding to albumin can lead to modifications that alter the function of albumin, like enabling albumin to bind with and transport fatty acids. These alterations can be easily examined using EPR and a spin-probe. Cancer-specific findings were measured using 6-doxyl stearic acid(2-(14-carboxytetradecyl)-2-ethyl-4,4-dimethyl-3-oxazolidinyloxy. EPR provides a sensitive non-invasive method of characterizing serum albumin, providing valuable diagnostic information and monitoring disease prognosis [50] [51].

3.2.5 Free radicals and delayed cerebral ischemia

Looking deeper into the impact of free radicals on health, this study [52] provided an assessment of radicals in delayed cerebral ischemia (DCI) patients. DCI is caused by lack of oxygen due to arterial vasospasm (narrowing of the artery), leading to infarction (tissue death, necrosis, or stroke), poor neurological outcomes, and mortality. It has been suggested that free radicals have a significant role in the development of DCI. Studies have explored the relationship between free radical concentration in peripheral venous blood and development of DCI. Using EPR and a spin probe, it was found that symptomatic DCI patients had significantly higher concentration of ROS radicals in the blood than asymptomatic DCI patients [52] [53].

Notably, spin probe cyclic hydroxylamine 1-hydroxy-3-methoxycarbonyl-2,2,5,5-tetramethylpyrrolidine (CMH) is used to provide sensitive and accurate measure of reactive

oxygen species, furthermore, it enables the preservation of biological samples for at least six months without losing signal intensity in EPR analysis [54].

3.2.6 Oximetry

An adequate supply of oxygen is necessary to maintain healthy and normal functioning of the body systems. Thus, oximetry has been developed to monitor oxygenation in the blood, which indicates the normalcy of the oxygen supply available. Decreased oxygen supply in the human tissue leads to necrosis, also known as gangrene, which is common among diabetic individuals. Diabetes causes neuropathy (nerve damage) and atherosclerosis, a condition in which plaque or fatty deposits in the inner layer of blood vessels resulting in inadequate circulation. Both of these conditions contribute to poor oxygenation and wound healing. A technique using EPR has been developed to monitor wound oxygenation in animals. The partial pressure of oxygen p_{O2}, is measured. This technique is limited to pedicled skin flaps and cannot be used on excisional wounds. Supplementary oxygen can be used to enhance wound healing and prevent gangrene and amputation [55]. While this application is limited, it shows the potential of EPR to provide information that may not be available without paramagnetic detection.

3.2.7 Biological electron transfer

EPR has recently become widely utilized in biomedical and cancer research. One important example I wanted to look at is the investigation of energy transfer among cells and their impact on health.

Biological electron transfer plays a critical role in cell energy processes and systems functioning; thus, it also contributes to the development and progression of disease within the body. Electron transfer is mediated by reduction/oxidation units (redox) which alter the blood content of transferrin, ceruloplasmin, labile iron pool, neutrophils, and platelets. Cancer cells generate

excessive amounts of free radicals which can react to other cellular macromolecules like lipids and DNA [56].

Colorectal cancer is the second most common type of cancer and the second most common cause of cancer-related death. EPR is used to examine the activity of the redox blood content and determine the difference in the blood"s radical concentration between rectal cancer patients and healthy patients. Cancer patients have higher concentration of NO and iron radicals [57]. Through this study, EPR has been deemed a cost-effective diagnostic tool for cancer. It enables accurate diagnosis by examining the blood albumin and analyzing the results [58].

3.2.8 Irradiated blood

Human exposure to irradiation can occur in a number of ways including medical treatment, imaging, or exposure to toxins, for example. Exposing blood to radiation limits the complication associated with blood transfusion, where the host body rejects the new blood. Perhaps the most common ways to be exposed to radiation is in X-ray and radioactive pharmaceutical technetium-99m. The latter used as a diagnostic tool in many conditions and procedure as it has a long half-life (6 hours) and enables acquisition of clear scans.

In this study [59], EPR and Fourier transform infrared (FTIR) spectroscopies were used to explore the effect of irradiation on human blood. FTIR spectra revealed changes in the biochemical composition of irradiated blood, mainly proteins, and the use of hierarchical cluster analysis (HCA) was useful to quickly distinguish irradiated and non-irradiated blood samples. FTIR spectrometry can provide superior information to conventional biochemical methods. It uses very small amounts (measured in microliters), requires no sample pre-treatment, and provides fast results.

EPR results indicated increased concentration of oxidized hemoglobin in irradiated blood. The resulting oxidized product, methemoglobin, can cause additional health problems, such as a decrease in the carrying capacity of oxygen in the blood and resulting hypoxemia (decreased blood oxygen levels) [59].

Using EPR in biomedical/biochemical research can enable fast and accurate diagnosis through early detection of health conditions. Further investigation can progression of disease and support pharmaceutical development of more effective treatments [60].

Spin trapping and spin labeling are essential techniques which have been used to detect and identify free radicals in biological samples, like reactive oxygen species (ROS), as they stabilize the radicals and extend their spin lifetimes, enabling efficient detection of ROS with sensitivity and accuracy.

Spin Traps act as radical scavengers producing stable adducts that can be measured by EPR [61]. Spin labels are paramagnetic agents that interact with detectable molecules like radicals; it enables detection of dynamic changes in complex biochemical systems. Spin probes are molecule with stable free radical that can couple with other molecules and enable its detection using EPR [62].

3.3 Oxidative stress

Oxidative stress is caused by oxidative damage, it has been deemed a significant indicator for deteriorating health, and a participant in the development of chronic and life-threatening disease. Oxidative stress is caused by an increased free radical concentration in the body. Quantifying oxidative stress is a complex procedure that is made significantly easier using EPR.

Measurement using NO and ROS; prior to EPR, oxidative stress measurement was extremely complex and needed a lot of time and precision to execute. The traditional ways to measure oxidative stress depended on examining the impact and biomarkers of oxidation by direct measurement of ROS. ROS can be measured using fluorogenic probes, which are small-molecule sensors that unmask brilliant fluorescence upon exposure to specific stimuli. This enables detection of ROS under the microscope [63].

H_2O_2, OH^-, and ROO^- can be measured after staining with 5-(and -6)-carboxy-2′,7′-dichlorodihydrofluorescein diacetate (DCFDA). This spin probe is able to enter the cells and reacts to become DCFH within the cell, which then reacts with H_2O_2 to generate the fluorescent 2′,7′-dichlorofluorescein (DCF). The fluorescence intensity of DCF provides a semi-quantitative measure of the peroxide content produced by the cell.

Indirect measurements of quantifying the ROS concentration is done through the observation of oxidative damage. While this is a promising approach, it is yet to be developed and is made difficult by the extremely short half-life of radicals. For example, hydroxyl radicals have a half-life of less than one nanosecond. Currently, indirect measurements are performed by examining oxidative damage to cellular lipid, protein, and nucleic acids [64].

Protein damage is evidence by Protein carbonyl (PC), a biomarker of oxidation, assessment of cellular PC content provides significant evidence of oxidative stress in clinical experiments. PC results from the oxidation of protein and amino acid residue. It can be measured using 2,4-dinitrophenylhydrazine (DNPH). DNPH reacts with PCs and forms Schiff base producing dinitrophenylhydrazone products, which can be analyzed spectrophotometrically at 375 nm. The amount optical absorption correlate to the protein oxidization levels [64].

Lipid peroxidation is also used to access the damage made by ROS to the cells. Malondialdehyde (MDA) is one of the best studied end-products of peroxidation of polyunsaturated fatty acids. The MDA level in the cell is used to estimate oxidative stress levels, it can be measured using thiobarbituric acid reactive substances (TBARS).

MDA reacts with TBARS in acidic medium at 100 ^{o}C and produces pink/red product that can be then extracted with butanol and its absorbance is measured with a spectrophotometer at 520-535 nm or by fluorimeter. While these methods are fast and relatively simple, aldehydes (other than MDA) can react with TBRAS and alter the results, significantly degrading the accuracy of the measurements.

Plasma MDA may also be measured using high-performance liquid chromatography (HPLC), and by gas chromatography-mass spectrometry (GC-MS) [64].

Moreover, 8-Hydroxy-2′-deoxyguanosine (8-OHdG) is one of the major oxidative products that indicates the presence of DNA damage. 8-OHdG occurs from hydroxylation of deoxyguanosine residues. 8-OHdG residues are removed from the DNA by the automatic enzyme repair systems. Once detached, they circulate in the blood until filtered by the kidney and expelled in the urine.

Measuring the 8-OHdG concentration of in the blood and/or urine can be used to estimate the extent of DNA damage.

8-OHdG is measured using HPLC along with an electrochemical detector (ECD). While this process is sufficiently sensitive and accurate, it is inconvenient and extremely costly. Other ways to measure DNA oxidation include enzyme-linked immunosorbent assay (ELISA) and immunohistochemical analysis [64].

Moreover, assessment of antioxidants status can indicate oxidation; in order to maintain hemostasis (balance) among the body systems, the amount of damage by free radicals is mitigated by the antioxidant system. When the redox hemostasis (balance of antioxidants and radicals) is disturbed, it causes oxidative stress.

Redox hemostasis is regulated by enzymatic and non-enzymatic elements. Enzymatic antioxidants include Superoxide Dismutase (SOD), Catalase, Glutathione Peroxidase (GPx), and Glutathione S-Transferase (GSTs), Nonenzymatic Antioxidants, including Glutathione, Vitamin A, Vitamin C, and Vitamin E, and Total Antioxidant Capacity [64].

The quantification of oxidation stress can be performed from measurements of the free radical and antioxidant concentration in the blood and body-tissues using EPR [65].

EPR studies on living rats detected the presence of NO radicals in the brain. The process involved administration of NO scavengers, sample collection, rinsing with NaCl, freezing in liquid nitrogen (77 K), and then comparing the intensity of the measured NO-Fe-DETC spectrum with the calibration curve.

Imaging of NO is also used to continuously monitor free radicals. The method uses the characteristic EPR spectra that are observed when nitric oxide is combined with iron dithiocarbamates. The spectrum of the reaction product is a nine-line pattern, the difference can be easily observed from the initial nitronyl nitroxide spectrum.

The high concentration of NO and the large of trap molecules needed to detect a signal limit the use of EPR in this area. Trapping can remove NO being investigated. The sensitivity can be improved by using more specific and stable NO traps.

In vivo EPR can be a powerful tool. Measurements of both NO radicals and pO_2 can be performed simultaneously. This would provide valuable information on the degree oxygenation, the radical concentration, and rate of deterioration. Development of better and safer trapping agents would significantly expand the scope of in vivo EPR experiments and provide higher quality information [65].

In comparing EPR to traditional means of measurement, EPR is potentially more convenient, accurate and sensitive and does not need invasive procedures. It can safely detect free radicals, peroxidation of lipids and overall measurement of oxidation [66]. EPR offers a reliable option to enable effective change in clinical practice. It can save time, money, and effort by decreasing the needed time to collect and analyze samples and limit human error incidents.

3.4 Sickle Cell Disease

An example relating exploration of the blood content and oxidation in diseased status is Sickle cell disease (SCD). It is an inherited genetic disorder affecting the lives of 5% of the global population. It is one of the most prevalent blood disorders, impacting more than 300,000 children newborns each year. It results from a genetic mutation and requires life-long treatment to manage.

3.4.1 Sickle Cell

SCD causes the cells to change shape from the normal round to a crescent shape (sickled), which makes it hard and sticky, and compromises its ability to carry oxygen. Sickled red blood cells cannot bend and move easily within the blood vessels. This leads to blockage and hinders the blood flow throughout the body. Inadequate blood flow leads to many health problems like stroke, pain crises, and susceptibility to infection. While treatment plans can reduce symptoms and enhance the quality of life, blood and bone marrow transplant are the only known cures for SCD [67].

SCD is caused by Hemoglobin S which caused valine to replace glutamic acid in position 6 on the Beta-globin chain. This leads to the substantial impacts on RBCs that are sickling, increased susceptibility to hemolysis [68]. Cell free hemoglobin is usually bound by haptoglobin and cleared, but in SCD it acts as scavenger for vasoactive nitric oxide and pro-oxidant.

3.4.2 EPR and Sickle Cell disease

Reference [69] carried out a study in which healthy and SCD blood samples were collected into a 3.8% Sodium Citrate solution (volume ratio 1:9), the plasma was separated by centrifugation at

2000 rpm for 10 minutes and then 8100 rpm for another 10 minutes, the blood plasma was then separated and stored at -80 ^{0}C.

EPR was performed at 3.65 K in a Bruker Elexys X-band EPR system. Methaemoglobin (MetHb) and plasma mixtures were incubated at 37 C, in a 3-mm diameter quartz EPR tube, then frozen instantaneously in liquid nitrogen, and then stored at -80 ^{0}C prior to measurement. EPR spectra were obtained with a microwave power 1 mW, modulation amplitude 10 G, and accumulation of 5 scans.

EPR spectra contain a distinct signature associated with the unpaired electrons in the ferric form of iron in metHb and can be easily distinguished from that of copper II ions and other free radicals. EPR spectra of SCD patients shows a single peak due to metHb presence. However, the plasma of many SCD patients had shown a unique double peak that was attributed to a component of the plasma rather than metHb. This component may dominate the spectra, making measurements of the metHB concentration challenging and sometimes not possible [69].

3.4.3 Traditional methods of detecting SCD

High-performance liquid chromatography (HPLC) is a method used to identify the relative proportions of the different types of hemoglobin. The electrophoresis variation of this technique uses an electric current to detect both (1) the presence of abnormal hemoglobin and (2) differentiate the types of hemoglobin (A1, A2…etc.).

Another method to detect if a patient has the sickle cell disease in described in Reference 57. It involves collecting a blood sample in vacuum tubes containing EDTA (ethylenediaminetetraacetic acid) and anticoagulant. Then the tubes can be stored at 2 – 8 C for a maximum of 1 hour before they are subsequently mixed with a disodium hydrogen phosphate (Na_2HPO_4), sodium dithionite ($Na_2S_2O_4$) reagent mixture. The reagent is prepared by mixing 3 volumes of Na_2HPO_4 with 2

volumes of $Na_2S_2O_4$ to get a final pH of 6.8. This solution must be used immediately after preparation [70].

Five drops of freshly prepared reagent are mixed with 1 drop of blood, the slide is prepared with a drop of the mixture and coverslip is sealed using petroleum jelly, paraffin wax, or varnish. Sickling can be observed immediately in SCD and is clearest within 1 hour. Genetic testing may also be done to identify SCD [70] [71].

All in all, while EPR is expensive and requires a sophisticated analysis, it may be easier and less invasive than the more-commonly used traditional methods. EPR has the following advantages over currently used methods: it is easier, faster, and does not require a lot of experience to perform, while having these limitations: it is very costly, and requires sophisticated knowledge in the field.

3.4.4 Oxidative stress in SCD patients

SCD causes increased oxidative stress, which could be the root cause of the short lifespan typically associated with SCD. In the US, SCD patient life expectancy is 25 years less than the average of general population [72].

Ferrihemoglobin (Fe^{3+}) contains iron in the +3 oxidative state, whereas ferrohemoglobin (Fe^{2+}) contains iron in the +2 reduced state [73]. MetHb increases with the addition of NO (from oxidation or breathing). Patients with the SCE disease have increased concentrations of methemoglobin in the blood.

Human serum albumin (HSA) has a substantial role in mitigating the oxidation caused by methemoglobin, however, while MetHb induced haem oxtgenase I (HO-I) - which indicates oxidation - HAS limited the benefits of HO-I. The study findings indicate that metHSA is present in SCD [74] and has a role in reducing the oxidative effect of free haem. This reduces the protein oxidation and possibly limits the amount of damage that would result from the increased HO-I

levels. Methemoglobin increases substantially in the whole plasma of SCD patients when NO is added.

In this study [74] the plasma of many SCD patients showed a double peak, while some only showed one. Hemoglobin A and C were examined by EPR and showed identical results (single peak, as the high-spin ferric hemoglobin) this indicates that differences in SCD plasma are not related to the hemoglobin mutation itself, as seen in Figure (3.1) [74].

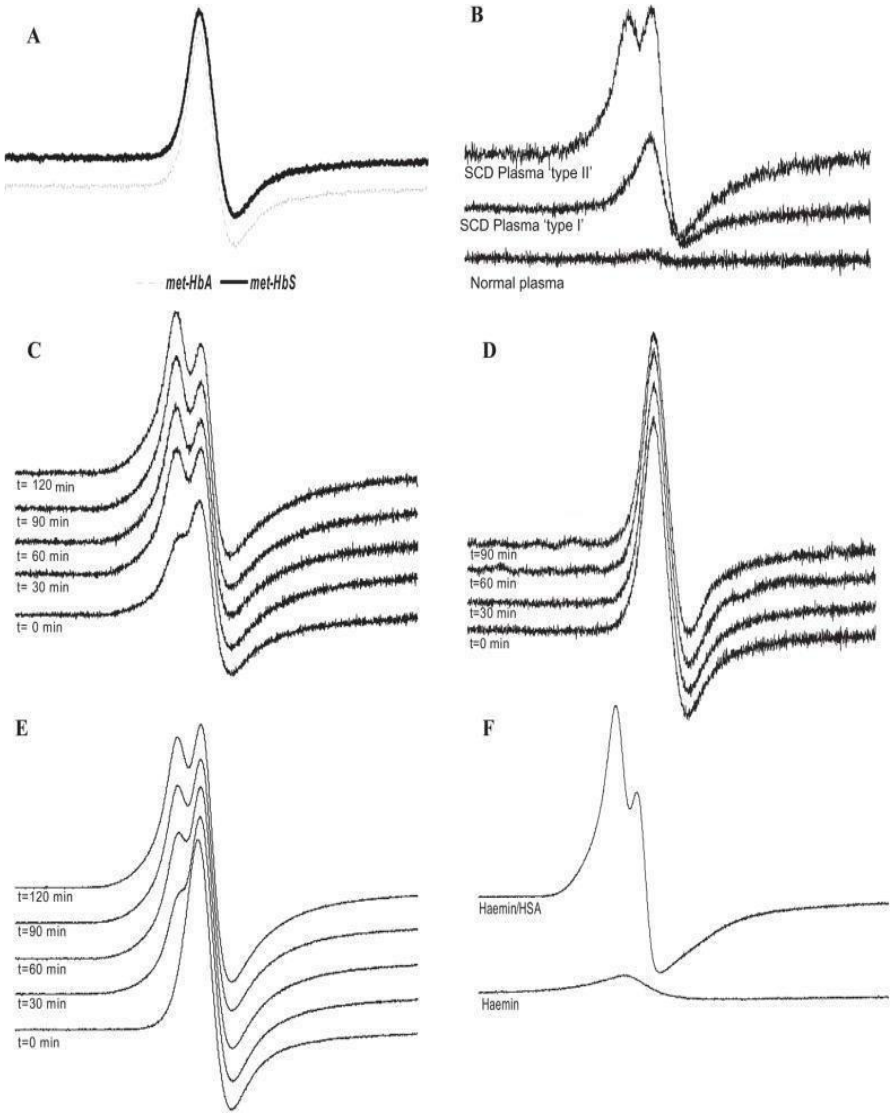

Figure 3.1 Sickle Cell Disease Spectra [74]

Figure (3.1) shows the spectra of SCD: A shows EPR spectra of MetHB of HbA and HbS. In B, the first and second waves are of SCD representatives" blood plasma compared to the EPR spectra of normal plasma. C shows the spectra taken after adding 10 uM of MetHB to SCD plasma incubated at 37 C for 0-120 minutes. Spectra D shows 10 uM of MetHB added to normal plasma incubated at 37 C for 0-120 minutes. Spectra E is of 100 uM MetHB in normal plasma incubated at 37 C for the indicated times (0, 30, 60, 90, 120 minutes). Spectra F is of 100 uM hemin and 30 mg/ml of Human Serum Albumin (HSA). All spectra were obtained at 3.65 K.

The sample was tested at 37 ^{0}C, requiring no extreme temperature change. The samples were centrifuged, which does not seem necessary as EPR is able to detect non-clear sample and examine the blood without extraction [74].

3.5 Cancer studies

3.5.1 Magnetic centers in cancer patients' blood

As it has been indicated earlier, oxidation results in disease, this can be seen in the blood of cancer patients too.

Aside from iron, copper has been found to be another indicator of malignancy in human blood. Normally, Copper is produced as ceruloplasmin in the human liver and then transported through the body in the bloodstream. However, cancer cells may also produce extra ceruloplasmin. An extremely high level of copper is typically found in cancer cells and plasma of patients with malignant tumors. Tumor cells acquire copper from the plasma in the bloodstream, thereby increasing the copper concentration in those cells [75].

Whole blood studies have been performed in an X-band Bruker spectrometer (EMX-10) at 170 K. Nitrogen gas flow was used to avoid water condensation on the spectrometer cavity. The settings used were: 20 mW microwave power, 100 kHz modulation frequency, 1 mT second modulation amplitude. Recording of EPR spectra took place in a sweep range 650 mT. The spectra was smoothed using an adjacent averaging method to increase the ability to discern weak signals [75].

Initially, the sample is frozen, human blood spectra measured at 170 K, it was seen in healthy and ill individuals. Figure (3.2) shows EPR spectrum of Fe^{+3} ion in whole blood. The first component observed in the curve is g at 4.30 to 4.37 which has the lowest amplitude and narrowest line width. The amplitude of the second component with g at 4.23 to 4.27 is greater than the amplitude of the first one. The third component is g at 4.11 to 4.13, having the highest amplitude and greatest line width [75].

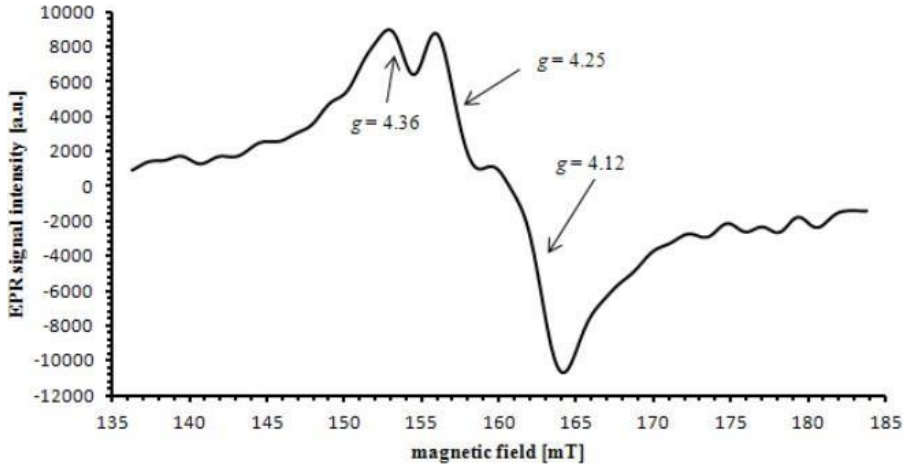

Figure 3.2 Fe^{+3} ion in the whole blood [75]

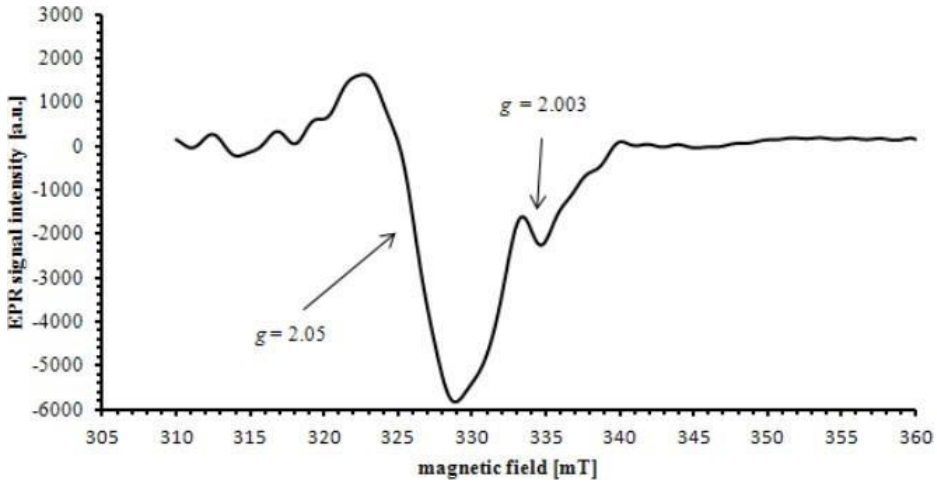

Figure 3.3 EPR Spectra of Whole Blood from 68-Year old female breast Cancer Patient [75]

Figure (3.3) show the EPR spectrum of whole blood from 68-year-old female breast cancer patient, shows the signal from Cu^{2+} ions. The line g at 2.05, which is consistent with the literature value given to the Cu^{2+} ions present in the blood g at 2.049, while the signal g at 2.003 is present in the blood of about 30% of cancer patients and is believed to indicate the presence of free radicals [75].

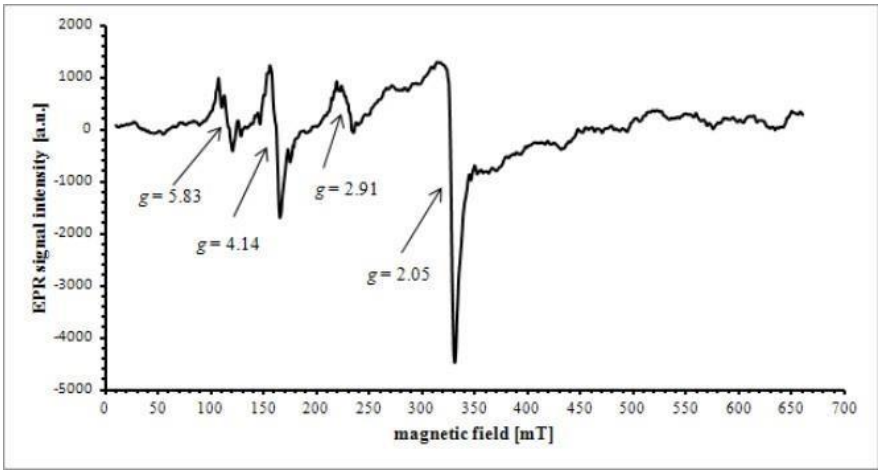

Figure 3.4 EPR spectrum of whole blood of 68-year-old female breast cancer patient [75]

Figure (3.4) showing EPR spectrum of whole blood of 68-year-old female breast cancer patient. It shows signals from Cu^{2+} in ceruloplasmin (g = 2.05), high spin Fe^{3+} in transferrin (g = 4.14), high spin Fe^{3+}in methemoglobin (g = 5.83), and low spin ferriheme complex (g = 2.91) at 170 K [75].

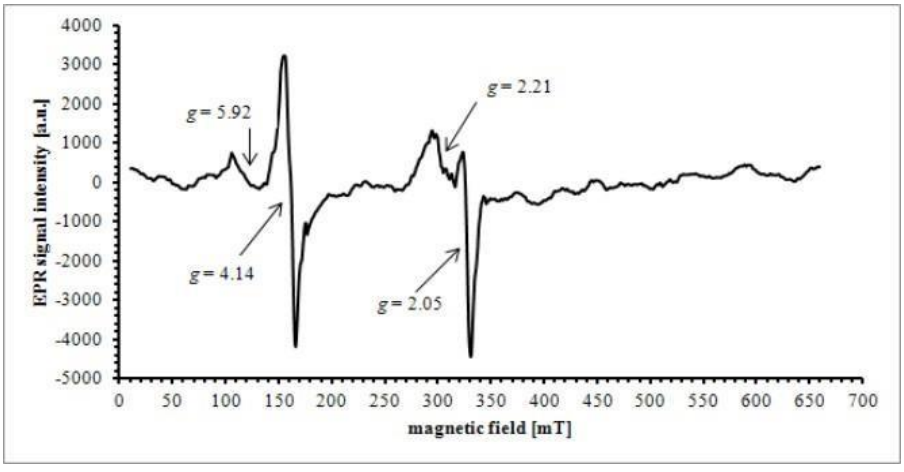

Figure 3.5 EPR spectrum of whole blood of 51-year-old female breast cancer patient [75]

Figure (3.5) illustrates EPR spectrum of whole blood of 51-year-old female breast cancer patient, showing signals of Cu^{2+} (g= 2.05) Fe^{3+} (g = 4.14, g = 5.92) and ferriheme complex (g=2.21) [75].

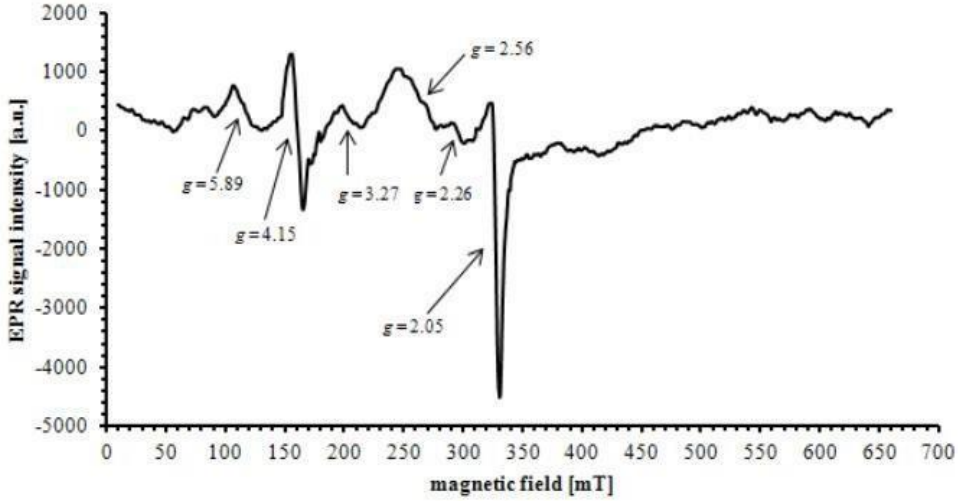

Figure 3.6 EPR spectrum of whole blood 51-year-old female, breast cancer patient [75]

Figure (3.6) indicates EPR spectrum of whole blood 51-year-old female, breast cancer patient. It shows signals of Cu^{2+}, (g= 2.05), high-spin Fe^{3+} (g= 4.15 and 5.89), low spin ferriheme complexes (g= 2.26 and 2.56), and cytochrome (g= 3.27) [75].

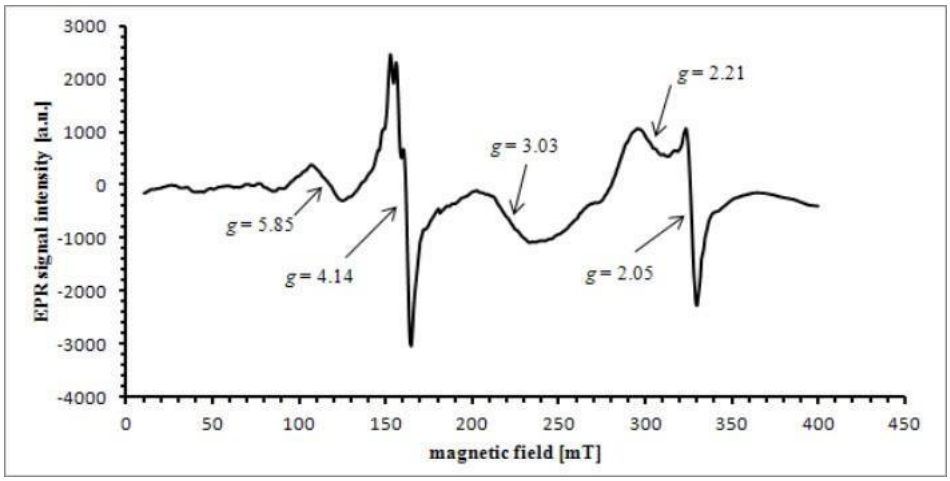

Figure 3.7 EPR spectrum of whole blood of a healthy person [75]

Figure (3.7) is of EPR spectrum of whole blood of a healthy person showing signals of Cu^{2+} (g=2.05), high spin Fe^{3+}(g=4.14 from transferrin) and (g= 5.85 from methemoglobin), low spin ferriheme complexes (g=2.21) and cytochrome (g=3.03) [75].

The figures above show that EPR spectra of cancer patients is similar to that of healthy individuals. This suggests that EPR technique cannot directly diagnose cancer. However, since it is able to detect free radicals and paramagnetic changes in the human body (blood and tissue) it may be useful for early detection of cancer/or malignancy. It may have a role in prevention of disease; however, it requires further developments.

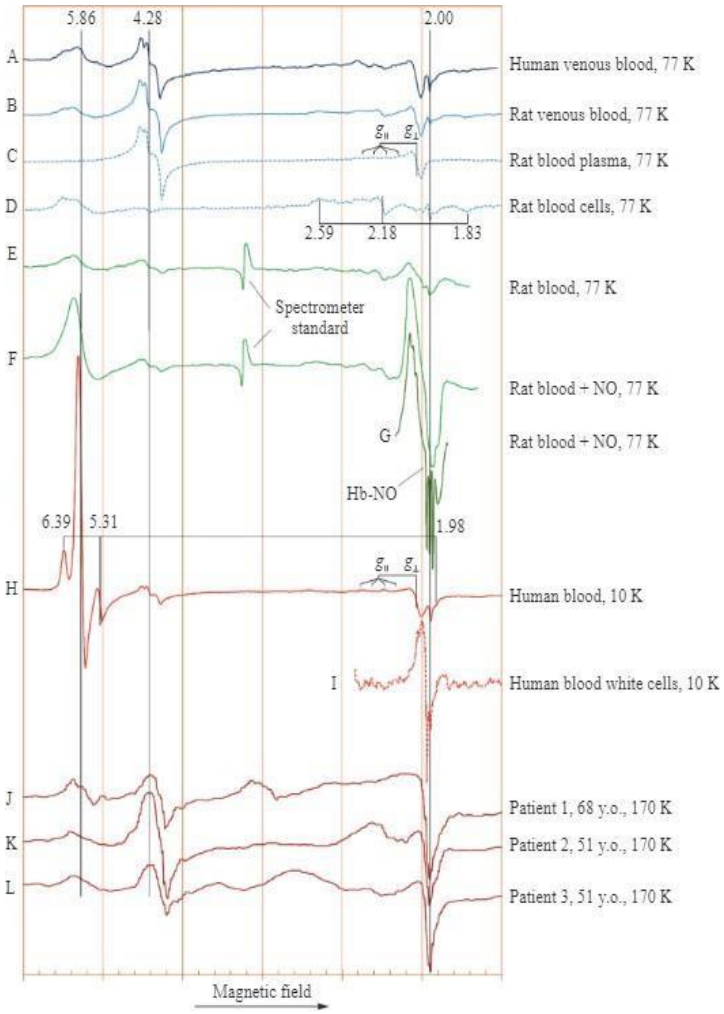

Figure 3.8 Group of EPR spectra from different studies [75]

Figure (3.8) shows different EPR spectra from several studies [76]. A and B show the similarities between human and rat blood, they are almost identical. C, shows the g at 4.28 and 2.05 are caused by plasma components. In D, g at 2.59, 2.18 and 1.83 are related to cell fractions of the blood, g at 4.28 is caused by high-spin ferric iron in transferrin. Cu^{2+} ions from ceruloplasmin show the signal g_1 =2.05 and g_{11} that shows four lines (difficult to distinguish). D and E resulted from different experiments and show consistent results. E and F illustrate the impact of NO gas inhalation prior to blood extraction, where the level of MetHb increased. The spectra also show a new EPR signal caused by the complex of NO with ferrous Hb, Hb-NO and shows in more detail in G. Moreover, H shows the spectrum of whole human blood like A, however the differences seen are due to measurement at different temperatures. The intensity of the ferric haem signal increased (g-5.86), compared to other signals, and two more lines appeared. Spectra I is of isolated white blood cells and can be attributed to non-heme iron complexes and signals of free radicals. It is similar to spectrum of activated microphages in other studies (microphage is a type of white blood cell, they are activated when the body is fighting infection). J-L are spectra of breast cancer patients showing signals of transferrin, ceruloplasmin, as well as external copper signals (which can be due to contamination, from the copper needle used [76].

Variability of EPR spectra is caused by individual physiological and biochemical characteristics, and the blood preparation method. This means that a long-term monitoring of the patient is likely to provide better indicator for cancer/malignancy development which facilitates early detection and enables examination of the blood (and individual differences) over time.

EPR is used as a detection and diagnosis tool for cancer patients. Spin traps are commonly combined with EPR in cancer studies to enable examination of the mechanism of chemical, radiation-induced, and hormonal carcinogenesis and their role in development of cancer. As well as investigating the differences between tumors, providing diagnosis, and assess the impact of medical treatment on malignant tumors [75] [76].

3.5.2 Iron ion complexes in blood

Tumors in animal studies are induced with certain known-carcinogenic compounds to enable examination of the specific-type spectra. Paramagnetic centers in humans" and animals" tissue and blood are molecules containing Fe^{+3} (transferrin and hemoglobin), Cu^{+2} ions in ceruloplasmin, and free radicals like ROS and others.

Figure (3.9) shows EPR spectra of a patient and a donor with colorectal cancer. The most prominent alteration is in g = 2.0-2.4 [77].

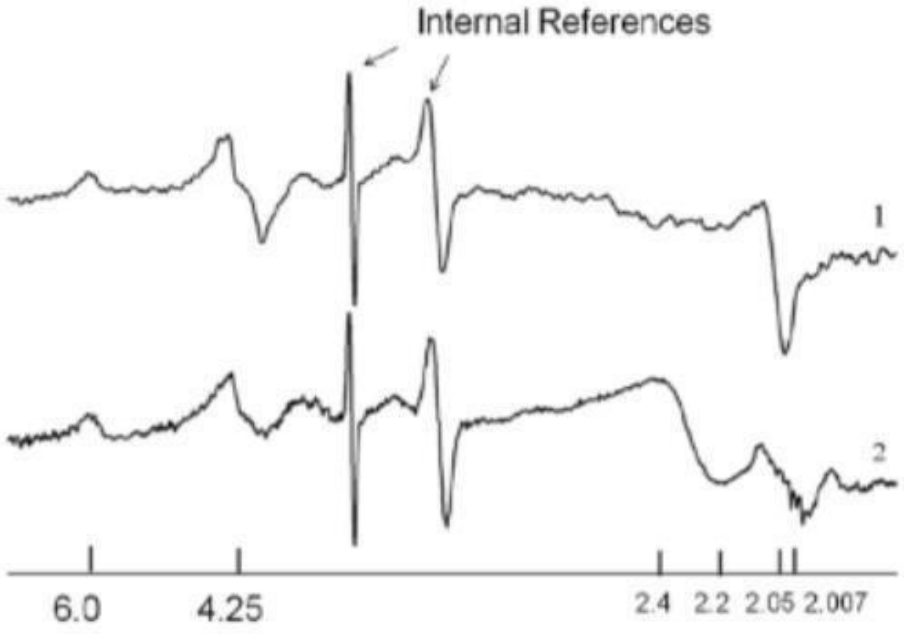

Figure 3.9 EPR Spectra of blood of healthy individual (1) and colorectal cancer patient (2) [77]

A triplet signal is typically seen in EPR spectra, which indicates pathological changes, it was observed in patients with carcinoma, sarcoma, and hepatoma tissues. It is due to the nitrogen interaction with iron ions in nitrosyl-iron protein complexes of hemoproteins and cytochromes. The triplet signal is an EPR marker of malignant tumor growth, the signal g iso= 2.007), it can be seen in Figure (3.10) [77].

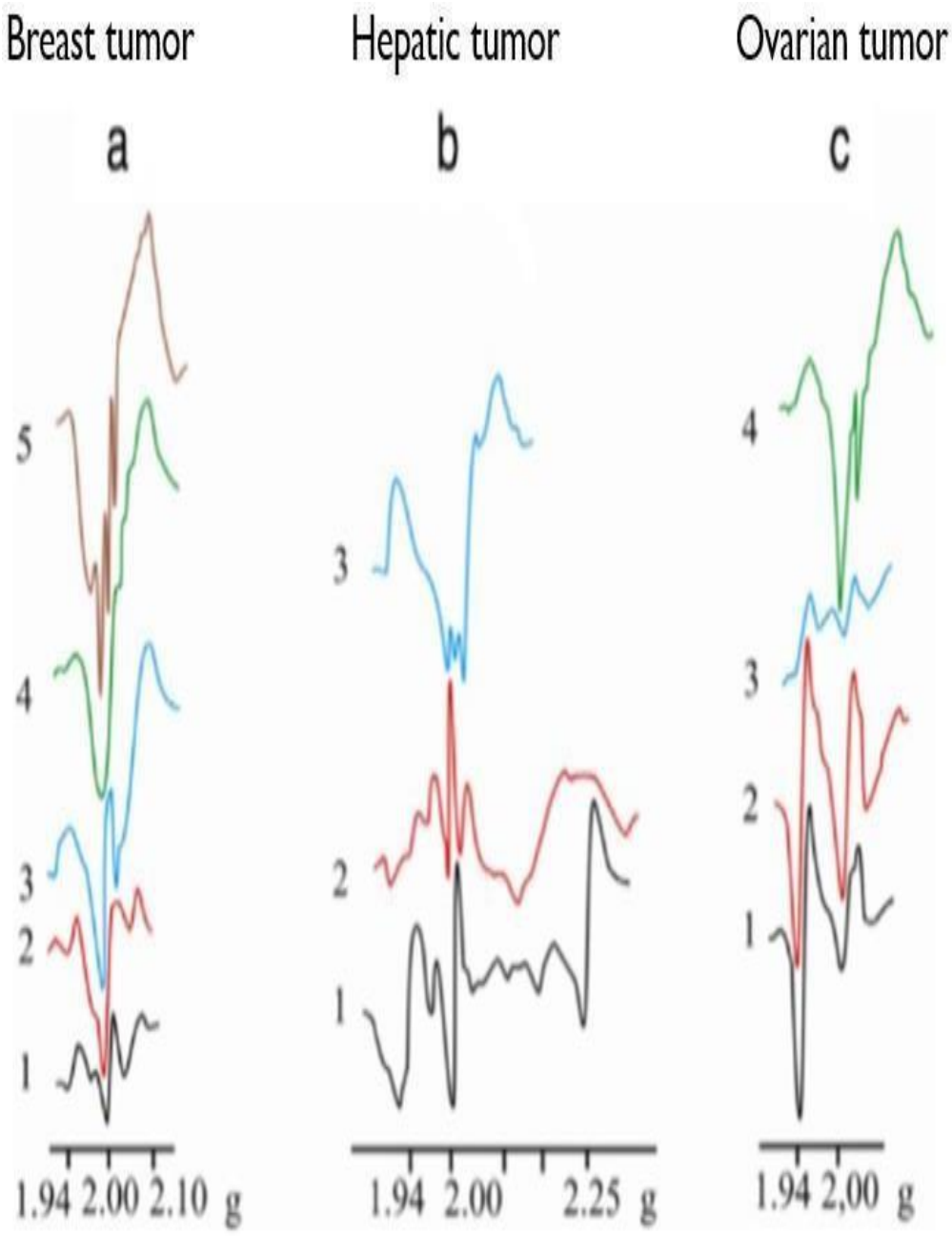

Figure 3.10 Triplet Signal in EPR Spectra of Blood Samples of Breast (a), Hepatic (b), and Ovarian (c) Cancer patients [77]

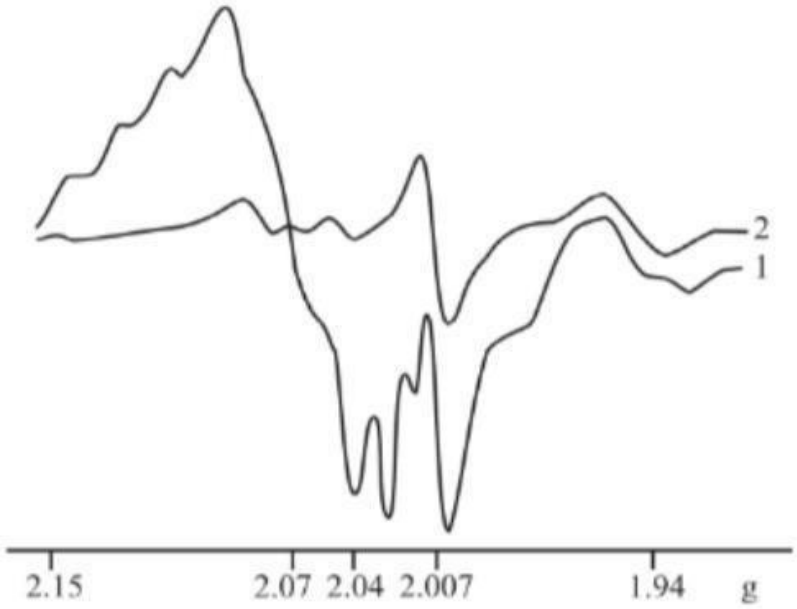

Figure 3.11 EPR spectra of lung tissue, Cancer (1) and Healthy (2) individuals [77]

Figure (3.11) confirms the detection of triplet marker in affected lung tissue in comparison with healthy lung tissue [77].

A study found it possible to diagnose oral squamous cell carcinoma by examining peripheral blood using EPR. Blood was extracted, centrifuged, and serum albumin was stored at -80 ^{0}C until analysis. Spin probe was used 16-doxyl stearic acid; due to the high attraction for albumin to stearic acid, leading to high binding (>99.9% of the spin probe to albumin). The samples were thawed for 2 hours prior to examination and incubated for 10 minutes at 37 ^{0}C. Modification to albumin peptides can be used as diagnostic indicators in early cancer stages.

Adding a fatty acid spin probe enables measurement of different albumin binding variables. The binding variables of the spin probe at different combinations of ethanol concentration is important to the accuracy of testing. Particularly for evaluating the structural and functional changes occurring after binding albumin and tumor proteins [78].

In an experiment 40 blood samples were collected, 20 of healthy volunteers, and 20 patients with melanoma. Immediately after collection blood was stored in liquid nitrogen at 77 K [79].

Measurement temperature 77 K, X-band, Bruker EMX-10 EPR spectrometer, operating at 9.4 GHz, Microwave power 20 mW, modulation frequency 100 kHz, second modulation amplitude 1 mT [79].

Figure (3.12) is illustrating EPR spectra of modified albumin binding capacity [80].

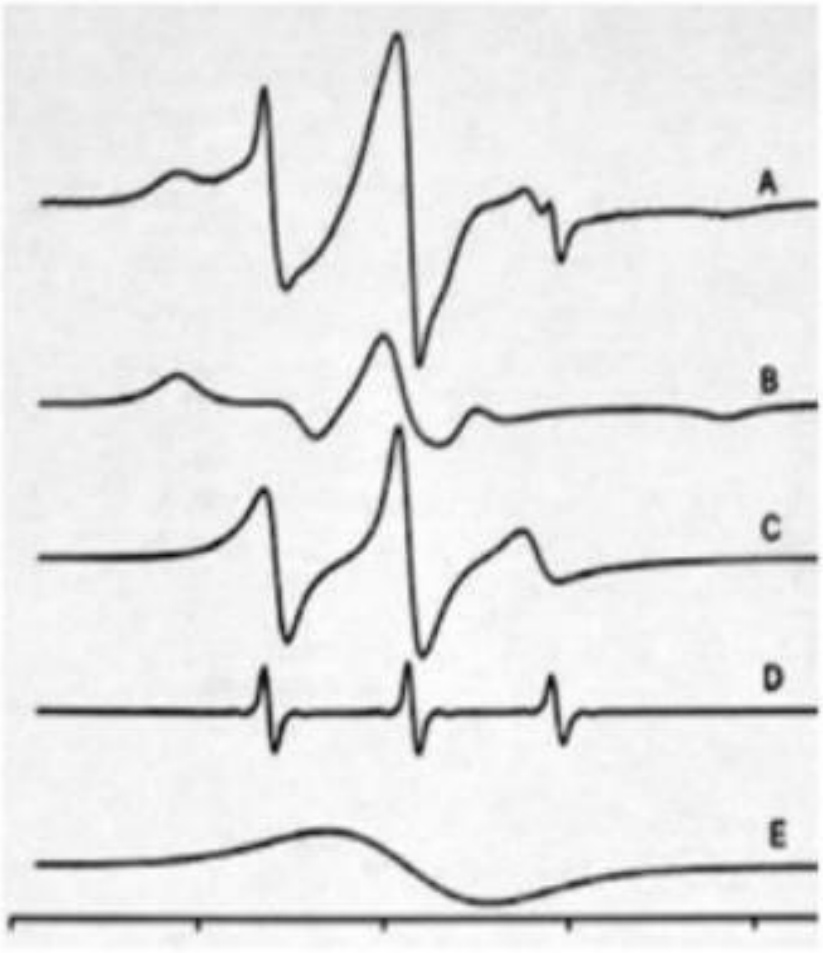

Figure 3.12 EPR spectra of modified albumin binding capacity(a) signals of fatty acid binding at sites 2 different sites (b, c) and unaffiliated fatty acid (d), and fatty acid molecules(e) [80]

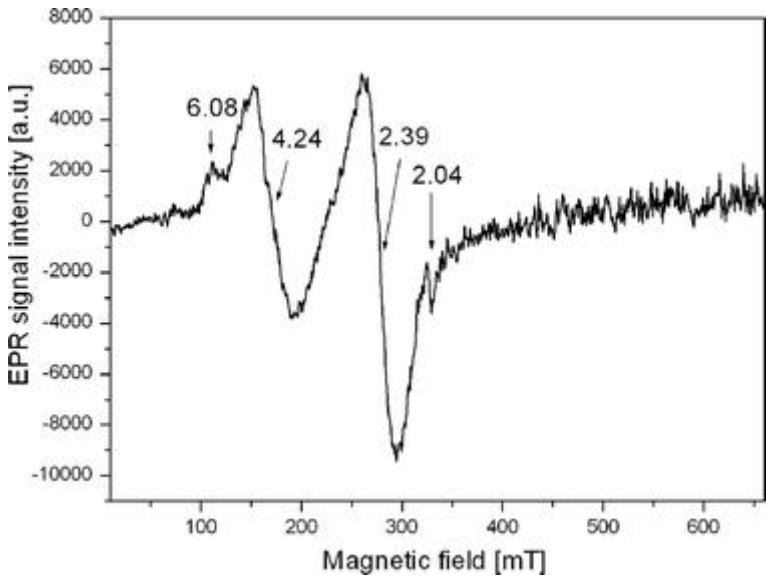

Figure 3.13 Blood EPR Spectra of Healthy Person [81]

Figure (3.13) shows signals of iron as transferrin and metHB and Copper as ceruloplasmin, as well as free radicals [81].

Figure (3.14) and Figure (3.15) are illustrating the EPR spectra of patient with melanoma of type 1 and type 2 respectively [81].

In healthy spectra higher concentration of paramagnetic species is observed, the signal g at 2.04 can be used to distinguish from melanoma patients" spectra, the signal is attributed to copper ions in the blood. While melanoma patients" spectra had different components, at signals 6, 4, 3, and 2.3 attributed to iron complexes and free radicals. The different groups of melanomas differed in blood iron levels.

Plotted data in figure (3.16) show a linear relationship between transferrin saturation and the signal g at 4.2 among the sample and among women independent of men, unfortunately limited sample number limited discriminating linearity for men data.

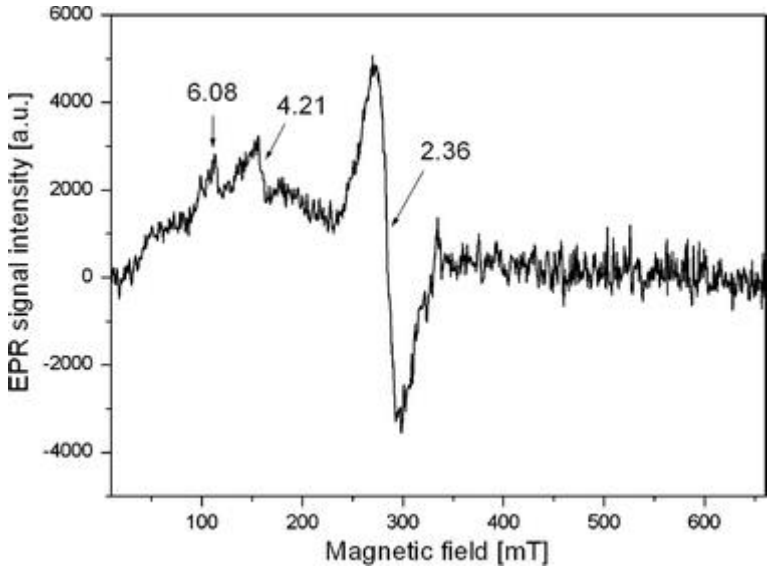

Figure 3.14 EPR Spectra of Melanoma patient blood type 1 [81]

Lowered level of iron in blood, on average 78 (μg/dl), whereas the norm median is 97 (μg/dl) in Figure (3.15) [81].

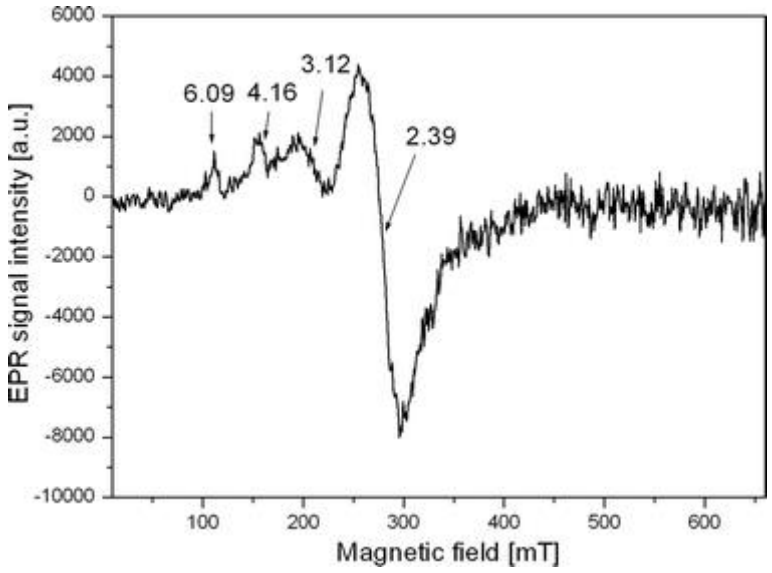

Figure 3.15 EPR Spectra of Melanoma patient blood type 2 [81]

Thus, the correlation of the iron ion concentration in blood and transferrin saturation with the amplitude of the EPR line at g = 4.2 is determined as seen in Figure (3.16) [81].

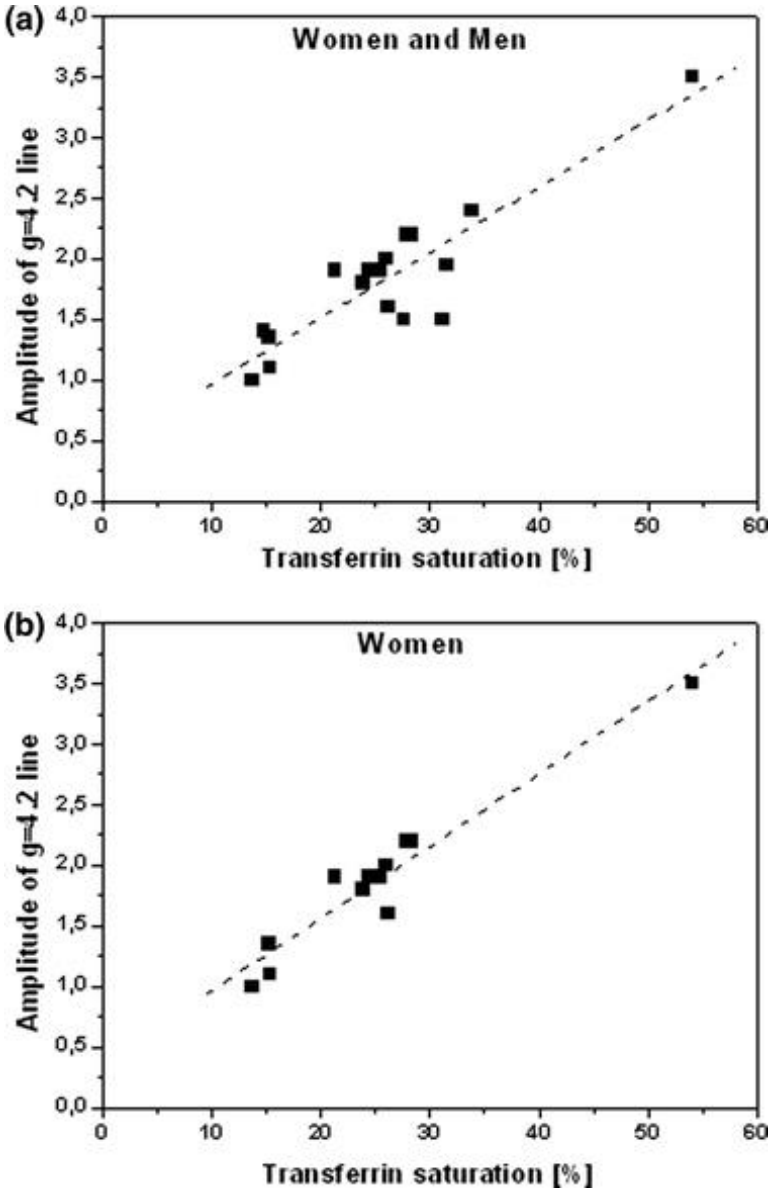

Figure 3.16: Correlation between Fe^{+3} and Transferrin Saturation [81]

Due to the small number of males in the study the correlation has not been determined. The analysis did not reveal the presence of free radicals, it suggested that the cause is their short

lifetime, requiring application of spin trap. EPR signals of healthy people show more types and higher concentration of paramagnetic signals than patients with melanoma. We may conclude that, in monitoring patients, changes to the amplitude of g-values, and decreased paramagnetic signals can indicate illness. The triplet marker can be a good indicator for malignancy.

3.5.3 Urologic cancer in anemic patients

Urologic cancer is that affecting the urinary system and male reproductive organs, which include kidney, bladder, ureter, penis, urethra, prostate, and testicles. A link between urological cancers and Anemia has been suggested in the literature [78].

Anemia is known to be associated with some types of cancer (not all), the incidence and severity of anemia depends on the type and stage of malignant-tumor progression.

The experiment used venous blood stored in quartz flask with liquid nitrogen. Spectra taken at 9.38 GHz and microwave power of 50 mW. Samples were divided into 3 groups: urological cancer patients (48 patients with bladder cancer, 46 patients with kidney cancer, stages I-IV, in pre-surgery period), control group 1: 39 donors from the blood transfusion unit (conventionally healthy) and 43 outpatients from non-oncology unit (anemia syndrome registered in 20% of the outpatients), and control group 2: 26 professional sportsmen, serum samples used to check correlation between transferrin measured by EPR and serum iron measured by absorption photometry (conventionally) [78].

The results are presented as plots in Figure (3.17) and Figure (3.18) to provide data associating levels of iron/copper and urological cancer [78].

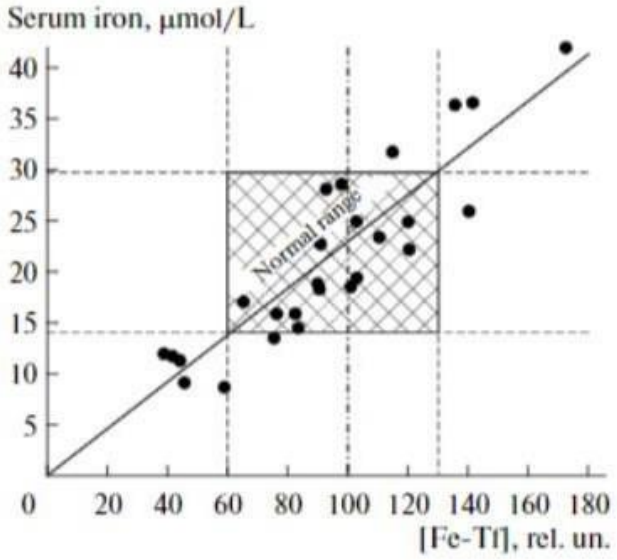

Figure 3.17 Correlation between Serum Iron and transferrin [78]

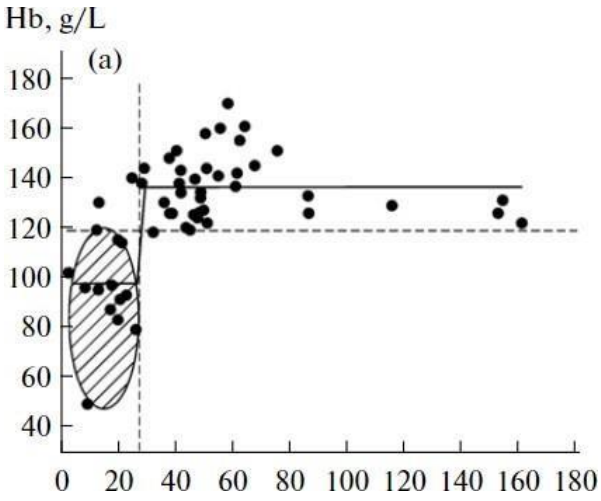

Figure 3.18 Relations of Blood Hemoglobin and Transferrin in Urological Cancer Patient [78]

Figure (3.19) is showing the relationship between the blood hemoglobin content and transferrin (Fe^{3+}) signal in venous blood from non-oncology outpatients [78].

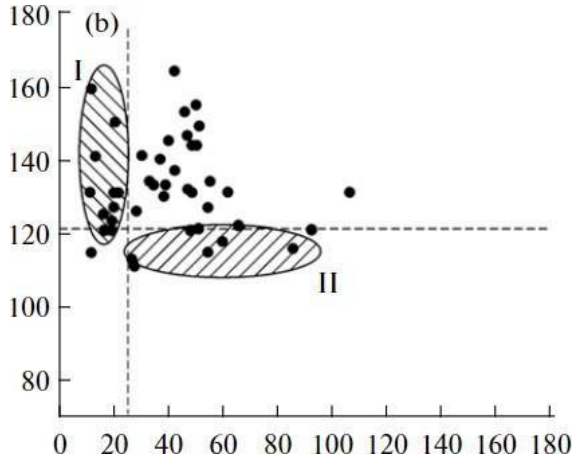

Figure 3.19 Relation of Blood Hemoglobin and Transferrin in non-oncology Patients [78]

Figure (3.20) is showing the relationship between the blood hemoglobin content and transferrin (Fe^{3+}) signal in venous blood from sportsmen [78].

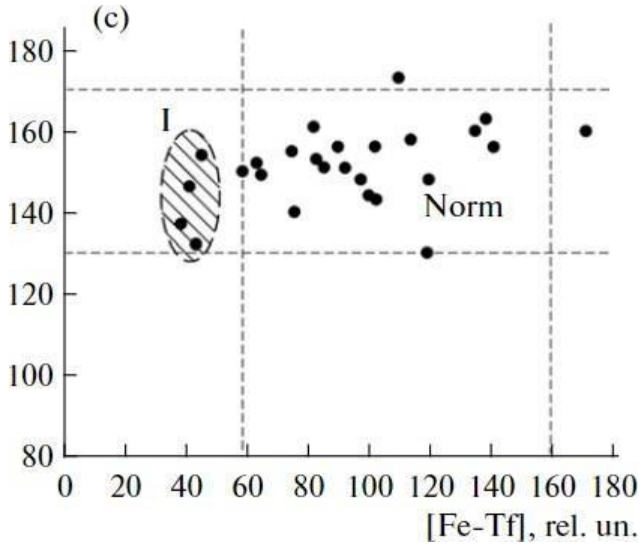

Figure 3.20 Relation of the blood hemoglobin content and transferrin (Fe^{3+}) signal in venous blood from sportsmen [78]

Missing data; data of serum iron measurement for urological cancer patients were not available as they are not endorsed by the state. Availably of the data could have provided a better point of view and enabled more sophisticated comparison.

This experiment aimed to estimate the paramagnetic centers in venous blood of anemia patients who also have urological cancer and used venous blood. Figure 3.16 shows correlation of serum iron and transferrin from sportsmen, it is apparent that about 40% of the values are above or below the norm, variation values is also substantial among the sample. It is important to note that sportsmen typically go under a lot of physical pressure and possible traumas on regular basis, therefore, their blood iron levels may fluctuate more than the average person. For most urological cancer patients figure (3.18) shows extremely low transferrin concentration that was barely visible in EPR analysis. However, no correlation between stage of cancer and transferrin level was established. Possible causes of low iron transferrin in urologic cancer patients can be related to immune response depleting iron-containing-compounds like hemoglobin. Another reason can be consumption of iron by the cancer cells particularly in stage I samples.

Figure (3.19) and Figure (3.20) shows no correlation between low transferrin and Cu^{2+} levels, similarly no correlation as found for other groups (b). Ceruloplasmin is an indicator of inflammation, increased ceruloplasmin- copper can be related amplified oxidative process as ceruloplasmin is utilized as antioxidant. Overall, decreased levels of transferrin iron can be a strong indicator for urological cancer, using EPR as a monitoring tool is superior to one-time measurement for detection. Moreover, testing for iron-transferrin, and copper-ceruloplasmin in anemic patients can enable early detection and diagnosis of urological cancer. Transferrin levels are impacted by extreme physical loads, thus individuals under high physical stress like professional athletes can have significant differences between routine measurements [78].

3.6 Liver Tissue EPR

The liver is an important vital organ that maintains the body's hemostasis through performing most of the required metabolic regulation and toxin filtration. It is similar to blood; in that it is affected by the major changes in the whole body. Using EPR to detect anomalies in liver tissue can facilitate early detection of disease and prevention.

The experiment: lyophilized (freeze-dried) sample of human liver, temperature range 4-300 K, X-Band spectrometer 100 kHz field modulation. Resonance absorption has been measured as a first derivative of the absorbed power versus magnetic field [82].

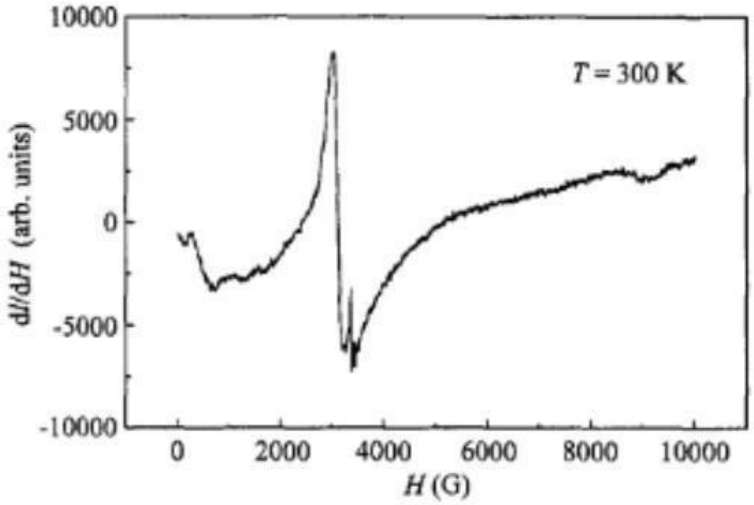

Figure 3.21 EPR Spectrum of Liver Tissue at Room Temperature [82]

Complex spectrum is given by liver tissue is illustrated in Figure (3.21). We can see g= 2.1 and 2, which are attributed to free radicals When we decrease the temperature, several spectral changes can be seen the broad signal at 2.1 becomes more asymmetrical, it shifts to the lower field and gradually broadens, the intensity decreases even more below 8 K, the free radicals signal at g= 2 disappears as can be seen in Figure (3.22) [82].

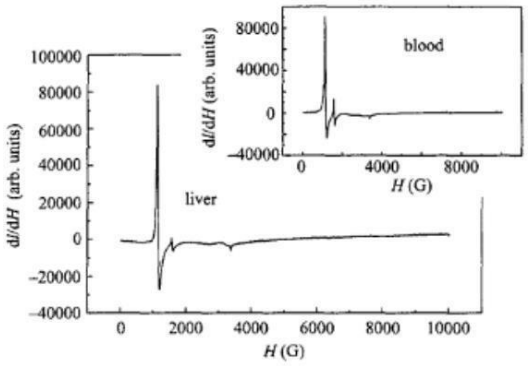

Figure 3.22 EPR Spectrums of Liver and Blood Samples at 4 K [82]

Two signals appear in this figure g at 5.8, attributed to Fe^{2+} ions from hemoglobin g at 4.3, intensity is relatively small; it is the typical signal of high-spin Fe^{3+} ions, attributed to nonheme iron (transferrin). In the liver spectrum g at 2.1 may be attributed to Fe^{3+} ions (ferritin) [82].

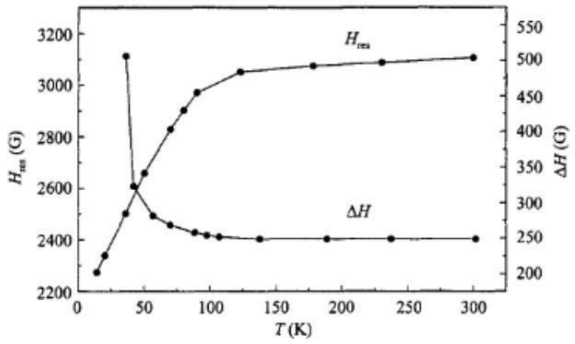

Figure 3.23 Temperature changes and Impact on the Field and EPR Line Width and Ferritin Nanoparticles [82]

Figure (3.23) shows the temperature dependence of the resonance field and linewidth of EPR signal of ferritin particles. Figure (3.24) shows the relation between resonance shift and EPR linewidth of ferritin nanoparticles plotted on double logarithmic scale indicating a linear relationship with a slope 3.03 [82].

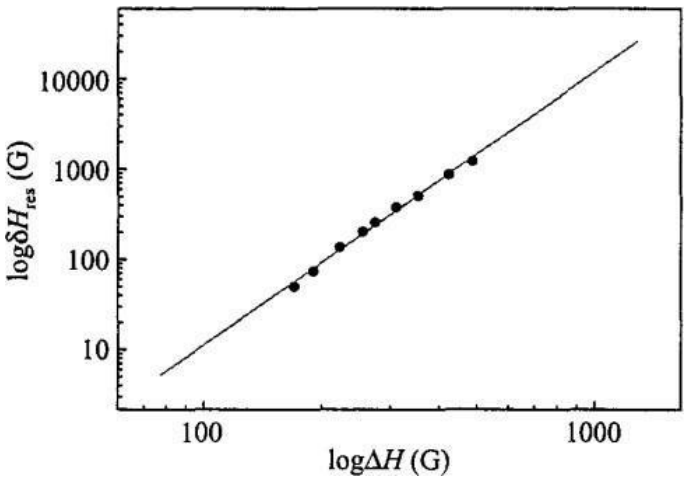

Figure 3.24 Relations between Resonance Shift and EPR Line Width for Ferritin Nanoparticles [82]

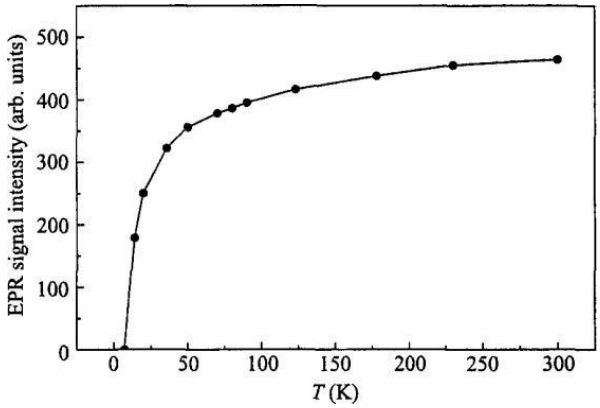

Figure 3.25 EPR Signal Intensity as Function of Temperature for Ferritin Nanoparticles [82]

Therefore, the broad signal at g at 2.1 arises in magnetic resonance spectra of human liver tissue is due to superparamagnetic behavior of small magnetic iron particles as shown in Figure (3.25).

The intensity of the line decreases as the temperature decreases, below 8 K this signal 2.1 disappears, reflecting the formation of antiferromagnetic phase of magnetically blocked particles.

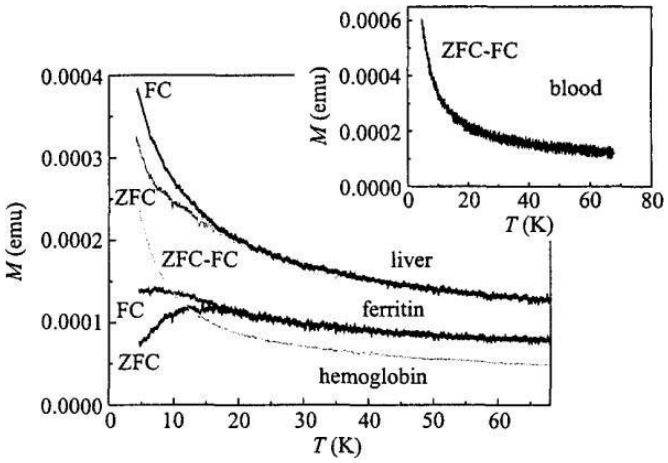

Figure 3.26 Temperature Dependence of Magnetization at the Applied Field 0.1 T for Human Liver and Blood [82]

Figure (3.26) shows the temperature dependence of magnetization measured in zero field cooled and field cooled (ZFC-FC) magnetization measurement curves split at low temperature, indicating the existence of the irreversible processes. These curves decompose into two main magnetic contributions. A reversible paramagnetic contribution originating from the Fe^{2+} ions of hemoglobin similar to that observed in the blood sample. Where both ZFC and FC branches overlap over the whole temperature range, irreversible magnetic contribution originating from the Fe^{3+} ions of ferritin, which shows a typical blocking process of an assembly of superparamagnetic particles. In the ZFC regime with increasing temperature the fraction of ferritin particles for which temperature is above their blocking temperature increases. Which initially favors alignment of the magnetic moments with applied field whereas a further increase in temperature enhances thermal fluctuations and result in reduction of induced magnetization. This concludes that two forms of magnetic ions exist in liver tissue, hemoglobin at 5.8 ferritin at 2.1, which are characterized by the irreversible magnetization processes [82].

Ferritin grains show antiferromagnetic order at low temperatures and transition into superparamagnetic state as temperature increases. Examining the EPR spectrum of blood present a lot of similarity to the liver tissue spectrum.

It is, therefore, safe to assume that the three-line signal indicating malignancy (seen in blood EPR) would be seen in liver tissue as well, particularly for liver-related- malignancy (hepatoma) Unfortunately, the current literature does not provide such experiment.

3.7 Bone marrow

It is the spongy soft tissue inside the bones, it generates new blood cells, it has many blood vessels and there are two types [83]. Red bone marrow contains blood stem cells, which can develop into RBCs, WBCs, and platelets, and yellow bone marrow is mostly fat.

Studying tumor affected bone marrow by EPR was done on 20 female rats of similar characteristics were given cancer (control group), 18 female patients (45-71 years old) with breast cancer in different stages (T2-3, N1, N2, M0) and 11 female patients (41-68 years old) with polytraumas (control group). Bone marrow samples were collected from the sternum (breastbone) and iliac crest. Then samples frozen in liquid nitrogen at 77 K. X-band EPR was used. Oxidation of the 1-hydroxy-2,2,6,6-tetramethyl-4-oxo-piperidine hydrochloride (TEMPONE-H) to the stable nitroxyl radical TEMPONE was used to trap superoxide [84].

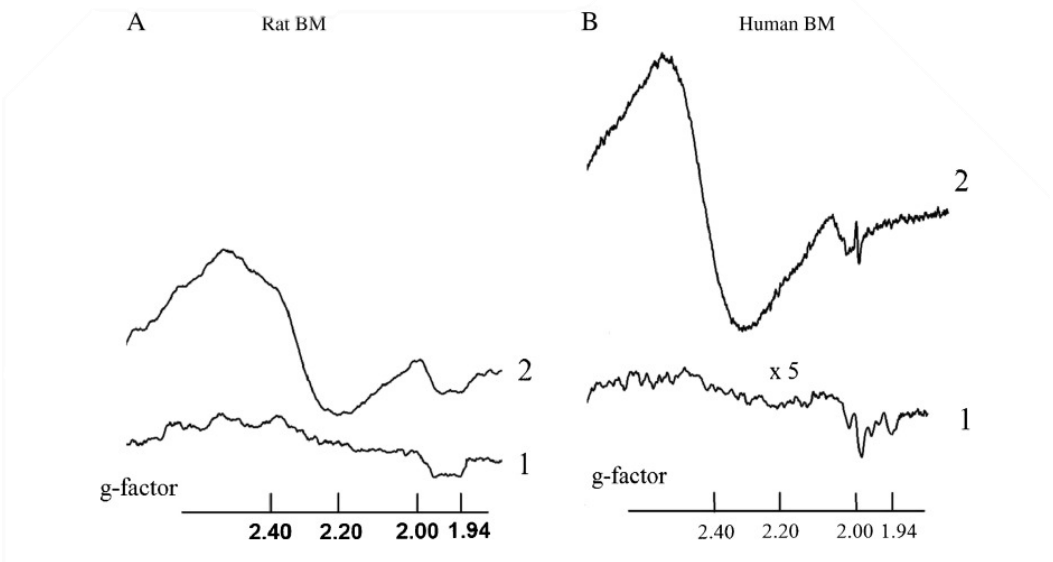

Figure 3.27: A-EPR Spectra of Healthy Rat (1) and Carcinoma and Breast Cancer Affected Rat (2) Bone Marrow. B-EPR Spectra of Healthy Human (1) and Carcinoma and Breast Cancer Affected Human (2) [84]

The rat bone marrow EPR spectra and human are shown in Figure (3.27), 1 is assigned to the healthy sample 2 is for carcinoma and breast cancer. The most intriguing in nature is an intensive broad signal at g ≈ 2.20–2.60 that appears in the tumor affected BMs. The signal with the similar spectroscopic parameters is to be reported arising "sometimes" in "a part" of the pathologically changed tissues attributed to iron complexes [84].

These are thought to be caused by loose or "free" iron loosely attached to molecules of phosphate, nucleotides, and amino groups. The free iron concentration is increasing in the earlier and latest stages of disease. This signal could serve as a measure to estimate the liable iron pool (LIP) and thus estimate the grade of tumor invasion.

Cells with increased LIP have higher concentration of ROS and thus increased oxidation, therefore, estimating and tracking the concentration overtime may be used to monitor tumor progression. The EPR signal with g ≈ 2.00 is usually ascribed to the free radical centers practically completely localized in mitochondria. Signal at g ≈ 1.94 is related to the activity of the iron-sulfur cluster N_2 of NADH: ubiquinone oxidoreductase (complex I) which is responsible for the proton pumping in this largest and is the most complicated enzyme in the electron transport chain (ETC) of mitochondria [84].

Iron metabolism by tumor cells, and mitochondrial dysfunction greatly participate in tumorigenesis. Bone marrow can reveal changes in its microenvironment through metabolic disorders and producing superoxide radicals in stromal cells (stem cells making the body"s connective tissue) [84]. The study presented suggests that based on the EPR spectra free iron (LIP) can be used as a tool to measure the influence of metabolism changes and mitochondrial dysfunction, as tumor metabolites can reprogram mitochondrial activity to increase the production of superoxide radicals.

3.8 Melanoma

3.8.1 Skin cancer

One of the most serious types of cancer, which can be easily observed in a skin examination by a professional. I wanted to explore the possibility of using EPR to detect superficial skin anomalies that may be malignant.

Melanoma is abnormal malignant skin growth, usually associated with increased levels of melanin. Early detection of skin cancer is vital to give the patients the best possible outcome. In early stages, the tumor can be resected (removed) and the patient would be completely cured. However, in later stages with tumor progression it gets deeper into the tissue and can affect the lymph nodes; making it difficult and at times impossible to remove.

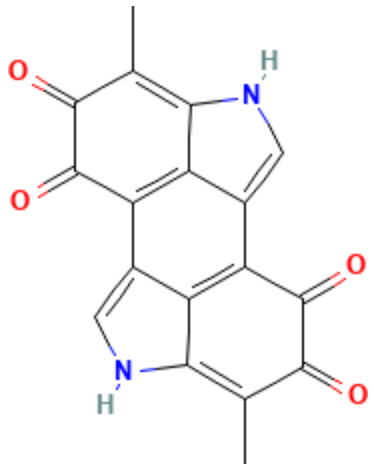

Figure 3.28 Chemical Structure of Melanin [79]

Melanin $C_{18}H_{10}N_2O_4$, is an irregular light absorbing polymer, it is responsible for the pigmentation (skin color) in most mammals. It is a cation chelator and can act as a free radical sink. Melanin has been seen as a potential target for anti-melanoma therapy since the 1990's [85] [79]. Some of its proprieties are ultra-violate light absorption, melanin also has redox and electron delocalization proprieties, which give rise to the semiquinone free radicals that can be detected

by EPR. Melanin is paramagnetic, which enables us to use EPR and detect its concentration in tumor cells thereby gauging its progression and improving patients' outcomes. There are two main types of melanomas: pigmented and non-pigmented [79]. The chemical structure of Melanin is illustrated in Figure (3.28).

EPR measurement was done in-vivo and non-invasively using clinical L-band spectrometer. Figure (3.29) shows the chamber and measuring loop used for in-vivo detection [86].

EPR signals were monitored in pigmented and non-pigmented melanomas during tumor growth. Pigmented and non-pigmented melanomas were induced in 5-week-old female rats. Non-pigmented melanoma subjects were the control group.

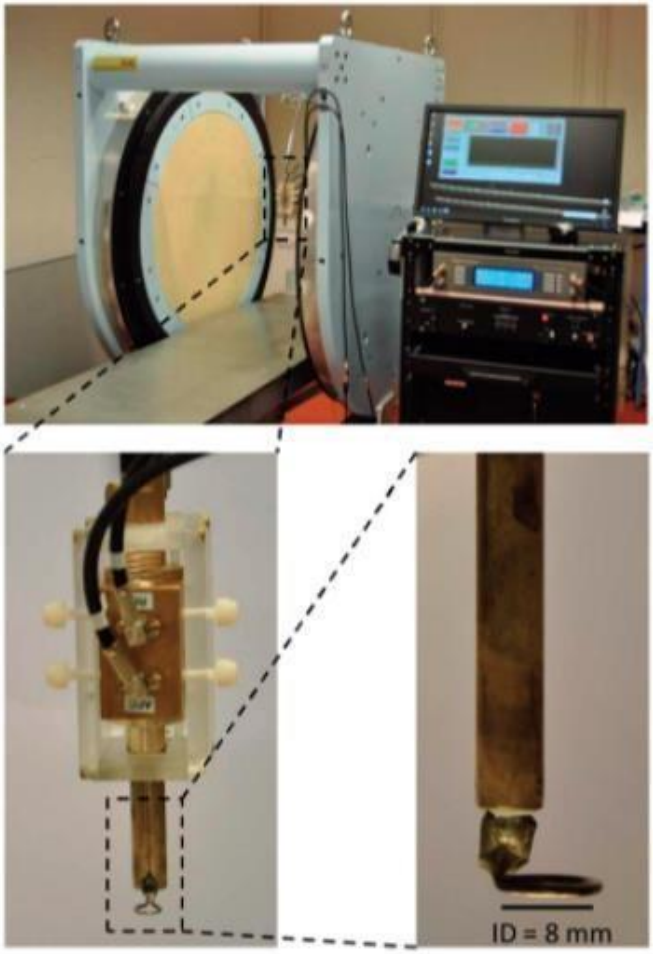

Figure 3.29 Clinical L-Band EPR Spectrometer [86]

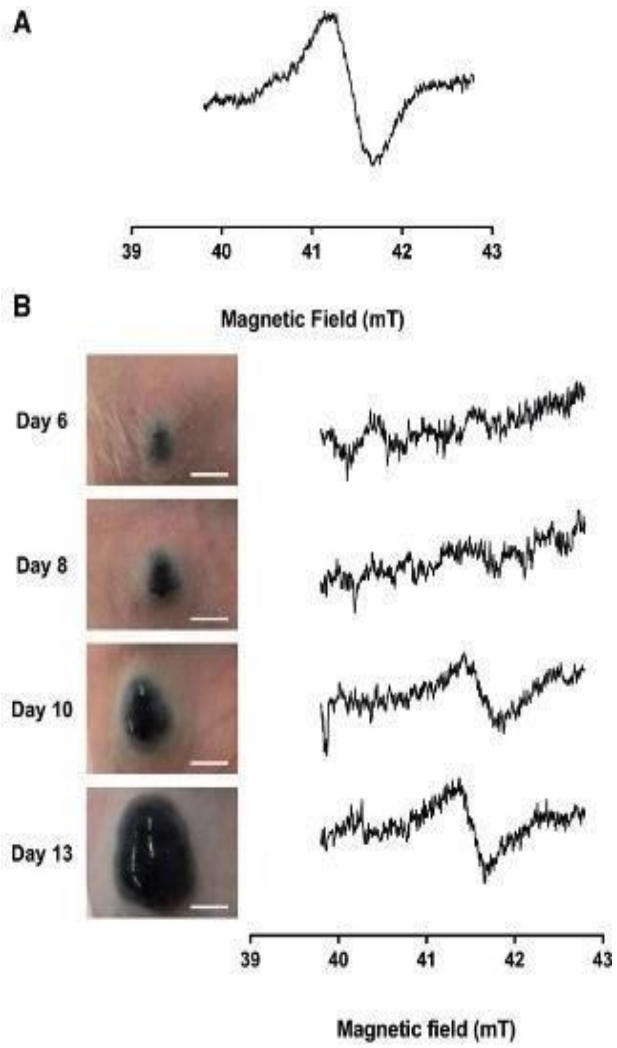

Figure 3.30: A-Typical Spectrum of Melanoma, B- Tumor Size and Corresponding EPR Signal for Tumor Containing Melanin [86]

In Figure (3.30), A shows the Typical melanin signal taken at day 10 after inoculation, the same signal is obtained from synthetic melanin B Shows the increase of EPR signal peak to peak amplitude during tumor growth between day 1 and day 13. In C, no signal was measured in non-pigmented melanoma subjects. The spectra show the correlation of tumor area or size and EPR signals detected. We can see that non-pigmented melanoma has no paramagnetic signals. Pigmented melanoma signals originate from the melanin radicals. The study has uncovered a

correlation between EPR signal of endogenous melanin radicals recorded in-vivo and melanoma size [86].

EPR is useful in detecting pigmented melanoma and estimating its progress. In the case of non-pigmented melanoma, EPR is not efficient; it doesn"t enable us to detect cancer nor its progress. Temperature measurement was not mentioned, as the rat was alive during measurement, room-temperature is assumed, this might have caused the lack of signal in non-pigmented melanoma as well. While the current findings indicate the validity of using EPR to detect skin cancer progression, it is vital that more research is done before this method is established in practice.

In my opinion, it seems that while EPR is very useful in detecting paramagnetic elements, it is superior as a monitoring tool, where a sample is repeatedly taken and measured to detect differences and account for individual norms. This will make early detection possible (as early as possible) giving patients the chance to have the best possible outcome. It is also imperative to expand our research to bigger sample sizes (human) and perhaps explore the variability of skin-color, lifestyle, and other possible factors, to ensure sensitive and accurate detection before this is introduced into medical practice. The unpaired electrons localized on the oxygen atoms in indol-5,6-quinone groups is the paramagnetic centers in the melanin polymer as shown in Figure (3.31) [86].

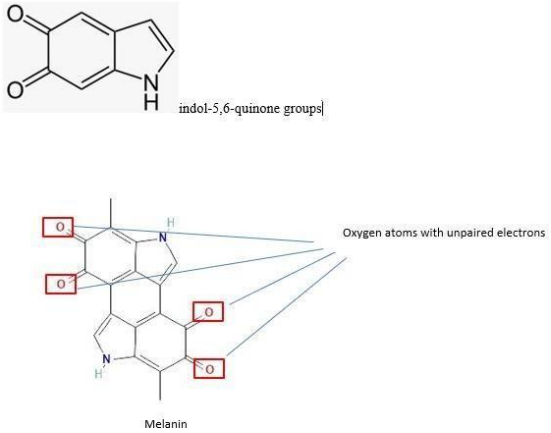

Figure 3.31 Paramagnetic centers in Melanin [86]

The skin is the most exposed part of our bodies to the harmful sun rays, which can lead to melanoma; a malignant increased production of melanocytes on the skin, which contain increased concentration of melanin. 1 in 5 Americans will be diagnosed with skin cancer by the age of 70 More than 9000 people are diagnosed every day, and At least 2 people die of skin cancer in the US every hour if detected early, the 5 year survival rate is 99%, and it can be cured, however it can spread and cause other tissue to be affected too like when it spreads to the lymph nodes and leads to lymphoma [87].

3.8.2 Melanoma Vs. Skin pigmentation mole (naevi)

Types of melanin; there are 3 recognized types of melanin; eumelanin: dark colors in hair, eyes, and skin. It has 2 types: brown and black, pheomelanin: pinkish pigment coloring the lips, nipples, and red hair, and neuromelanin: controls colors of neurons. The main focus of this research is eumelanin and pheomelanin (which concern melanomas and moles on the skin, most common type of skin cancer) as seen in Figure (3.32) [88] [89].

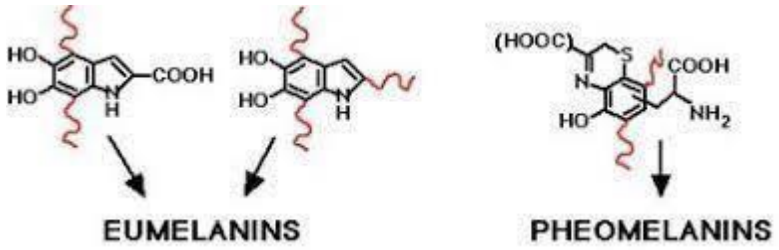

Figure 3.32 Chemical Structure of Eumelanin and Pheomelanin [88]

Ex-vivo studies using x-band EPR found differences in the amplitude of spectra for Eumelanin and Pheomelanin. Ration between the height of major EPR peak of Eumelanin and the height of the weak "shoulder" EPR peak of Pheomelanin; which shows differing proportions between the two

types. [Detection of pheomelanin is possible using x-band, but not currently doable using L-band) [86] [90].

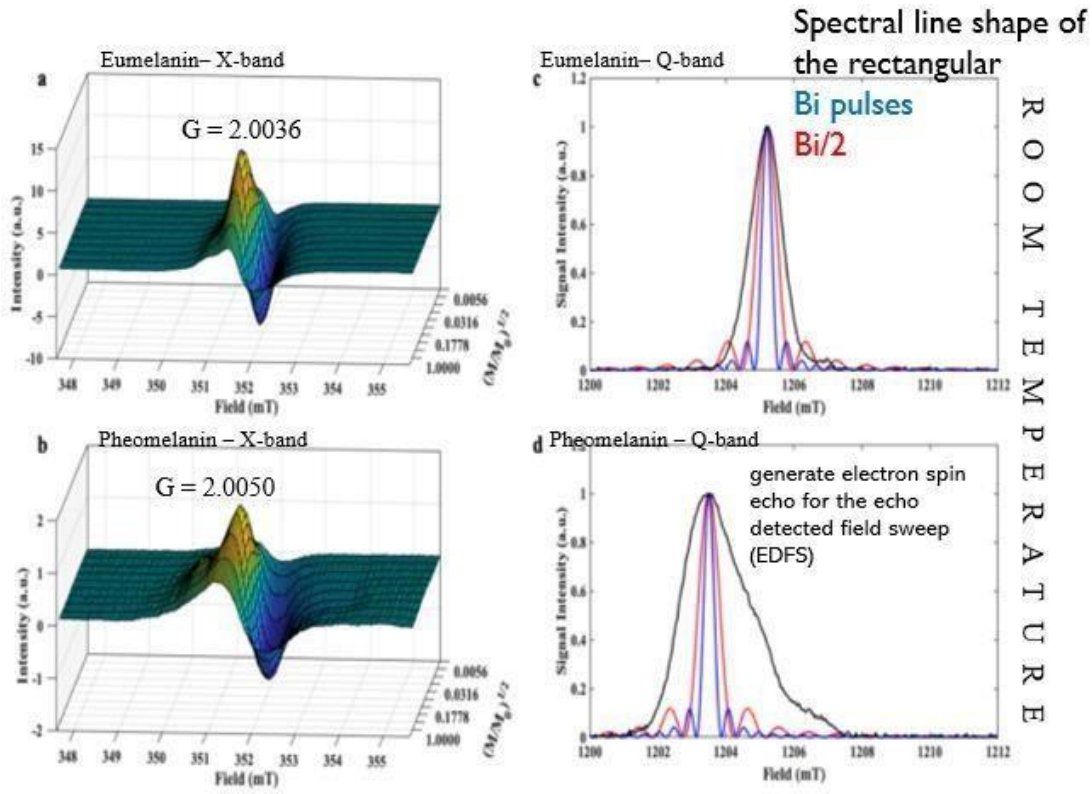

Figure 3.33 EPR Spectra of Eumelanin and Pheomelanin using X-Band and Q-Band Spectrometers [90]

The figure (3.33) shows EPR spectra recorded at increasing microwave power (maximum power value, M0 =144.5 mW), A Shows eumelanin spectrum (g iso = 2.0036 +/- 0.0002), free radical signal delta B = 0.5 +/- 0.1 mT at M= 1.46 mW, commonly interpreted as originating from the presence of carbon-centered g ≈ 2.0032) and semiquinone g ≈ 2.0045) free radical species, caused by hydration level and pH of the sample, respectively. (measured at X band 9.87) B-Pheomelanin spectrum (g iso = 2.0050 +/- 0.0002), free radical signal recorded higher g value ≈ 2.0050), broader line shape (peak to peak amplitude delta Bpp = 3.2 +/- 0.1 mT, which is attributed to the semiquinone free radical species (measured at Q band 33.8) C- And D – the red

and blue curves represent spectral line shape of the rectangular bi/2 and bi pulses respectively, to generate electron spin echo for the echo detected field sweep (EDFS) spectra acquisition [89].

3.8.3 Comparing nevus pigmentosus (moles) and malignant melanoma

Discriminating between moles and cancer is seldom possible with the naked eye, thus, a biopsy is usually taken to further examine the tissue and diagnose cancer. Using EPR to distinguish Melanoma offers fast, easy, non-invasive way to ultimately provide a diagnosis. Continuous wave electron paramagnetic resonance (CW PMR) uses a continuous microwave field of constant frequency is applied on the sample while magnetic field B_0 is swept until the resonance condition is met; it is recorded by observing the reflected microwave radiation. EPR imaging involves spatial imaging of the distribution of free radicals in vivo [91].

3.8.4 EPR experiment with Skin cancer

1 melanoma samples embedded in paraffin wax before EPR measurement, paraffin embedded nevus pigmentosus were used as control samples. Spin probe reagent 4-hydroxy-2,2,6,6-tetramethylpiperidin-1-oxyl (TEMPOL by GC) and 1,1-diphenyl-2-picrylhydrazyl (DPPH by HPLC). 9 GHz EPR spectrometer was used for measurement. Samples were cut to 3x4x3 mm to suit the 5 mm diameter EPR rode as in the Figure (3.34).

EPRI, imaging was done using Bruker E500 ELESYS system at room temperature, high sensitivity TM resonator added, system operated in x-band (9.6 GHz) and 100 kHz modulation frequency, water-cooled gradients allow magnetic field gradient up to 10 mT/cm along the X and Y axes. 2D images reconstructed from complete set of projections collected as function of the magnetic field gradient suing back projections algorithm Xepr software package [92].

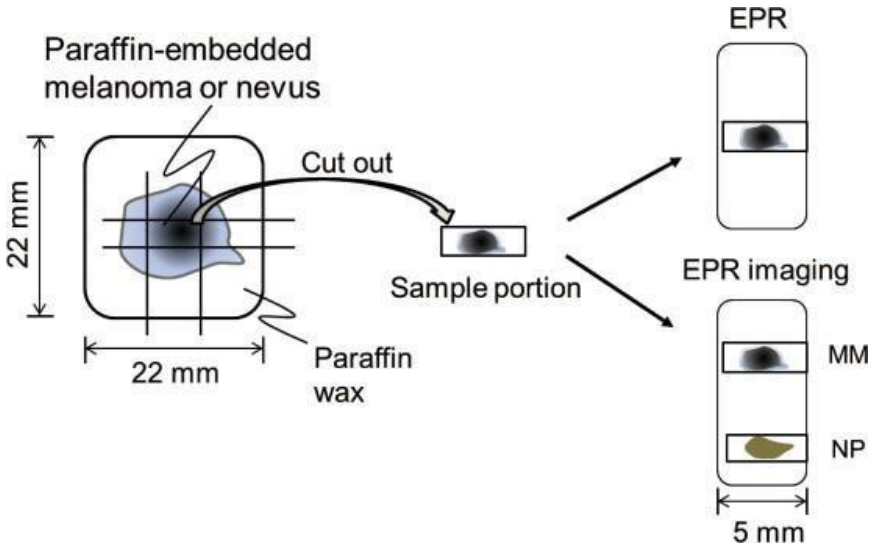

Figure 3.34 Schematic description of the experiment for EPR and EPRI [92]

3.8.5 The analysis of EPR and cancer

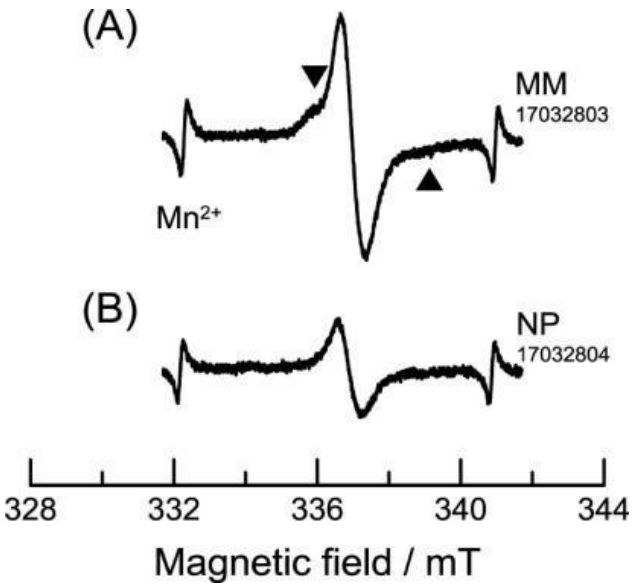

Figure 3.35 Typical Spectra of Melanoma (A) and Moles (B) [92]

The figure (3.35) shows typical EPR spectra of malignant melanoma (MM) and nevus pigmentosus (NP). Melanin radicals in g= 2.00 region. MM spectrum shows 3-line pattern with

peak-to-peak linewidth deltaHpp 0.65 +/- 0.01 mT (A). NP spectrum is similar but with deltaHpp 0.69 +/- 0.01 mT [73]. Statistical analysis suggests that NP tend to be broad. G value is approximately 2.005 for both samples. Unequal 3-lines pattern was observed in the Figure (3.36). Spectral pattern is similar to previously reported pheomelanin radicals.

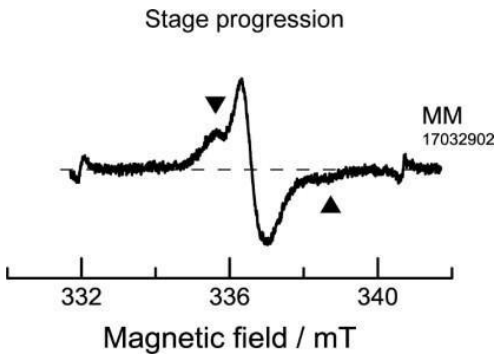

Figure 3.36 EPR Spectrum of Paraffin Embedded Melanoma Sample Showing Additional Signal of Pheomelanin-related [92]

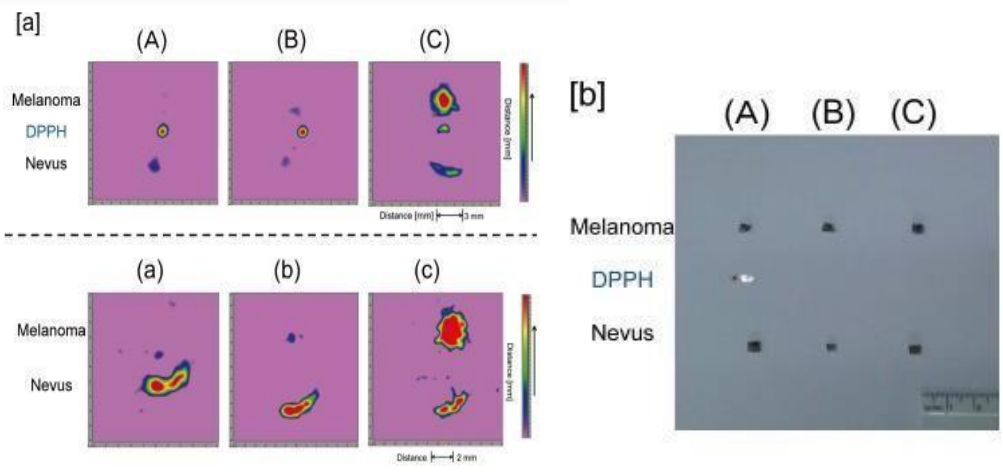

Figure 3.37 Melanoma and Nevus samples set by DPPH Radical, Stages of Melanoma [92]

As seen in Figure (3.37), the top row of images is melanoma and nevus set by DPPH, a known radical [10]. Melanoma stages correspond to the images a, b, c, stages: IA, IIC, and IV, respectively. The bottom row is without DPPH. We can see that while melanoma earlier stages show weaker intensity than nevus, in its later stages, melanoma has significantly higher intensity. Signal intensity in the figure is relevant to other samples measured. Measurement was done at room temperature [92].

Monitoring melanoma/mole can provide better outcomes than attempting to detect the problem when using EPR. This experiment [10] shows that a single image may not be enough to confirm diagnosis, a set of images repeated regularly would provide optimal measure for diagnosis. As seen EPR spectra of melanoma and nevus are different and can be distinguished from one another. However, the current melanoma research using EPR is relatively limited, more research is needed to ascertain the potential of EPR in the field and develop it to utilize in clinical practice. It is important to note that while racial differences exist in the risk of developing melanoma, studies do not address this difference, it may be useful to further research. It is established that melanin is protective against UV lights, thereby defending the skin against skin cancer caused by over-exposure to the sun, thus indicating the need to assess samples with different base-levels of melanin. Moreover, using X-band spectrometer is more beneficial than L-band; as it allows for clearer and more sensitive measurement. It is indicated that major developments can be done in the medical field using EPR and evidence-based practice, altering things from diagnosis to treatment, predicting that utilizing such scientific findings can improve treatment and outcome.

3.9 EPR and food analysis

Consumed food has a huge impact on human health; antioxidant and free radical content can contribute to the development of oxidative stress and by that deterioration of health.

3.9.1 Food Analysis

Decomposition of organic material like food is attributed to increased presence of free radicals due to oxidation. Oxidative deterioration rate has been associated with levels of antioxidants in the food, in its raw state. Antioxidant-rich food help in maintaining the balance between free radicals and antioxidants; thus, preventing development of oxidative stress [93].

While radicals resulting from oxidation are typically highly reactive, current evidence provides consistent reports of stable radicals in dry food, investigation into the cause suggest that it can be due to heat treatment of carbohydrates, oxidation of proteins, and the Maillard reaction [94] [95].

The Maillard reaction occurs when food containing sugar and amino acids undergoes heat treatment, resulting in a distinct golden-brown color, it is commonly seen in cooking and plays an integral role in determining the quality and safety of dairy products through the ultra-high-temperature (UHT) treatment [96].

3.9.2 Oxidation of antioxidants produces stable radicals in dry food

Polyphenols are the most abundant plant-based dietary antioxidants, they include flavonoids, phenolic acids, and others. Studies have shown that consumption of polyphenols decreases the risk of developing chronic disease and limits the impact of oxidative stress in humans, most notably in fighting cancer, diabetes, and cardiovascular disease. In the first experiment EPR was used to detect free radicals in food (licorice-flavored sweets) and non-invasively in the living rat bodies after ingestion [97]. Radicals detected in food and in living rats were stable. It is, therefore, shown that oxidation of polyphenols produces stable radicals [96].

Studying stable radicals using EPR provides quantitative measure, estimates the rate of oxidation, and provides insight into the impact of external influences like heat and light [94].

3.9.3 Bread

Bread is one of the most consumed stable foods around the world, it is typically made of wheat, however, other grains like, rice, rye, and barely are also used in bread making. All tested types of flour and grains of wheat and rye show a very weak and complex EPR signal, whereas baked bread shows a similar but more intense signal. The intensity of bread signals varies between samples, which may be attributed to the roasting and baking time, position in the bakery and time of testing the sample after baking (the signal intensity is halved after 10-14 days) [98].

Free radicals in bread are mainly caused by heat application as bread is baked, the concentration is estimated to be 50- 100 times higher in the baked bread, in comparison to the grains and flour. The crust of bread has recorded 2-5 times higher concentration than the middle-part of the same bread, which may be attributed to the Maillard reaction as the crust is directly exposed to the heat as the bread bakes.

3.9.4 Whole milk powder and formula

Milk is another stable that is consumed globally, milk formula has been an essential sustenance for infants everywhere. It is known to be a ‘‘very healthy‟ choice in the past, however, in recent years it is deemed unfitting to a healthy diet. Alas, using EPR to determine the antioxidant and free radical content can provide better understanding of the benefits/risks of consuming milk and formula.

Several processes contribute to milk oxidation; oxidation of fatty acids produces thiobarbituric acid, a lipid peroxidation marker that can be detected by EPR, lactose crystallization and browning, and slow and storage induced Maillard reaction (sugar and amino acids). These

processes are linked to moisture development, changes of water activity, production of antioxidants, and action of oxygen. Continuous EPR monitoring revealed increased free radicals' concentration, as well as the presence of two distinct radical species, "white radical" which requires oxygen and contributes to lipid oxidation, and "brown radical" that does not require oxygen and is present in the late stages of the Maillard reaction browning effect [99] [100].

3.9.5 Ginger

Ginger root has been known to have healing properties in many cultures, which has been scientifically confirmed. Ginger is rich in active antioxidants including compounds like 6-Gingerol, which is a major pharmacologically active component derived from ginger root [101].

In a study measuring the concentration of antioxidants in ginger have shown that it is rich antioxidants, or oxygen species scavengers.

Ginger was heated to 80 ^{0}C for 2 hours to explore the impact of heat on the concentration of antioxidants. After which EPR was used to detect antioxidant found that unlike other foods, although decreased, subjecting ginger to heat does not strip it of its antioxidant proprieties [102] [103].

3.9.6 Sterilized herbs

Due to the possibility of unhygienic practices in herbs farming and harvesting, it is advised that herbs are sterilized to be fit for human consumption. Using EPR to detect possible changes caused by the sterilization process can ensure safety of consumption and quantify the free radicals' content in herbs.

Investigations into the impact of sterilization on free radicals' concentration. An experiment was done to detect the difference in herbs free radical concentration before and after steam sterilization, it was found that sterilization produces a very small number of free radicals. Concentration of radicals in both samples was estimated at $\sim 10^{18}$ spin/g [104].

All in all, exploration of free radicals and antioxidants behavior using EPR enables understanding of the impact of external factors like heat and sterilization. Interestingly, this behavior seems different among food-material, prompting the need for more research to be done. Insight into the concentration of free radicals and antioxidants in foods and their behaviors when exposed to environmental conditions can assist in developing higher quality processed food products that sustain optimal taste and health benefits.

3.9.7 Coffee

An estimate of 2 billion cups of coffee are consumed daily around the world but the caffeine jolt is not the only benefit. Coffee has been associated with reduction of neurodegenerative disease, prevention of DNA damage, and in treatment of diabetes; as it lowers blood sugar levels [105].

While moderate coffee consumption has been linked to better cardiovascular health, high consumption of more than 6 cups per day may lead to high blood pressure, increase blood-lipids, and declining cardiovascular health [106] [107].

EPR was able to detect strong concentration of antioxidants in coffee, which had been reported to negatively correlate with the roasting time of coffee beans. On the other hand, studies show that free radicals were detected in roasted, ground, and instant coffee. Instantaneous EPR monitoring revealed that concentration of radicals increased during roasting, cooling also affects radicals" concentration. High flow air cooling increases radicals' concentration, while cooling with nitrogen or in low-oxygen environment has no substantial impact on detected radicals. Current evidence indicate differences in radical concentration can be based on type of coffee (e.g.,

Arabica, Robusta), roasting time, storage, and whether it is ground coffee or whole beans [106] [107] [108].

Longer roasting time increases radicals signal, storage within normal air environment increases radicals, unlike storing under nitrogen which prevents oxidation and thus has lower radicals' concentration. Stronger radicals signal is detected in ground coffee compared to whole beans and bean halves. Instant coffee has lower concentration of radicals than ground coffee, which may be attributed to the drying process, as moisture is removed, thus oxidation is decreased [108].

Further exploration of coffee has indicated the importance of investigating the concentration of radicals' differences among several types. Several reasons have contributed to making this decision, firstly, globally high coffee consumption indicates the possible impact it can have on health and global morbidity. Secondly, the research topic choice has been urged by the health impact of increased radicals' concentration. Specifically, that it results development of oxidative stress, which increases the risk of most chronic illnesses. Additionally, studies exploring coffee have not examined Arabic coffee, and due to insufficient comparable data, it was decided to include several prominent types to provide comparable results.

Over the years many controversies have been raised around coffee's benefit and harm scientific studies confirmed the positive impact of coffee on health like preventing DNA damage [108] [109], reducing the risk of neurodegenerative, cerebrovascular, and cardiovascular diseases [110]. Coffee has also been evidenced to have anti-tumor effect, thereby reducing the risk of cancer [101] [111].

Antioxidant and free radicals in Coffee have been investigated using EPR. That measured oxidants like 2,2'-azino-bis(3-ethylbenzothiazoline-6-sulphonic) acid (ABTS), 4-hydroxy-2,2,6,6-tetramethylpiperidine-1-oxyl (TEMPOL), 2,2-diphenyl-1-picrylhydrazyl (DPPH) and potassium peroxodisulfate (K2S2O8) [112]. Moreover, antioxidant properties of coffee components, caffeic acid and caffeine, against ABTS, DPPH, and hydrogen peroxide (H_2O_2) [112].

Coffee contains polyphenols which confirms its strong antioxidant content. Melanoidins are another antioxidant found in coffee, they are formed as a result of the Millard reaction throughout the roasting process [113] [114].

Moreover, roasted coffee contains high levels of acrylamide; consumption of which has been linked to increased risk of cancer. Coffee's acrylamide content has prompted limitations on consumption and fear of its link to cancer [115], however, it has been found that the concentration of acrylamide in coffee is not stable; it decreases over time [116] [117].

Coffee has to be roasted prior to consumption in all types; therefore, radicals' formation cannot be avoided. It starts to degrade the second it is roasted, as heat breaks down the soluble fats in the coffee.

Free radicals in coffee result from the heat-treatment of carbohydrates, including The Millard reaction during the roasting process, which impacts the coffee by toasting its sugar-content and depleting it natural moisture [118].

The Millard reaction occurs when food containing sugar and amino acids undergoes heat treatment, resulting in a distinct golden-brown color; it is commonly seen in cooking. It plays an integral role in determining the quality and safety of food like high-quality specialty coffee and dairy products going through the ultra-high-temperature (UHT) treatment [119] [95].

Exposure to light expedites the oxidation of coffee, it is also notable that cooling the coffee beans after roasting can have a substantial impact on the resulting concentration of radicals, the faster coffee is cooled the more radical content it would have [120].

Oxidation of proteins and fats in coffee can also be due to exposure to heat and storage conditions. Halving or grinding the coffee also results in higher oxidation rates, as it increases surface area that is exposed to oxygen, moisture, and light. Interestingly, oxidation of antioxidants produces free radicals in most dry foods like coffee. Coffee contains polyphenols include flavonoids, phenolic acids among others. Coffee is roasted polyphenols breakdown forms free radicals, resulting in increased concentration of radicals. Consumption of polyphenols

decreases the risk of developing chronic disease and limits the impact of oxidative stress in humans, fighting cancer, and other chronic diseases, however, as they oxidize, resulting free radicals contribute to the development of chronic diseases. Several paramagnetic centers exist in coffee, free radicals are the most prominent and available. There are many sources of oxidation in coffee, which vary between coffee types, roasts, brewing methods, and possibly other environmental factors. It is notable that roasting, grinding, storing, as well as brewing the coffee all cause an increase in free radical concentration. It is likely that steps taken in coffee planting and harvesting, as well as climate factors involved have an impact as well, however, it is difficult to standardize and quantify [96] [121].

Detection of radicals using EPR is determined by the g-value, comparing to the standard free radical DPPH, which has a g value of 2.0036. Real-time coffee monitoring using EPR has revealed increased free radical concentration during the roasting process [96]. Concentration of radicals in Arabica coffee was substantially higher than Robusta.

It is traditionally measured passively by measuring the oxidation rates and antioxidant activity (AA), methods of measuring AA include [118]: Oxygen radical absorbance capacity ORAC, Total radical trapping antioxidant parameter TRAP, Ferric reducing antioxidant power FRAP, Trolox equivalent antioxidant capacity TEAC (Randox), Using 2,2-azinobis(3-ethylbenzthiazoline)-6-sulforic acid ABTS and Thiobarbituric acid reactive substances TBARS to estimate oxidation rates. In all the aforementioned methods, antioxidant activity depends on multiple parameters like time, temperature, nature of substance, and concentration of antioxidant and other compounds. Antioxidant activity cannot be measured directly, thus measurement of oxidation is used as an indicator. Measurement is also based on long-living synthetic free radicals (like DPPH), antioxidant activity is synonymous with power, and both relate to concentration of antioxidants [118].

Methods like TEAC, TRAP, and FRAP are based on reduction reactions of free radicals or Fe^{+3} complexes. It is noteworthy that radicals used in measurement are synthetic and have significant differences to the radicals in the human body. Moreover, these methods are time-consuming and require a multitude of devices and detectors to show results.

Measurement using potentiometric method with mediator solution K_3[Fe (CN)6]/K4[Fe $(CN)_6$], was successful in measuring antioxidant activity in foods and beverages.

This study has examined the antioxidant activity in both Robusta and Arabica coffees and found that Roasting decreases the antioxidant content, thereby we can deduce an increase in the free radical concentration. On the other hand, it was found that antioxidants like melanoidins, are formed as a result of roasting [118].

The study [91] used 15 types of coffee, prepared as package instruction to be examined in its consumed-state using x-band spectrometer. Coffee was examined in real-time during the roasting process, as bean, powder, and prepared. Lyophilized coffee (freeze dried), and instant coffee (spray dried), results are shown in Figure (3.38) [108].

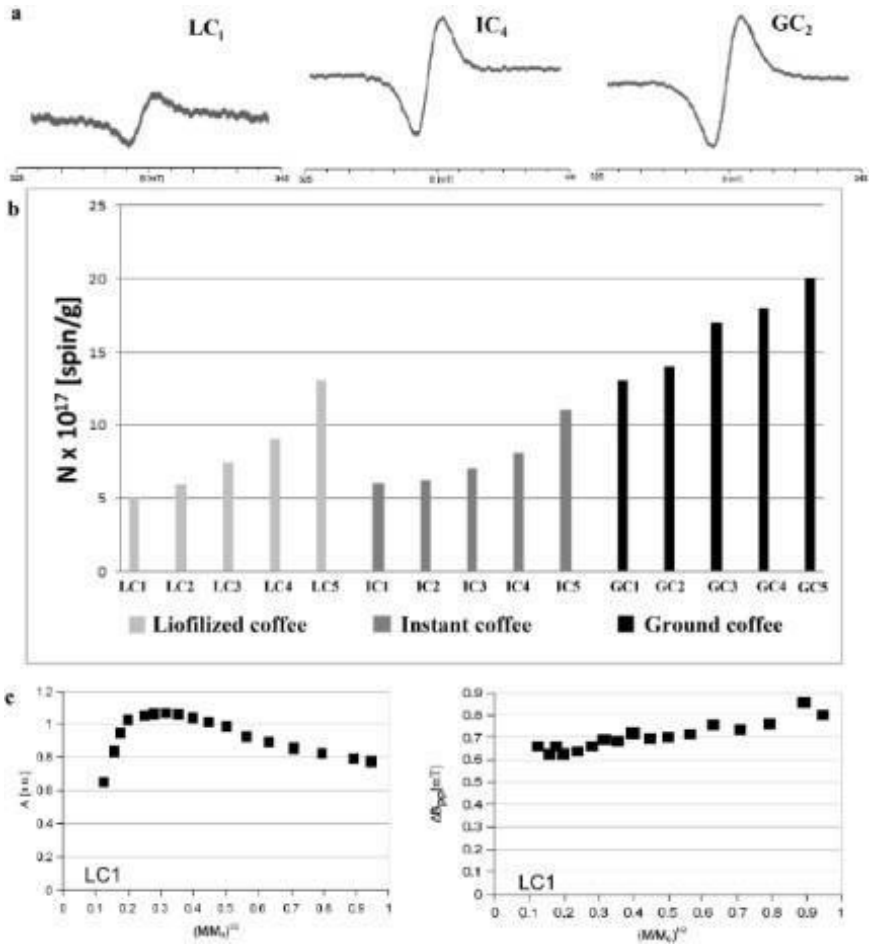

Figure 3.38 EPR data for the 15 samples. A- The EPR spectra were measured at room temperature. B – comparison of free radical concentration of the 3 different groups (of samples): lyophilized (LC1), instant (IC4), and ground (GC2) coffee. C- Influence of microwave power (M/Mo) on amplitude (A) and linewidths (DBpp) of the EPR spectra of lyophilized LC1 coffee sample [108]

This second experiment [108] uses coffee beans rather than other preserved coffee, using single origin coffees in their original state (not ground, nor freeze dried or preserved). The samples used are from: Ethiopia, Brazil, Peru, India, Colombia, and Robusta beans. Measured at room temperature, results are shown in Figure (3.39).

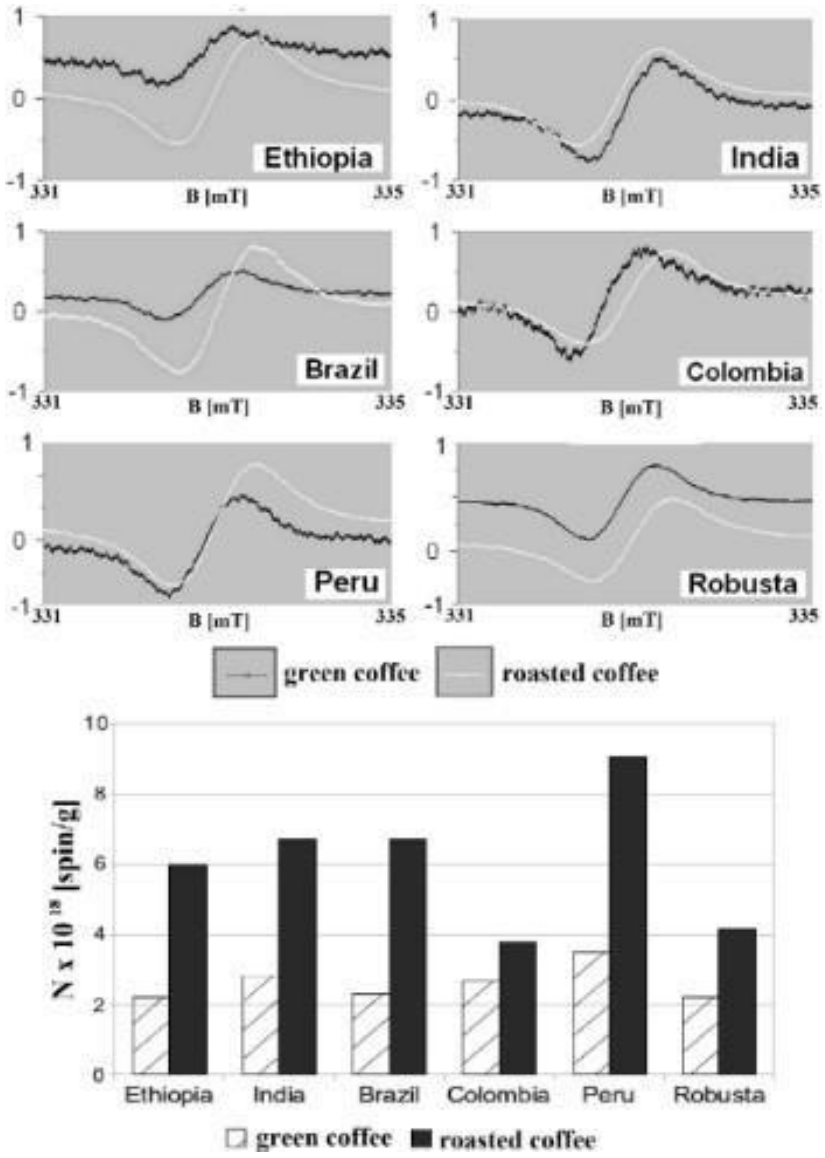

Figure 3.39 EPR spectra and radical concentration for the examined 6 different green and roasted single-origin coffee samples, measured at room temperature. The samples originate from: Ethiopia, Brazil, Peru, India, Colombia, and Robusta [108]

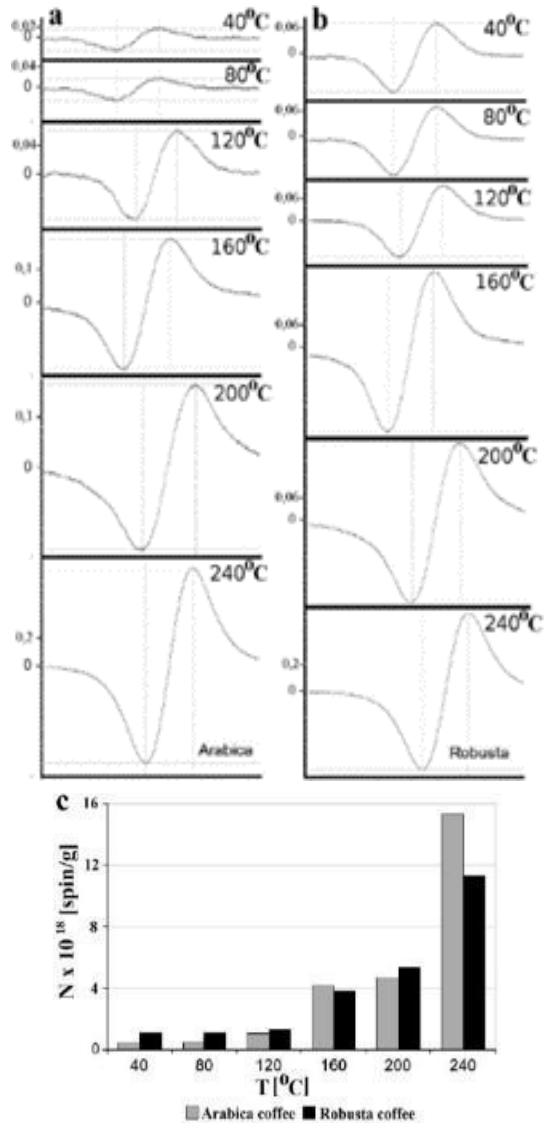

Figure 3.40 EPR data for the examined coffee beans roasted at different temperatures (A-Arabica, B-Robusta) at room temperature. B – induction of magnetic field. C- Free radicals" concentrations (N) in Arabica and Robusta beans roasted at the indicated temperatures [108]

Figure 3.40 shows a comparison between Arabic and Robusta coffees showing EPR spectra and radical concentration of both, roasted at the indicated temperatures, measured at room temperature. It is evident that higher roasting temperatures yield higher concentration of radicals [108].

The study concluded that free radicals in coffee beans increase when roasting, commercially available coffee products contain about the same number of radicals as roasted beans (10^16-10^18 spin/g). Interestingly, the concentration is higher in coffee ground than in instant and lyophilized coffees. Origin of coffee was also found to have an impact on free radical concentration, coffee beans from Peru had the highest concentration [108].

Another study [122] examined coffee in-situ, measuring radicals and EPR spectra of the coffee roasting process.

Spectra a in the figure 3.40, shows the weak signal of radicals in green coffee beans (g= 2.0053) which decreased during the early stages of roasting spectra a-c. a progressive increase was seen in later stages in spectra f-h with a g value of 2.0039, which shows that the increase resulted from the roasting process.

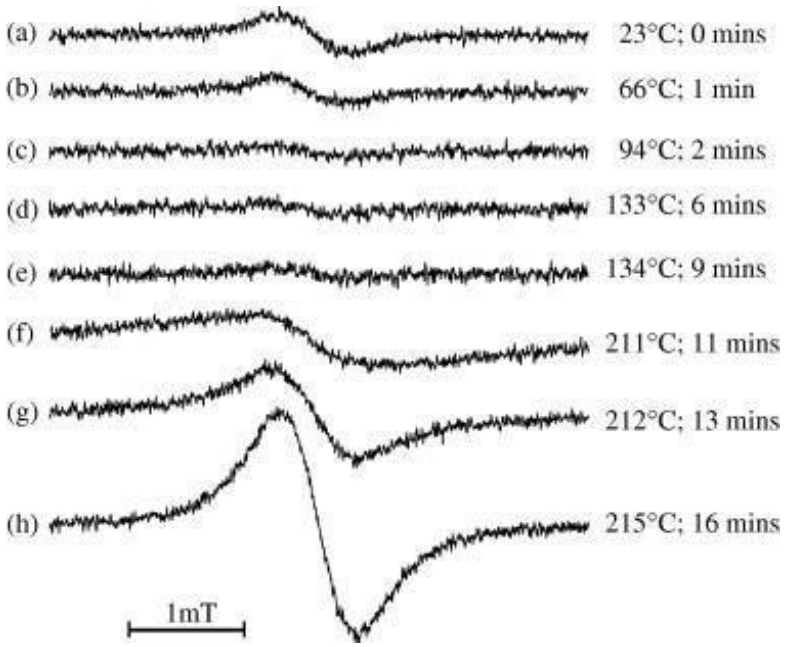

Figure 3.41 EPR spectra of Robusta half-bean roasted in air at the indicted times and temperatures [122]

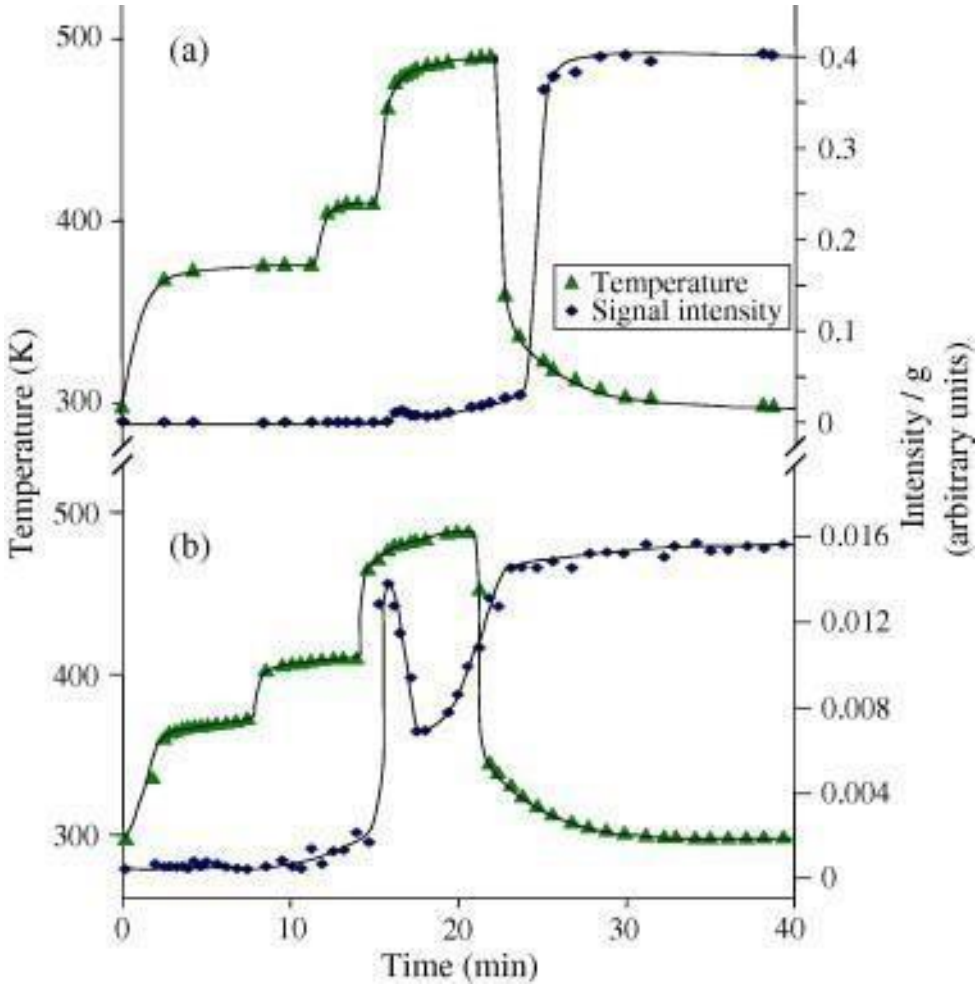

Figure 3.42 Variation in intensity of the free radical EPR signal as a function of time and temperature during the roasting of a Robusta half-bean (a) in air, and (b) in N_2 atmosphere [122]

The complete set of results showing the variations of spectral intensity with time and temperature are summarized in Figure (3.42) showing Robusta coffee signal variation and Figure (3.43), showing Arabica signal variation.

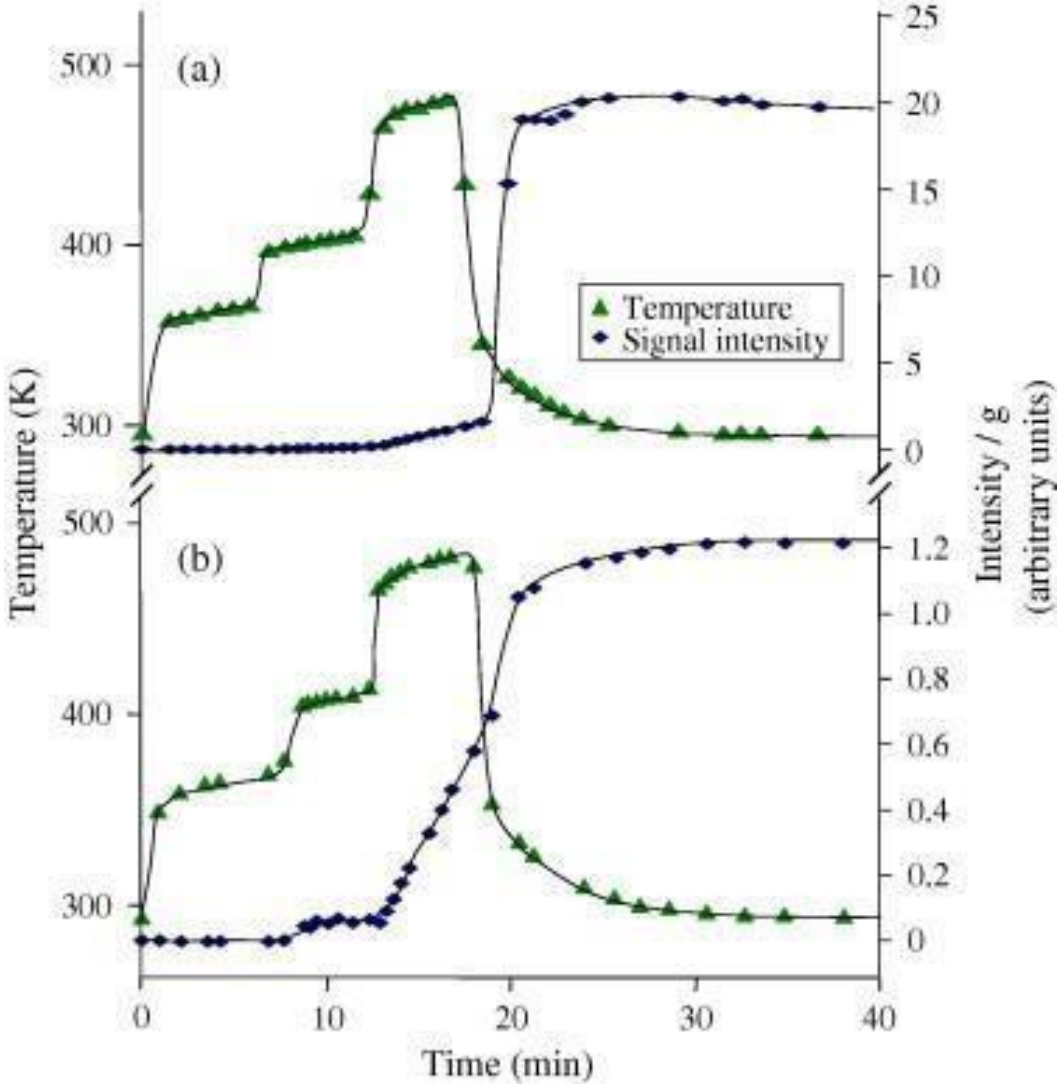

Figure 3.43 Variation in intensity of the free radical EPR signal as a function of time and temperature during the roasting of an Arabica half-bean (a) in air, and (b) in N_2 atmosphere [122]

Free radical signals were in the 5% range for both Arabica and Robusta (6% Arabica, 3.8% Robusta) While similar results have been found, it is clear that variation exist depending on origin, species, roasting time, and possibly other factors. A small increase in radical concentration during the cooling process is attributed to changes in spin-lattice relaxation processes [122].

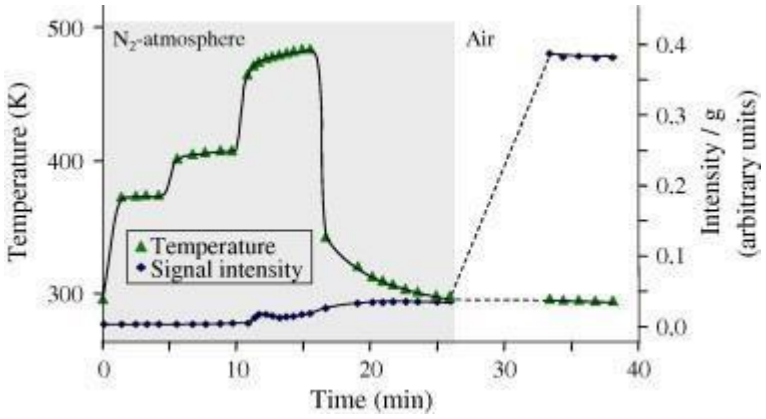

Figure 3.44 Variation in intensity of the free radical EPR signal as a function of time and temperature during the roasting of a Robusta half-bean in a N_2 atmosphere and then being exposed to air during cooling [122]

Samples roasted under N_2 and cooled in air showed a substantial increase in radical concentration as per the Figure (3.44).This study shows that EPR is able to monitor the concentration of free radicals in samples and discern variation through time. It is noted that atmospheric factors may have contributed to the variation of EPR signals, particularly between Robusta and Arabica, as they tend to be grown in different areas, and are examined under different circumstances. Samples roasted in air (both Arabica and Robusta) had significantly higher concentration than those under N2, which may be due to higher oxidation rate in normal air [122]. Along with free radicals and antioxidants, coffee contains other paramagnetic centers like Fe3 and Mn2, in lower concentrations, which can be quantified by EPR spectroscopy [119].

While coffee has been studied extensively, no studies were found comparing the free radical concentration of Arabic coffee and American coffee. Arabic coffee is different in roasting, mix, and preparation, which may significantly impact the concentration of radicals and antioxidants, lending it different health benefits than regular/American coffee. Thus, I have decided to examine coffee and assess the free radical concentration in different types. This study will aim to provide a comparison between several coffee types and estimate the free radical content of each.

CHAPTER 4

METHODOLOGY

4.1 The setup

Oxidative stress is now believed to cause much more damage than previously assumed; therefore, investigating the concentration of free radicals in commonly consumed foods could make an important positive impact to one's life. Consumption of foods with high free radical concentrations is believed to enhance the oxidative stress level in an individual [123].

Arabic coffee is consumed throughout the world, yet there are not any reports of its free radical concentration. The study described here investigates the free radical content of Arabic coffee and compares it to the results of this and other investigations of other types of coffee. This may help identify which coffees may contribute to oxidative stress.

For this experiment, 7 samples were investigated: green Arabic coffee beans, and home roasted as it is traditionally done with the addition of cardamom, Arabic coffee grounds, Espresso, American, European, and Turkish coffees. The main focus of this experiment is to assess the radicals' content and compare among the different types.

Arabic coffee is indigenous to Yemen, it is small, hard, and olive-green in color, known sub-types include Mocha, Khawlani, and Harari coffee. Harari also comes from Ethiopia and is one of the most expensive types of coffee in the world [124]. The level to which coffee is roasted depends on the region ranging from blonde to dark roast, however lighter roasts are more popular. Coffee is prepared by mixing it with spices like cardamom, and other, it is ground and mixed with water, then boiled for about 15 minutes before it is served.

Coffee types were chosen based on popularity, amongst which Arabic coffee was prepared traditionally, starting with green beans, home-roasted, and ground. The samples were then shipped from Bahrain to Arizona State University, to the User Facility in the school of molecular science laboratory.

Samples had been purchased from the same supermarket in Bahrain, with close expiry date to avoid effect of storage and usability. The coffee was studied directly as a pure solid.

Samples were cut, weighed, and placed in EPR quartz tubes for measuring, as quartz has minimal levels of paramagnetic impurities. Each spectra used the same weight-sample, as illustrated in Table (4.1).

Table 4.1: The samples of EPE experiment

Sample	Type	weight (gm)
1	Turkish Coffee	0.014
2	Espresso Coffee	0.02
3	European Coffee	0.018
4	Ground Arabic Coffee	0.03
5	American Coffee	0.02
6	Roasted Arabic Coffee	0.01
7	Green Arabic Coffee	0.018

4.2 The spectrometer

The spectrometer used in this study is Bruker ELEXSYS E580 as illustrated in Figure (4.1). It can work using multifrequency, from X to S, L, and Q bands. It also includes SpinJet Arbitrary

Waveform Generator which enhances sensitivity and selectivity, with an amplifier that provides an exceptionally wide detection bandwidth of 1 GHz. The spectrometer offers FT-EPR and Electron Spin Echo techniques to detect EPR spectra and spin relaxation times. It enables measurement of spin density distribution ad distance through miniscule interactions between electrons and nuclear spins, as long as long-distance ranges by dipolar coupling between electrons. It also facilitates measurement of correlation and exchange rates and laser triggered experiments to assess chemical reactions, seen in Figure (4.1) [125].

Figure 4.1 Bruker ELEXSYS E580 [125]

4.3 Measurement

The samples were measured at both room temperature (298 K) and low temperature (106-113 K) in a Bruker ELEXSYS E580, Billerica, Massachusetts, United States. Several microwave power

levels were used to determine under which conditions the EPR response became saturated; 1 mW, 0.25 mW, 0.016 mW, 0.06 mW, and 0.004 mW. The A.C. magnetic field modulation was carried out at 3 different levels, 10 G, 5 G and 3 G. The offset level had been settled to be 0.0 % in the spectrometer. The amplifier gain was set to 60 dB. The sweep direction was up, and the sweep width was carried out at 200 G and 6000 G. The average monitoring frequency was 9.4 GHz. The modulation frequency was 100 kHz.

In this study, 47 distinct conditions had been conducted to perform 47 runs, and each run had been repeated several times (2-16) times, and the average of those trials had been taken in order to increase the precision.

The measurement temperature was the room temperature for all runs. However, some runs had been conducted for prepared coffee samples at 298 K and 107 K. No spin traps had been used in this experiment.

Spectra were recorded as first derivatives of the absorption using 100 kHz modulation frequency. The data had been corrected accordingly using a baseline adjustment in order to minimize the contribution of instrumental noise to the intensity measurements. The g value had been determined in order to identify the substances in the coffee samples.

CHAPTER 5

RESULTS AND ANALYSIS

5.1 The experiment

Seven coffee samples were characterized at room temperature and low temperature (107-111) K using Electron Paramagnetic Resonance. Measurements were performed at several microwave powers (1 mW, 0.25 mW, 0.06 mW, 0.016 mW, and 0.004 mW) to evaluate at what level of power saturated the defect transitions. An A.C. modulation of 3 G, 5 G and 10 G was used to optimize the signal to noise intensity, without significantly broadening the EPR peak linewidth.

Figure (5.1) shows spectra of the coffee samples measured at temperature of 298 K.

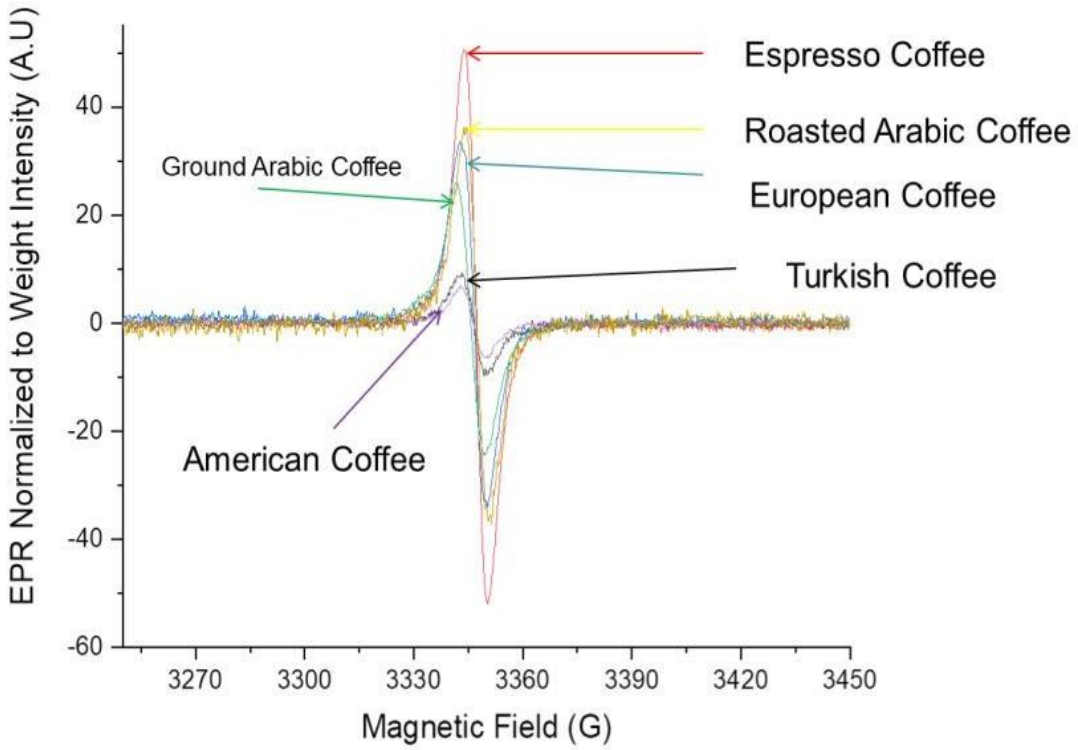

Figure 5.1 Spectra of Coffee Samples measured at room temperature (298 K) with a microwave power of 0.06 mW and a modulation field of 3 G.

Figure (5.1) shows that the Espresso coffee has the largest EPR signal, indicating that the concentration of paramagnetic centers is highest in this type, while the American coffee has the lowest.

The effect of the sample temperature on the intensity of EPR signal is displayed in Figure (5.2).

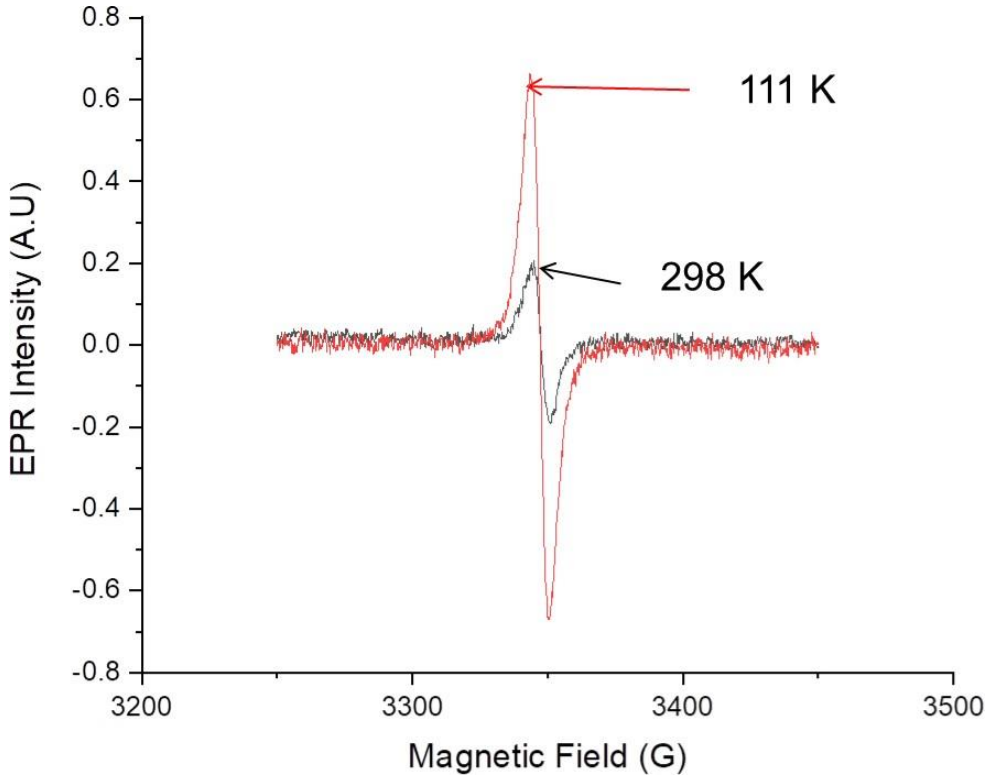

Figure 5.2 EPR Intensity of Roasted Arabic Coffee at 298 K and 111 K temperatures, modulation field of 10 G and microwave power of 1 mW.

All other coffee samples show similar changes with temperature. At 111 K,the EPR intensity signal is higher by a factor of 3.1 over that at room temperature (300K), while the temperature ratio is 2.7. The 13% difference is presumably a result of a very small change in T_2 over this wide temperature range.

Figure (5.3) illustrates the EPR Signal intensity for measurements of Turkish coffee under different field modulations and applied microwave power.

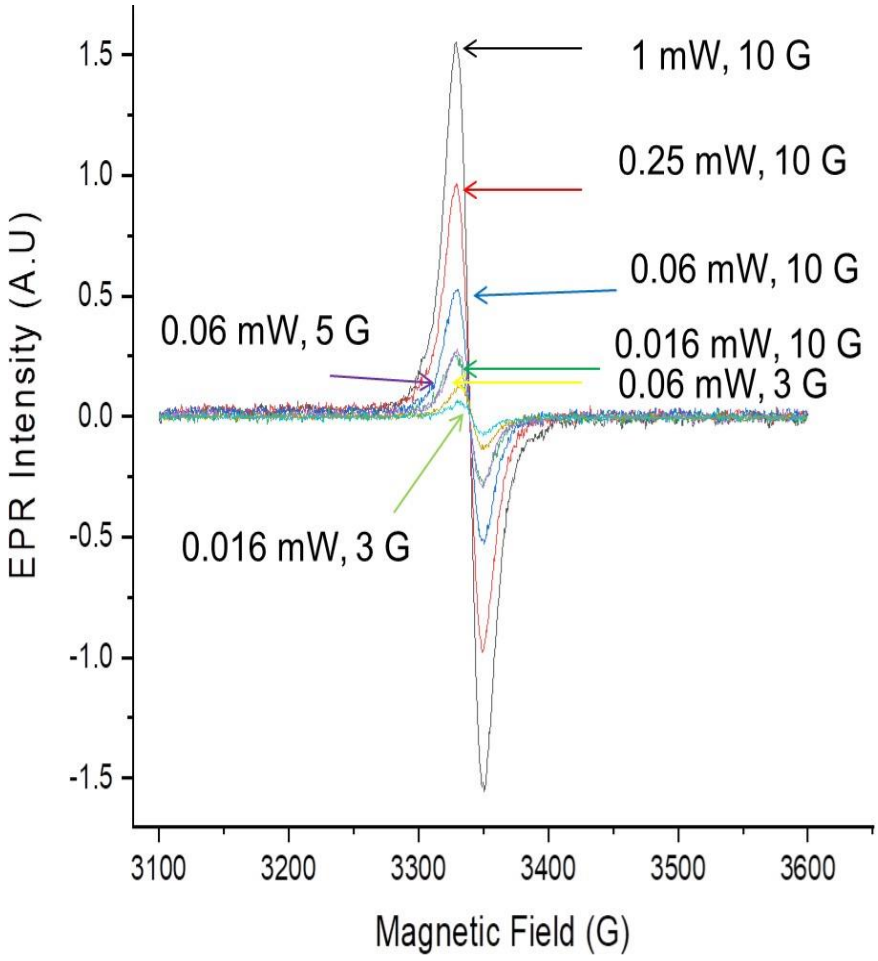

Figure 5.3 EPR Intensity Signals for Turkish coffee sample for a variety of modulation fields and microwave power, all at the measurement temperature of 298 K

Figure (5.4) is illustrating the difference in EPR intensity signal for green, roasted, and ground Arabic coffee at 107 K

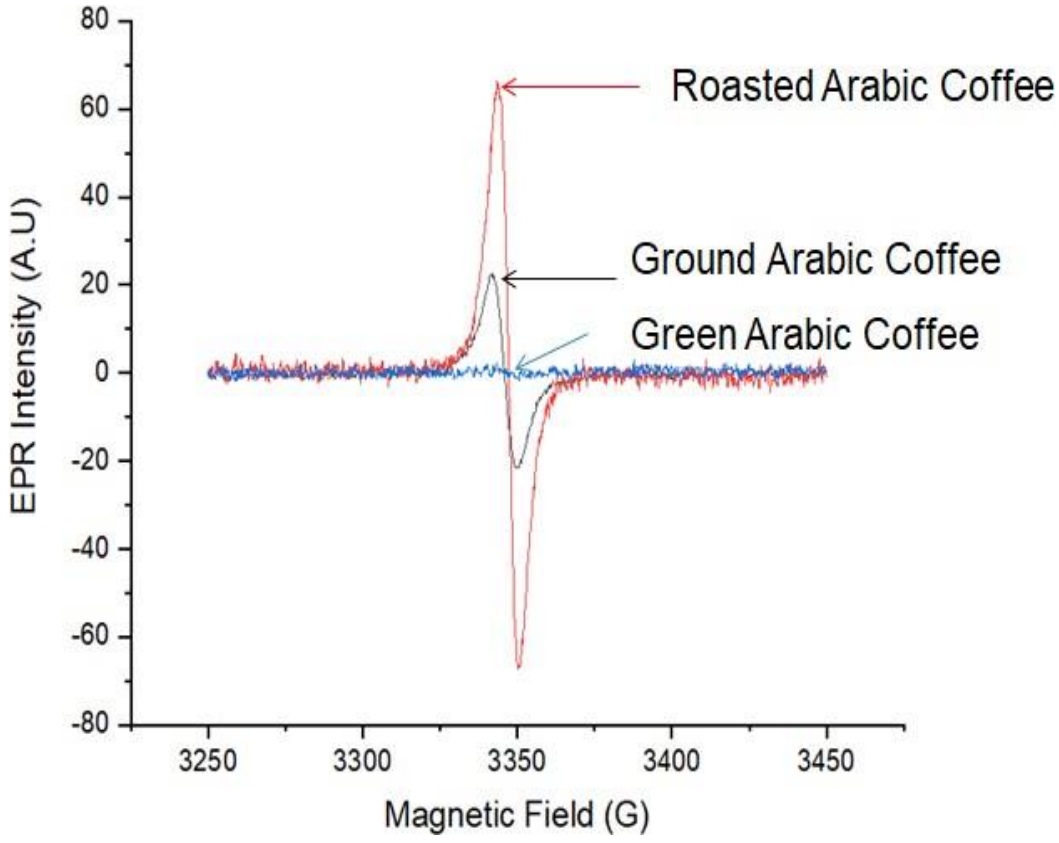

Figure 5.4 The results of EPR measurements of Roasted, Green and Ground Arabic Coffee at 107 K with a field modulation of 3 G and microwave power of 0.016 mW

The figure shows that green Arabic coffee has substantially different levels of paramagnetic centers than roasted and ground coffee. Roasted coffee showed the highest paramagnetic signal amongst the 3 samples.

Figure (5.5) illustrates the EPR measurement results of Turkish coffee characterized at 107 K and different microwave powers (0.06 mW, 0.016 mW, and 0.004 mW), while Figure (5.6) illustrates the EPR signal for the Turkish coffee sample at identical microwave power of 0.06 mW but different modulation frequency (3 G, 5 G and 10 G).

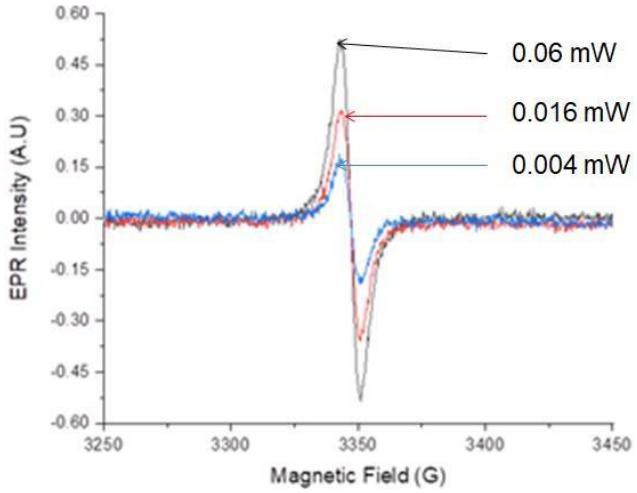

Figure 5.5 The EPR Signal of Turkish coffee for a range of microwave powers measured at a modulation field of 3 G and 107 K

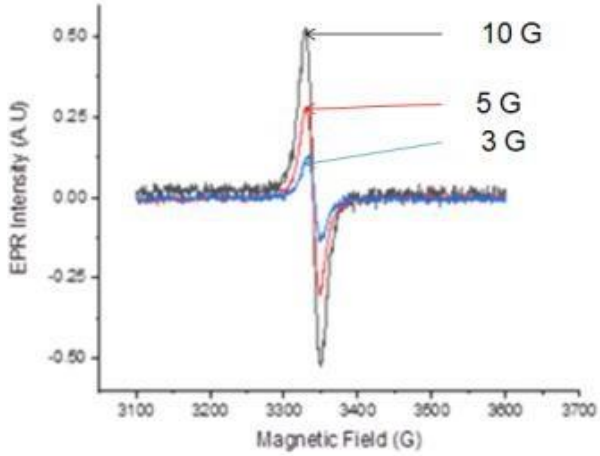

Figure 5.6: EPR spectra of the Turkish coffee sample measured at 0.06 mW microwave power and a range of modulation fields

Figure (5.5) shows a positive correlation between microwave power and EPR signal intensity. Figure (5.6) shows positive correlation between modulation frequency and EPR signal intensity. Figure (5.7) shows the results of integrating the EPR signal of the Turkish coffee sample at room temperature and different microwave power and modulation frequency. These values are proportional to EPR absorption (within an integration constant) since the EPR signals reported so far are a differential of the signal as a result of the EPR measurements use a lock-in technique.

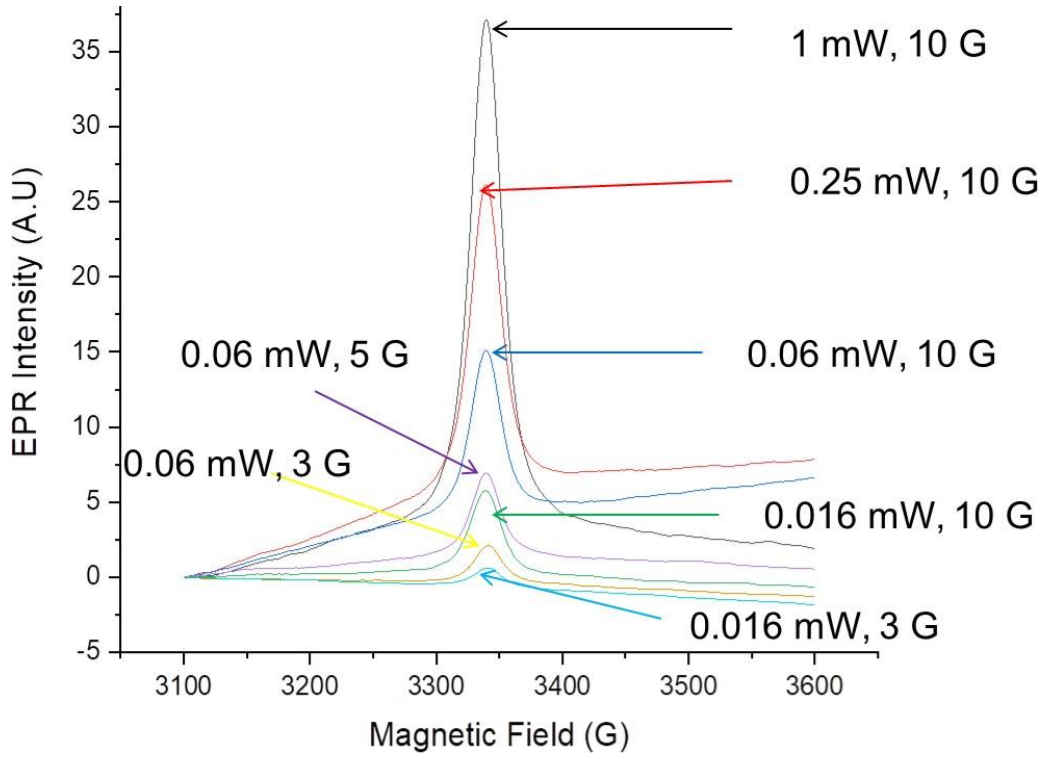

Figure 5.7 Absorption EPR Signal at different modulation frequency and microwave power

The average g-value for all the samples was 2.0096. The largest line width was 16.3 G for run 32 of the Espresso Coffee, measured at a 108 K, a microwave power of 1 mW, and a field modulation of 10 G. There is small EPR peak with a g value of 4.197 in the coffee spectra measured at 107 K.

Figure (5.8) is showing the relation between the square root of the microwave power and the peak to peak height.

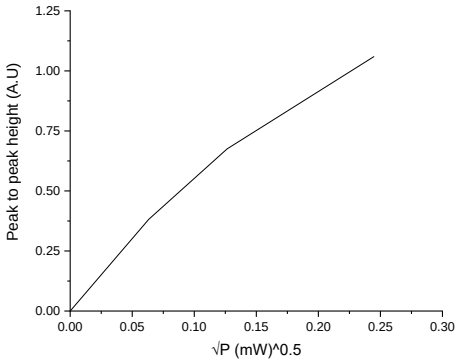

Figure 5.8: Square root of the microwave power and the peak to peak height relation

Figure 5.8 shows the peak-to-peak height of the EPR peak versus the square root of the microwave power. The deviation from linear at higher power levels indicates that saturation is occurring under these conditions. This is confirmed in Figure 5.9. Note that the peak-to-peak intensity of the 0.004 mW data set is significantly greater than those at higher power, validating our claim that the measurements carried out at high power were performed under saturated conditions. Figure (5.9) is illustrating the magnetic field versus the EPR Intensity divided by the square root of the microwave power.

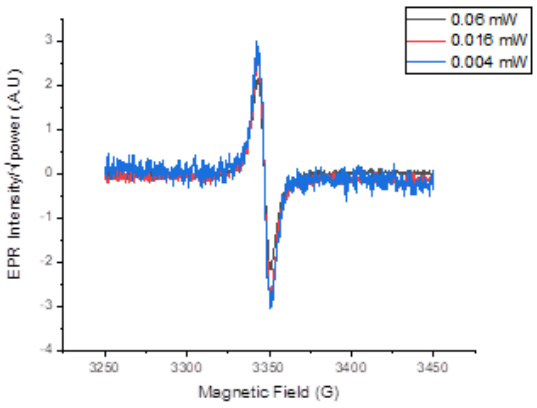

Figure 5.9: Magnetic field versus EPR Intensity divided by the square root of the microwave power

5.2 The analysis

All spectra showed peaks in the EPR spectra which are typically attributed to the presence of organic free radicals. The average g-value for the samples is 2.009 (≈2.01) which can be attributed to the presence of peroxyl radicals, ROS, known as hydrogen superoxide. This may result from lipid oxidation related to normal storing conditions [126] [127]. Several studies indicated that the g-value of 2.009 is an indicator of oxygen O^{-2} species, ROS, caused by oxidation [128].

For the green Arabic coffee at low temperature run, the spectra showed g-value of 1.98 which can be the result of transition metal impurity; Chromium complexes [129] (including Cr^{+3} [130], Cr^{+5} [131]), Manganese (Mn^{+2}) [119], and Copper (Cu^{+2}) [130] [132], have all been reported in the literature to correspond with the g-value found. These impurities may be natural components of coffee, they can also result from the steps of coffee processing; it is possible that oxidation, fermentation, soil and water contamination, roasting, storage, and transportation of the coffee have caused these impurities [133].

At low temperature runs, there is small peak at g-value of 4.197 which can be attributed to the presence of small amount of iron (Fe^{+3}) in the coffee samples. This has been previously reported in the literature on measurements of American coffee [119].

The experiment was conducted at several microwave powers to ensure no signal saturation. When the paramagnetic centers are in a non-saturated condition the measured signal intensities scale with the square root of power. In this experiment, it was found that by doubling the power, the signal will increase with a factor of 1.68, indicating that the power is saturated at the higher power levels Figure (5.5).

Also, it was found that, the cooler the temperature, the larger the peak intensity (Figure (5.4)). If the lifetimes of the paramagnetic centers do not change, then the EPR signal intensities should depend only on the population differences in the spin orientation and thus follow the Curie law. It was found that the signal at 107 K temperature is almost 3 times higher than the signal at 298 K

temperature.

This study found, Espresso coffee has the highest free radical concentration among the samples, given that it has the highest EPR peak height and greatest linewidth (16.3 G). The concentration of the radicals scales with the area under the curve of the signal.

As illustrated in Figure 5.6, the experiments performed at the smallest field modulation of 3 G resulted in a linewidth of 16 G. The experiments carried out with 5 G and 10 G field modulation resulted in spectra that contained distortions and were thus not suitable for use to perform quantitative analysis.

The two figures (5.8) (5.9) show that the higher powers indicate some saturation, therefore, the measurements carried out at low microwave power levels were used when comparing the concentration of free radicals in various tested coffee samples.

This study found that Espresso coffee has more radical content than other coffees, which could insinuate it is more harmful to one's health. This may also confirm the positive correlation between roasting time and radials' concentration, as espresso typically uses a darker roast [96] [121].

The findings of this study are consistent with current literature; radicals seem to increase with roasting, and possibly cooling rates, which is likely due to the normal oxidation processes including lipid oxidation, the Millard reaction and exposure to light [118] [119] [120].

The paramagnetic concentration of Arabic coffee results fell at about the average when compared to the other types of coffee studied here, revealing that radical concentration is not as high as Espresso coffee nor as low as American coffee. Figure (5.2) shows the spectra of 3 Arabic coffee samples: green, roasted, and ground, it is clear that the spectrum of roasted Arabic coffee contains a high concentration of radicals, however, in the green sample, the prominent peak is missing, It is well known that coffee contains high concentrations of antioxidants, like polyphenols, which breakdown into radicals upon oxidation; through roasting, cooling, and storing [96]. Therefore, it is foreseeable that the lack of paramagnetic centers observed in the green sample can be

attributable to compounds formed between the antioxidants and paramagnetic centers in the coffee [119]. However, upon roasting, these chemical species break apart, generating free radicals.

Ground coffee was prepared with the traditional addition of cardamom, which can explain the difference between the roasted and ground coffee as illustrated in Figure (5.4). It is not clear whether the difference in concentration is related to the addition of cardamom or the smaller ratio of coffee to cardamom in the sample, compared to the rest of the samples.

Marginal difference of power accuracy (7.3%) relating to consistency of peak heights from run to run was found in this experiment, which is moderate.

5.3 Conclusion

EPR spectrometry has a wide range of applications that can facilitate betterment of clinical practice and health. Paramagnetic centers indicating disease or malignancy can provide basis for early detection and prevention of disease. Using EPR to assess the concentration of antioxidants and radicals in food can limit human exposure to radicals, thereby enabling reduction of oxidative stress and subsequent damage. This thesis examined free radicals' content in Arabic coffee in comparison to other coffee types, revealing that Arabic coffee has an average concentration of organic radicals and the highest concentration is in Espresso coffee. It is notable that further exploration of Arabic coffee's radical concentration can be useful in assessing the impact of roasting, cooling, grinding, and storing. As well as thoroughly examine the impact of varying temperatures and any additions to the coffee mix (like cardamom).

5.4 Future Work

I believe future work should further investigate in-situ measurement of radicals in coffee, as well as possible impact on the radicals' content in blood. EPR is a promising technique to analyze health profile and prevent deterioration; it can be developed and efficiently used for early detection of health anomalies. EPR is able to provide the knowledge we need to develop better solutions to current health problems.

REFERENCES

1. Weil, J. A., & Bolton, J. (2007). Electron Paramagnetic Resonance: ElementaryTheory and Practical Applications - John A. Weil, James R. Bolton (2nd ed.). A John Wiley & Son, Inc. Publication
.
2. Spaldin, N. (2011). Magnetic Materials: Fundamentals and Applications (2nded.). Cambridge University.

3. Heidari, H. and Nabaei, V. (2019). SQUID Sensors. In Magnetic Sensors for Biomedical Applications (eds H. Heidari and V. Nabaei). https://doi.org/10.1002/9781119552215.ch5

4. Butta, M., Ripka, P., Atalay, S., Atalay, F. E., & Li, X. P. (2008). Fluxgate effect in twisted magnetic wire. Journal of Magnetism and Magnetic Materials, 320(20),e974–e978. https://doi.org/https://doi.org/10.1016/j.jmmm.2008.04.176

5. Goel, N., Babuta, A., Kumar, A., & Ganguli, S. (2020). Hall effect instruments, evolution, implications, and future prospects. Review of Scientific Instruments, 91(7), 071502. https://doi.org/10.1063/5.0009647

6. Gao, W., & Sammes, N. M. (1999). An Introduction to Electronic and Ionic Materials. In An Introduction to Electronic and Ionic Materials. WORLD SCIENTIFIC. https://doi.org/10.1142/3794

7. Callister, W. D., & Rethwisch, D. G. (2009). Materials Science and Engineering:An Introduction, 8th Edition. In Materials & Design (Vol. 12, Issue 1). John Wiley and Sons. http://linkinghub.elsevier.com/retrieve/pii/0261306991901019

8. Kleschyov, A., Wenzel, P., & Munzel, T. (2007). Electron paramagnetic resonance (EPR) spin trapping of biological nitric oxide. Journal of Chromatography. B, Analytical Technologies in the Biomedical and Life Sciences, 851, 12–20. https://doi.org/10.1016/j.jchromb.2006.10.006

9. Al Khatib, M., Costa, J., Baratto, M. C., Basosi, R., & Pogni, R. (2020). Paramagnetism and Relaxation Dynamics in Melanin Biomaterials. Journal ofPhysical Chemistry B, 124(11), 2110–2115. https://doi.org/10.1021/ACS.JPCB.9B11785

10. Skibsted, L. H. (2010). Understanding oxidation processes in foods. Oxidation inFoods and Beverages and Antioxidant Applications: Understanding Mechanismsof Oxidation and Antioxidant Activity, 3–35. https://doi.org/10.1533/9780857090447.1.3

11. Maghraby, A. M. (2019). Introductory Chapter: Electron Paramagnetic Resonance. Topics From EPR Research. https://doi.org/10.5772/INTECHOPEN.83028

12. Roessler, M. M., & Salvadori, E. (2018). Principles and applications of EPR spectroscopy in the chemical sciences. Chemical Society Reviews, 47(8), 2534–2553. https://doi.org/10.1039/C6CS00565A

13. Villamena, F. A. (2017). EPR Spin Trapping. In F. A. Villamena (Ed.), Reactive SpeciesDetection in Biology (pp. 163–202). Elsevier. https://www.sciencedirect.com/science/article/pii/B9780124200173000049

14. EPR: Theory - Chemistry LibreTexts. (n.d.). Retrieved January 7, 2022, from https://chem.libretexts.org/Bookshelves/Physical_and_Theoretical_Chemistry_Textbook_Maps/Supplemental_Modules_(Physical_and_Theoretical_Chemistry)/Spectroscopy/Magnetic_Resonance_Spectroscopies/Electron_Paramagnetic_Resonance/EPR%3A_Theory

15. Lewis, D. E. (2020). Yevgenii Konstantinovich Zavoiskii and the Battle for Electron Paramagnetic Resonance Spectroscopy. ACS Symposium Series, 113–122. https://doi.org/10.1021/BK-2020-1349.CH006

16. Barra, A. L., Caneschi, A., Gatteschi, D., & Sessoli, R. (2002). High-Frequency EPR Spectra for the Analysis of Magnetic Anisotropy in Large Magnetic Clusters.Journal of the American Chemical Society, 117(34), 8855–8856. https://doi.org/10.1021/JA00139A021

17. Al'tshuler, S. A., & Kozyrev, B. M. (1964). Electron Paramagnetic Resonance (C. P. Poole, Ed.). Kazan University .

18. Spasojević, I. (2011). Free radicals and antioxidants at a glance using EPR spectroscopy. Critical Reviews in Clinical Laboratory Sciences, 48(3), 114–142. https://doi.org/10.3109/10408363.2011.591772

19. Spaldin, N. (2011). Magnetic Materials: Fundamentals and Applications (2nded.). Cambridge University.

20. Kuppusamy, P., & Zweier, J. L. (2004). Cardiac applications of EPR imaging.NMR in Biomedicine, 17(5), 226–239. https://doi.org/10.1002/NBM.912

21. Orenha, R. P., & Galembeck, S. E. (2014). Molecular orbitals of NO, NO+, andNO-: A computational quantum chemistry experiment. Journal of Chemical *Education*, *91*(7),1064–1069. https://doi.org/10.1021/ED400618J/ASSET/IMAGES/ED400618J.SOCIAL.JPE G_V03

22. Draw the molecular orbital diagram of O2 and calculate the bond order. Is O2 diamagnetic or paramagnetic? Explain your answer. | Study.com. (n.d.). Retrieved February 6, 2022, from https://study.com/academy/answer/draw-the- molecular-orbital-diagram-of-o2-and-calculate-the-bond-order-is-o2-diamagnetic- or-paramagnetic-explain-your-answer.html

23. Discuss the formation of N2 molecule on the basis of MO theory. Predict its:(i) Bond order(ii) Magnetic character. from Chemistry Chemical Bonding and Molecular Structure Class 11 Haryana Board - English Medium. (n.d.). Retrieved February 6, 2022, from https://www.zigya.com/study/book?class=11&board=hbse&subject=Chemistry&book=Chemistry+Part+I&chapter=Chemical+Bonding+and+Molecular+Structure&q_type=&q_topic=BondIng+In+Some+Homonuclear+Diatomic+Molecules&q_category=&question_id=CHEN1108671

24. Sheikhshoaie, I., Ebrahimipour, Y., & Sheikhshoaee, M. (2012). Structural investigation of methanol {6-[(2-oxidopropyl)iminomethyl] phenolato} dioxidomolybdenum(VI) by X-Ray crystallography and DFT calculations.Walailak Journal of Science and Technology, 9(3), 207–216. https://doi.org/10.2004/WJST.V9I3.207

25. Solved a) Considering the molecular orbital diagram for | Chegg.com. (n.d.). Retrieved February 6, 2022, from https://www.chegg.com/homework-help/questions-and-answers/considering-molecular-orbital-diagram-ethylene- draw-molecules-kind-three-dimensional-repre-q56089763

26. VALENCE BOND THEORY HOMONUCLEAR DIATOMIC MOLECULESVALENCE BOND. (n.d.). Retrieved February 7, 2022, from https://slidetodoc.com/valence-bond-theory-homonuclear-diatomic-molecules-valence-bond/

27. File:Ammonia MO diagram.jpg - Wikimedia Commons. (n.d.). RetrievedFebruary 7, 2022, from https://commons.wikimedia.org/wiki/File:Ammonia_MO_diagram.jpg

28. Maciej Serda. (2013). Synteza i aktywność biologiczna nowych analogów tiosemikarbazonowych chelatorów żelaza. Uniwersytet Śląski, 343–354. https://doi.org/10.2/JQUERY.MIN.JS

29. Using the MO diagram of "NO", calculate the bond order. Compare it to "NO"^(+)? | Socratic. (n.d.). Retrieved February 7, 2022, from https://socratic.org/questions/59a5709a11ef6b7ac40bc96d

30. Introduction to Molecular Orbital Theory. (n.d.). Retrieved February 7, 2022,from https://www.ch.ic.ac.uk/vchemlib/course/mo_theory/main.html

31. Supplementary Illustrations. (n.d.). Retrieved February 7, 2022, from https://www2.chemistry.msu.edu/faculty/reusch/virttxtjml/Jmol-11/methanemos.htm

32. Bratasz, A., Kuter, I., Konior, R., Gościński, I., & Łukiewicz, S. (2004). NitricOxide as a Prognostic Marker for Neurological Diseases. Https://Home.Liebertpub.Com/Ars, 6(3), 613–617. https://doi.org/10.1089/152308604773934378

33. Song, K., Li, Y., Zhang, H., An, N., Wei, Y., Wang, L., Tian, C., Yuan, M., Sun,Y., Xing, Y., Gao, Y., & Santibañez, J. F. (2020). Oxidative Stress-Mediated Blood-Brain Barrier (BBB) Disruption in Neurological Diseases. Oxidative Medicine and Cellular Longevity, 2020. https://doi.org/10.1155/2020/4356386

34. Liguori, I., Russo, G., Curcio, F., Bulli, G., Aran, L., Della-Morte, D., Gargiulo, G., Testa, G., Cacciatore, F., Bonaduce, D., & Abete, P. (2018). Oxidative stress,aging, and diseases. Clinical Interventions in Aging, 13, 757. https://doi.org/10.2147/CIA.S158513

35. Kleschyov, A. L., & Terekhov, M. (2013). Electron paramagnetic resonance in a biomedical laboratory. BIOANALYSISVOL, 5(18), 2233–2237. https://doi.org/10.4155/BIO.13.200

36. Hogg, N. (2010). Detection of nitric oxide by electron paramagnetic resonance

spectroscopy. Free Radical Biology and Medicine, 49(2), 122–129. https://doi.org/10.1016/J.FREERADBIOMED.2010.03.009

37. Fujii, H., Wan, X., Zhong, J., Berliner, L. J., & Yoshikawa, K. (n.d.). In VivoImaging of Spin-Trapped Nitric Oxide in Rats With Septic Shock: MRI Spin Trapping. https://doi.org/10.1002/(SICI)1522-2594(199908)42:2

38. Mannaerts, D., Faes, E., Gielis, J., Van Craenenbroeck, E., Cos, P., Spaanderman,M., Gyselaers, W., Cornette, J., & Jacquemyn, Y. (2018).Oxidative stress and endothelial function in normal pregnancy versus pre-eclampsia, a combined longitudinal and case control study. BMC Pregnancy and Childbirth 2018 18:1, 18(1), 1–9. https://doi.org/10.1186/S12884-018-1685-5

39. Pei, Z., Fung, P. C. W., & Cheung, R. T. F. (2003). Melatonin reduces nitric oxidelevel during ischemia but not blood–brain barrier breakdown during reperfusion in a rat middlecerebral artery occlusion stroke model. Journal of Pineal Research,34(2),110–118. https://doi.org/10.1034/J.1600-079X.2003.00014.X

40. Lee, M.-C. (2013). Assessment of oxidative stress and antioxidant property using electron spin resonance (ESR) spectroscopy. Journal of Clinical Biochemistry andNutrition, 52(1), 1–8. https://doi.org/10.3164/JCBN.12-58

41. Baumane, L., Dzintare, M., Zvejniece, L., Meirena, D., Lauberte, L., Sile, V., Kalvinsh, I., & Sjakste, N. (2002). Increased synthesis of nitric oxide in rat braincortex due to halogenated volatile anesthetics confirmed by EPR spectroscopy. Acta Anaesthesiologica Scandinavica, 46(4), 378–383. https://doi.org/10.1034/J.1399-6576.2002.460408.X

42. Components of blood (article) | Khan Academy. (n.d.). Retrieved October 15,2021, from https://www.khanacademy.org/science/biology/human- biology/circulatory-pulmonary/a/components-of-the-blood

43. Heckl, C., Lang, A., Rühm, A., Sroka, R., Duffield, T., Vogeser, M., & Paal, M. (2021). Spectrophotometric evaluation of hemolysis in plasma by quantification of free oxyhemoglobin, methemoglobin, and methemalbumin in presence of bilirubin. Journal of biophotonics, 14(5), e202000461. https://doi.org/10.1002/jbio.202000461

44. Wilks, A. (2007). Heme Oxygenase. XPharm: The Comprehensive Pharmacology Reference, 1–8. https://doi.org/10.1016/B978-008055232-3.60506-9

45. Drummond, G. S., Baum, J., Greenberg, M., Lewis, D., & Abraham, N. G. (2019). HO-1 overexpression and underexpression: Clinical implications.Archivesof Biochemistry and Biophysics, 673, 108073. https://doi.org/10.1016/J.ABB.2019.108073

46. Chau, L.-Y. (2015). Heme oxygenase-1: emerging target of cancer therapy. Journal of Biomedical Science 2015 22:1, 22(1), 1–7. https://doi.org/10.1186/S12929-015-0128-0

47. Goldman, M., Uzicanin, S., Scalia, J., Scalia, V., & O'Brien, S. F. (2016). Impactof informing donors of low ferritin results. Transfusion, 56(9), 2193–2198. https://doi.org/10.1111/TRF.13691/ABSTRACT

48. Waldvogel-Abramowski S, Waeber G, Gassner C, et al. Physiology of iron metabolism. Transfus Med Hemother. 2014;41(3):213-221. doi:10.1159/000362888

49. Mrakic-Sposta, S., Gussoni, M., Montorsi, M., Porcelli, S., & Vezzoli, A. (2014).A quantitative method to monitor reactive oxygen species production by electron paramagnetic resonance in physiological and pathological conditions. Oxidative Medicine and Cellular Longevity, 2014. https://doi.org/10.1155/2014/306179

50. SC, K., A, G., G, M., & V, M. (2006). Electron spin resonance spectroscopy of serum albumin: a novel new test for cancer diagnosis and monitoring. Clinical Chemistry, 52(11), 2129–2134. https://doi.org/10.1373/CLINCHEM.2006.073148

51. Gurachevsky, A., Muravskaya, E., Gurachevskaya, T., Smirnova, L., & Muravsky, V. (2007). Cancer-associated alteration in fatty acid binding to albumin studied by spin-label electron spin resonance. Cancer Investigation,25(6), 378–383. https://doi.org/10.1080/07357900701407947

52. Ewelina, G., Krzysztof, S., Marek, M., & Krzysztof, K. (2017). Blood free Radicals Concentration Determined by Electron Paramagnetic Resonance Spectroscopy and Delayed Cerebral Ischemia Occurrence in Patients with Aneurysmal Subarachnoid Hemorrhage. Cell Biochemistry and Biophysics 201775:3, 75(3), 351–358. https://doi.org/10.1007/S12013-017-0820-7

53. K, B., M, E., M, L., & H, G. (2014). A high precision method for quantitative measurements of reactive oxygen species in frozen biopsies. PloS One, 9(3). https://doi.org/10.1371/JOURNAL.PONE.0090964

54. CM, D., A, L., S, V., PE, P., P, S., D, D., P, L., & B, G. (2015). Application ofElectron Paramagnetic Resonance (EPR) Oximetry to Monitor Oxygen in Wounds in Diabetic Models. PloS One, 10(12). https://doi.org/10.1371/JOURNAL.PONE.0144914

55. Burlaka, A. P., Vovk, A. v., Burlaka, A. A., Gafurov, M. R., Iskhakova, K. B., &Lukin, S. N. (2018). Rectal Cancer: Redox State of Venous Blood and Tissues ofBlood Vessels from Electron Paramagnetic Resonance and Its Correlation with the Five-Year Survival. BioMed Research International, 2018. https://doi.org/10.1155/2018/4848652

56. Liu, Z., Zhang, W., Fan, S., Wang, L., & Jiao, L. (2013). RETRACTED ARTICLE: Changes in the electron paramagnetic resonance spectra of albumin- associated spin-labeled stearic acid as a diagnostic parameter of colorectal cancer.World Journal of Surgical Oncology 2013 11:1, 11(1), 1–5. https://doi.org/10.1186/1477-7819-11-223

57. Polakovs, M., Mironova-Ulmane, N., Pavlenko, A., Reinholds, E., Gavare, M., &Grube, M. (2012). EPR and FTIR spectroscopies study of human blood after irradiation. Spectroscopy (New York), 27(5–6), 367–371. https://doi.org/10.1155/2012/365056

58. He, W., Liu, Y., Wamer, W. G., & Yin, J.-J. (2014). Electron spin resonance spectroscopy for the study of nanomaterial-mediated generation of reactive oxygen species. Journal of Food and Drug Analysis, 22(1), 49–63. https://doi.org/https://doi.org/10.1016/j.jfda.2014.01.004

59. Klare JP, Steinhoff HJ. Spin labeling EPR. Photosynth Res. 2009 Nov-Dec;102(2-3):377-90. doi: 10.1007/s11120-009-9490-7. Epub 2009 Aug 29. PMID: 19728138.

60. Eaton, S. S., & Eaton, G. R. (2015). Chapter One - Rapid-Scan EPR of NitroxideSpin Labels and Semiquinones. In P. Z. Qin & K. Warncke (Eds.), Methods in Enzymology (Vol. 563, pp. 3–21). Academic Press. https://doi.org/https://doi.org/10.1016/bs.mie.2015.06.027

61. Carini, M., Aldini, G., Orioli, M., & Facino, R. (2006). Electron Paramagnetic Resonance (EPR) Spectroscopy: A Versatile and Powerful Tool in Pharmaceutical and Biomedical Analysis. Current Pharmaceutical Analysis, 2(2),141–159. https://doi.org/10.2174/157341206776819328

62. Katerji, M., Filippova, M., & Duerksen-Hughes, P. (2019). Approaches and Methods to Measure Oxidative Stress in Clinical Samples: Research Applicationsin the Cancer Field. Oxidative Medicine and Cellular Longevity, 2019. https://doi.org/10.1155/2019/1279250

63. Swartz, H. M., & Khan, N. (n.d.). EPR Spectroscopy of Function In Vivo Origins, Achievements, And Future Possibilities. http://eknygos.lsmuni.lt/springer/54/197-228.pdf

64. Richards, T., Harrhy, J. H., Lewis, R. J., Howe, A. G. R., Suldecki, G. M., Folli, A., Morgan, D. J., Davies, T. E., Loveridge, E. J., Crole, D. A., Edwards, J. K., Gaskin, P., Kiely, C. J., He, Q., Murphy, D. M., Maillard, J.-Y., Freakley, S. J., &Hutchings, G. J. (2021). A residue-free approach to water disinfection using catalytic in situ generation of reactive oxygen species. Nature Catalysis 2021 4:7,4(7), 575–585. https://doi.org/10.1038/s41929-021-00642-w

65. Sickle cell disease - NHS. (n.d.). Retrieved October 2, 2021, from https://www.nhs.uk/conditions/sickle-cell-disease/

66. Lumb, A. B. (2017). Oxygen. Nunn's Applied Respiratory Physiology, 169-202.e3. https://doi.org/10.1016/B978-0-7020-6294-0.00010-1

67. Hanson, M. S., Piknova, B., Keszler, A., Diers, A. R., Wang, X., Gladwin, M. T.,Hillery, C. A., & Hogg, N. (2011). Methaemalbumin Formation in Sickle Cell Disease: Effect on Oxidative Protein Modification and HO-1 Induction. British Journal of Haematology, 154(4), 502. https://doi.org/10.1111/J.1365- 2141.2011.08738.X

68. Pant, L., Kalita, D., Singh, S., Kudesia, M., Mendiratta, S., Mittal, M., & Mathur, A. (2014). Detection of Abnormal Hemoglobin Variants by HPLC Method: Common Problems with Suggested Solutions. International Scholarly ResearchNotices, 2014, 1–10. https://doi.org/10.1155/2014/257805

69. Old, J., Harteveld, C. L., Traeger-Synodinos, J., Petrou, M., Angastiniotis, M., & Galanello, R. (2012). HAEMATOLOGICAL METHODS. https://www.ncbi.nlm.nih.gov/books/NBK190583/

70. Lubeck D, Agodoa I, Bhakta N, et al. Estimated Life Expectancy and Income ofPatients With Sickle Cell Disease Compared With Those Without Sickle Cell Disease. JAMA Netw Open. 2019;2(11):e1915374. doi:10.1001/jamanetworkopen.2019.15374

71. Mohammed, A. M., & Ahmad, A. (n.d.). MAGNETIC PROPERTIES OF METHEMOGLOBIN. Retrieved October 8, 2021, from www.ijset.net/journal/821.pdf

72. Hanson, M. S., Piknova, B., Keszler, A., Diers, A. R., Wang, X., Gladwin, M. T.,Hillery, C. A., & Hogg, N. (2011). Methaemalbumin Formation in Sickle Cell Disease: Effect on Oxidative Protein Modification and HO-1 Induction. British Journal of Haematology, 154(4), 502. https://doi.org/10.1111/J.1365- 2141.2011.08738.X

73. Kubiak, T., Krzyminiewski, R., & Dobosz, B. (2013). EPR Study of ParamagneticCenters in Human Blood. Current Topics in Biophysics, 36(1), 7–13. https://doi.org/10.2478/CTB-2013-0006

74. Svistunenko, D. A. (2021). EPR spectroscopy of whole blood and blood components: can we diagnose abnormalities? Journal of Biomedical Research,35(4), 294–300. https://doi.org/10.7555/JBR.35.20210011

75. Burlaka, A.P., Gafurov, M.R., Iskhakova, K.B. et al. Electron Paramagnetic Resonance in the Experimental Oncology: Implementation Examples of the Conventional Approaches. BioNanoSci. 6, 431–436 (2016). https://doi.org/10.1007/s12668-016-0238-5

76. Moergel, M., Kämmerer, P. W., Schnurr, K., Klein, M. O., & Al-Nawas, B. (2011). Spin electron paramagnetic resonance of albumin for diagnosis of oral squamous cell carcinoma (OSCC). Clinical Oral Investigations 2011 16:6, 16(6),1529–1533. https://doi.org/10.1007/S00784-011-0655-3

77. Krzyminiewski R, Kruczyński Z, Dobosz B, et al. EPR Study of Iron Ion Complexes in Human Blood. Appl Magn Reson. 2011;40(3):321-330. doi:10.1007/s00723-011-0219-3

78. MI, I., VN, C., VN, M., VIu, P., EP, Z., & GV, C. (2013). [Electron paramagneticresonance study of blood of anemic patients with urological cancer]. Biofizika, 58(2), 289–294. https://europepmc.org/article/med/23755556

79. Riley, P. A. (1997). Melanin. The International Journal of Biochemistry & CellBiology, 29(11), 1235–1239. https://doi.org/10.1016/S1357-2725(97)00013-7

80. Moergel, M., Kämmerer, P. W., Schnurr, K., Klein, M. O., & Al-Nawas, B. (2011). Spin electron paramagnetic resonance of albumin for diagnosis of oral squamous cell carcinoma (OSCC). Clinical Oral Investigations 2011 16:6, 16(6),1529–1533. https://doi.org/10.1007/S00784-011-0655-3

81. Krzyminiewski, R., Kruczyński, Z., Dobosz, B., Zając, A., Mackiewicz, A., Leporowska, E., & Folwaczna, S. (2011). EPR Study of Iron Ion Complexes in Human Blood. Applied magnetic resonance, 40(3), 321–330. https://doi.org/10.1007/s00723-011-0219-3

82. Mosiniewicz-Szablewska, E., Ślawska-Waniewska, A., Świątek, K. et al. Electron paramagnetic resonance studies of human liver tissues. Appl. Magn. Reson. 24, 429 (2003). https://doi.org/10.1007/BF03166946

83. Definition of bone marrow - NCI Dictionary of Cancer Terms - National CancerInstitute. (n.d.). Retrieved November 10, 2021, from https://www.cancer.gov/publications/dictionaries/cancer-terms/def/bone-marrow?redirect=true

84. Burlaka, A. P., Ganusevich, I. I., Gafurov, M. R., Lukin, S. N., & Sidorik, E. P. (2013). Electron paramagnetic resonance study of tumor affected bone marrow. Cancer microenvironment : official journal of the International Cancer Microenvironment Society, 6(3), 273–276. https://doi.org/10.1007/s12307-013-0137-z

85. National Center for Biotechnology Information (2021). PubChem Compound Summary for CID 6325610, Melanin. Retrieved November 10, 2021 from https://pubchem.ncbi.nlm.nih.gov/compound/Melanin

86. Desmet, C. M., Danhier, P., Acciardo, S., Levêque, P., & Gallez, B. (2019).Towards in vivo melanin radicals detection in melanomas by electron paramagnetic resonance (EPR) spectroscopy: a proof-of-concept study. Https://Doi.Org/10.1080/10715762.2019.1593402, 53(4), 405–410. https://doi.org/10.1080/10715762.2019.1593402

87. Guy, G. P., Machlin, S. R., Ekwueme, D. U., & Yabroff, K. R. (2015). Prevalenceand costs of skin cancer treatment in the U.S., 2002-2006 and 2007-2011. American Journal of Preventive Medicine, 48(2), 183–187. https://doi.org/10.1016/J.AMEPRE.2014.08.036

88. Glagoleva, A. Y., Shoeva, O. Y., & Khlestkina, E. K. (2020). Melanin Pigment inPlants: Current Knowledge and Future Perspectives. Frontiers in Plant Science, 11, 770. https://www.frontiersin.org/article/10.3389/fpls.2020.00770

89. al Khatib, M., Costa, J., Baratto, M. C., Basosi, R., & Pogni, R. (2020). Paramagnetism and Relaxation Dynamics in Melanin Biomaterials. Journal of *Physical Chemistry B*, *124*(11), 2110–2115. https://doi.org/10.1021/ACS.JPCB.9B11785

90. Cesareo, E., Korkina, L., D'Errico, G., Vitiello, G., Aguzzi, M. S., Passarelli, F., Pedersen, J. Z., & Facchiano, A. (2012). An Endogenous Electron Spin Resonance (ESR) signal discriminates nevi from melanomas in human specimens: a step forward in its diagnostic application. PloS one, 7(11), e48849. https://doi.org/10.1371/journal.pone.0048849

91. Subramanian, S., & Krishna, M. C. (2013). Electron paramagnetic resonance imaging. In Molecular Imaging Techniques: New Frontiers (pp. 112–127). FutureScience Ltd. https://doi.org/doi:10.4155/ebo.13.235

92. Nakagawa, K., Minakawa, S., Sawamura, D., & Hara, H. (2017). Characterizationof Melanin Radicals in Paraffin-embedded Malignant Melanoma and Nevus Pigmentosus Using X-band EPR and EPR Imaging. Analytical Sciences : The International Journal of the Japan Society for Analytical Chemistry, 33(12), 1357–1361. https://doi.org/10.2116/ANALSCI.33.1357

93. Andersen, M. L., & Skibsted, L. H. (2018). ESR Spectroscopy for the Study of Oxidative Processes in Food and Beverages 87. Modern Magnetic Resonance, 1781–1794. https://doi.org/10.1007/978-3-319-28388-3_25

94. Gonis, J., Hewitt, D. G., Troup, G., Hutton, D. R., Hunter, C. R., Gonis', J., Ton^, D. R. H., & Hunter3, C. R. (2009). The Chemical Origin of Free Radicals inCoffee and Other Beverages. Free Rad Res, 23(4), 393–399.

https://doi.org/10.3109/10715769509065260

95. Nagai, R., Koito, W., & Sakamoto, Y. (2014). Maillard reaction. In Encyclopediaof Meat Sciences (second, Issue 6, pp. 403–405). https://doi.org/10.1016/B0-12- 227235-8/00277-7

96. Pandey, K. B., & Rizvi, S. I. (2009). Plant polyphenols as dietary antioxidants in human health and disease. Oxidative Medicine and Cellular Longevity, 2(5), 270. https://doi.org/10.4161/OXIM.2.5.9498

97. B, G., C, B., & R, D. (2000). Free radicals in licorice-flavored sweets can Be detected noninvasively using low frequency electron paramagnetic resonance after oral administration to mice. The Journal of Nutrition, 130(7), 1831–1833. https://doi.org/10.1093/JN/130.7.1831

98. Yordanov, N. D., & Mladenova, R. (2004). EPR study of free radicals in bread. Spectrochimica Acta Part A: Molecular and Biomolecular Spectroscopy, 60(6), 1395–1400. https://doi.org/10.1016/J.SAA.2003.10.039

99. Marianne K. Thomsen, Lene Lauridsen, Leif H. Skibsted, and, & Risbo*, J.(2005). Two Types of Radicals in Whole Milk Powder. Effect of Lactose Crystallization, Lipid Oxidation, and Browning Reactions. Journal of *Agricultural and Food Chemistry*, *53*(5),1805–1811.https://doi.org/10.1021/JF0485483

100. Stapelfeldt, H., Meisen, B. R., & Skibsted, L. H. (1997). Effect of heat treatment, water activity and storage temperature on the oxidative stability of whole milk powder. International Dairy Journal, 7(5), 331–339. https://doi.org/10.1016/S0958-6946(97)00016-2

101. S. Ohfuji, W. Fukushima, T. Tanaka, D. Habu, A. Tamori, H. Sakaguchi,et al. Coffee consumption and reduced risk of hepatocellular carcinoma among patients with chronic type C liver disease: A case–control study. Hepatology Research, 36 (2006), pp. 201-208

102. Si W, Chen YP, Zhang J, Chen ZY, Chung HY. Antioxidant activities ofginger extract and its constituents toward lipids. Food Chem. 2018; 239:1117– 1125.

103. Sueishi, Y., Masamoto, H., & Kotake, Y. (2019). Heat treatments of ginger root modify but not diminish its antioxidant activity as measured withmultiple free radical scavenging (MULTIS) method. Journal of Clinical Biochemistry and Nutrition, 64(2), 143. https://doi.org/10.3164/JCBN.18-41

104. Pawłowska-Góral, K., Ramos, P., Pilawa, B., & Kurzeja, E. (2013). Application of EPR Spectroscopy to Examination of the Effect of Sterilization Process on Free Radicals in Different Herbs. Food Biophysics 2013 8:1, 8(1), 60–68. https://doi.org/10.1007/S11483-013-9284-5

105. Stevens, L. M., Linstead, E., Hall, J. L., & Kao, D. P. (2021). AssociationBetween Coffee Intake and Incident Heart Failure Risk. Circulation: Heart Failure, 181–188. https://doi.org/10.1161/CIRCHEARTFAILURE.119.006799

106. F, R.-A., & E, L.-G. (2018). Coffee Consumption and Cardiovascular Disease:

A Condensed Review of Epidemiological Evidence and Mechanisms.Journal of Agricultural and Food Chemistry, 66(21), 5257–5263. https://doi.org/10.1021/ACS.JAFC.7B04506

107. Bøhn, S. K., Ward, N. C., Hodgson, J. M., & Croft, K. D. (2012). Effects of tea and coffee on cardiovascular disease risk. Food & Function, 3(6), 575–591. https://doi.org/10.1039/C2FO10288A

108. Krakowian, D., Skiba, D., Kudelski, A., Pilawa, B., Ramos, P., Adamczyk, J., & Pawłowska-Góral, K. (2014). Application of EPR spectroscopyto the examination of pro-oxidant activity of coffee. Food Chemistry, 151, 110– 119. https://doi.org/10.1016/J.FOODCHEM.2013.11.035

109. K. Jiyoung, L. Siyoung, S. Jaesung, K. Hyo Won, K. Jaekyoon, J. YoungJin, et al. Caffeinated coffee, decaffeinated coffee, and the phenolic phytochemical chlorogenicacid up-regulate NQO1 expression and prevent H2O2-induced apoptosis in primary cortical neuron. Neurochemistry International, 60 (5) (2012), pp. 466-474

110. C. Chung-Jung, T. Allen. Dietary hyperglycemia, glycemic index and metabolic retinal diseases. Progress in Retinal and Eye Research, 30 (1) (2011),pp. 18-53

111. A. Nkondjock. Coffee consumption and the risk of cancer: An overview.Cancer Letters, 277 (2009), pp. 121-125

112. V. Brezová, A. Slebodová, A. Stasko. Coffee as a source of antioxidants:An EPR study. Food Chemistry, 114 (2009), pp. 859-868

113. Delgado-Andrade C, Morales FJ (2005) Unraveling the Contribution of Melanoidins to the Antioxidant Activity of Coffee Brews J Agric Food Chem 53:1403–1407

114. Cämmerer, B., & Kroh, L. W. (2006). Antioxidant activity of coffeebrews. European Food Research and Technology, 223(4), 469–474. https://doi.org/10.1007/S00217-005-0226-4/FIGURES/7

115. Swiss Federal Office of Public Health, 2002. 〈 http://www.bag.admin.ch/verbrau/lebensmi/Acrylamid/index.htm〉

116. D. Andrzejewski, J.A.G. Roach, M.L. Gay, S.M. Musser. Analysis of coffee for the presence of acrylamide by LC-MS/MS. Journal of Agricultural andFood Chemistry, 52 (2004), pp. 1996-2002

117. Summa, C. A., de la Calle, B., Brohee, M., Stadler, R. H., & Anklam, E. (2007). Impact of the roasting degree of coffee on the in vitro radical scavenging capacity and content of acrylamide. LWT - Food Science and Technology, 40(10),1849–1854. https://doi.org/https://doi.org/10.1016/j.lwt.2006.11.016

118. Yashin, A., Yashin, Y., Wang, J. Y., & Nemzer, B. (2013). Antioxidant and Antiradical Activity of Coffee. Antioxidants (Basel, Switzerland), 2(4), 230–245. https://doi.org/10.3390/antiox2040230

119. Pascual, E. C., Goodman, B. A., & Yeretzian, C. (2002). Characterizationof Free Radicals in Soluble Coffee by Electron Paramagnetic Resonance Spectroscopy. Journal of Agricultural and Food Chemistry, 50(21), 6114–6122.

https://doi.org/10.1021/JF020352K

120. Sage, E. (2012, February 15). What is the Shelf Life of Roasted Coffee? A Literature Review on Coffee Staling | Specialty Coffee Association News. Scanews; Science . https://scanews.coffee/2012/02/15/what-is-the-shelf-life-of- roasted-coffee-a-literature-review-on-coffee-staling/

121. A, G.-L., E, G., A, V., MA, R., & JA, M. (2009). Flavonoids as anti-inflammatory agents: implications in cancer and cardiovascular disease. Inflammation Research : Official Journal of the European Histamine ResearchSociety ... [et Al.], 58(9), 537–552. https://doi.org/10.1007/S00011-009-0037-3

122. Goodman, B. A., Pascual, E. C., & Yeretzian, C. (2011). Real time monitoring of free radical processes during the roasting of coffee beans using electron paramagnetic resonance spectroscopy. Food Chemistry, 125(1), 248–254. https://doi.org/https://doi.org/10.1016/j.foodchem.2010.07.072

123. Pham-Huy, L. A., He, H., & Pham-Huy, C. (2008). Free radicals, antioxidants indisease and health. International journal of biomedical science : IJBS, 4(2), 89–96.

124. Rose | Blog | Best types of coffee beans you use in Arabic coffee preparation. (n.d.). Retrieved February 10, 2022, from https://rosethermos.com/types-of-coffee-beans

125. FT/CW System | Multifrequency FT EPR | Bruker. (n.d.). Retrieved April1, 2022, from https://www.bruker.com/en/products-and-solutions/mr/epr- instruments/epr-research-instruments/elexsys-ii-e580.html

126. Extrusion Chemistry of Wheat Flour Proteins: I. Free Radical Formation - Scientific Figure on ResearchGate. Available from: https://www.researchgate.net/figure/A-Typical-room-temperature-electron-paramagnetic-resonance-EPR-signal-from-extruded_fig1_228584587 [accessed 1 Apr, 2022]

127. Marnett, L. J., & Hancock, A. B. (1991). Peroxyl Free Radicals: Biological Reactive Intermediates Produced during Lipid Oxidation. Advances in Experimental Medicine and Biology, 283, 65–70. https://doi.org/10.1007/978-1-4684-5877-0_6

128. Tidahy, H. L., Siffert, S., Lamonier, J. F., Zhilinskaya, E. A., Aboukaïs, A., Yuan, Z. Y., Vantomme, A., Su, B. L., Canet, X., Deweireld, G., & Frère, M. (2007). Characterisation of new Pd / hierarchical macro-mesoporous ZrO2, TiO2 and ZrO2-TiO2 catalysts for toluene total oxidation. Studies in Surface Science and Catalysis, 160, 201–208. https://doi.org/10.1016/S0167-2991(07)80027-9

129. Gielzak, K., Wojciechowski, W. (1995). Magnetic Properties of Chromium (III) Complexes with Some Amino Acids. Chem. Papers 49(2) 54-58

130. Gudepu, S., Boda, R., Shareefuddin, D., Chary, M., & Sayanna, R. (2013). EPR and Optical Studies on Mixed Alkali-Alkaline Earth Oxide Borate Glasses Doped With Cu 2+ Ion.

131. Aboukaïs, A., Zhilinskaya, E., Filimonov, I., Nesterenko, N., Timoshin, S., & Ivanova, I. (2006). EPR investigation, before and after adsorption of naphtalene, of

mordenite containing Fe^{3+} and Cr^{5+} ions as impurities. Catalysis Letters, 111. https://doi.org/10.1007/s10562-006-0134-7

132. Taiwo, F. (2003). Electron paramagnetic resonance spectroscopic studies of iron and copper proteins. Journal of Spectroscopy, 17. https://doi.org/10.1155/2003/673567

133. Leveque, P., Godechal, Q., Gallez, B. (2008) EPR Spectroscopy and Imaging of Free Radicals in Food. Isreal Journal of Chemistry. 48; 19-26